Mechanism regulating multiple fission cell cycle in eukaryotic algae

Jong, Lin Wei

Doctor of Philosophy

Department of Genetics
School of Life Science
The Graduate University for Advanced Studies,
SOKENDAI

Contents

Abstract

Several eukaryotic cell lineages proliferate by multiple fission events, during which cells grow to severalfold of their original size and undergo rounds of cell division without intervening growth. For example, the unicellular volvocine green alga *Chlamydomonas reinhardtii* forms two to 32 daughter cells, in a mother cell wall by one to five rounds of successive cell division, and daughter cells hatch out of the mother cell wall. In this case, the number of successive cell divisions varies depending on the cell size achieved. In contrast, in some species, such as multicellular members of volvocine green algae, a defined number of successive cell divisions occur during multiple fission resulting in coenobium (a colony containing a fixed number of cells), with the daughter cells linked by cytoplasmic bridges during incomplete cytokinesis before the extracellular matrix forms surrounding the cells in colony form. The regulatory mechanism of the multiple fission cell cycle has been well studied in *C. reinhardtii*; however, it has remained unclear how the mechanism evolved and resulted in the occurrence of a defined number of successive cell divisions as observed in multicellular volvocine algae. To address this issue, I first examined the relationship between the number of successive cell divisions and cell size at which cells are committed to cell division in three species of volvocine algae. Volvocine algae include unicellular *Chlamydomonas*, four-celled *Tetrabaena*, eight to 32-celled *Gonium* and others, up to *Volvox* spp. which consists of up to 50,000 cells. As shown previously, *C. reinhardtii* was committed to cell division when the cell had grown at least two-fold and underwent one to four successive cell divisions depending on the cellular growth in G1 phase. In contrast, I found that *Tetrabaena socialis* and *Gonium pectorale* produced four and eight daughter colonies by two and three successive divisions, respectively, which were committed to cell division only when the cells had grown four- and eight-fold, respectively. As previously shown in *C. reinhardtii*, the cell size checkpoint for cell division(s) existed in the G1 phase in *T. socialis* and *G. pectorale*. These results suggest that evolutionary changes in cellular size for commitment largely contributed to the emergence and evolution of multicellularity in volvocine algae.

To assess whether a similar evolutionary change occurred in other lineages of eukaryotic algae and to find any possible common factor contributing to the evolution of multiple fission cell cycle. I also characterized cyanidialean red algae, namely, *Cyanidioschyzon merolae*, which proliferates by binary fission, *Cyanidium caldarium*, and *Galdieria sulphuraria*, which form up to four and 32 daughter cells (autospores), respectively, in a mother cell before hatching out. I found that a two, four, and seven-fold growth of newly born daughter cells is required to commit to cell division(s) for *C. merolae*, *Cy. caldarium*, and *G. sulphuraria*. In the cyanidialean red algae, the cell size checkpoint for cell division(s) was shown to exist in the G1 phase in this study, as shown also in volvocine green algae. In addition, I found that abnormally enlarged, genetically altered *C. merolae* cells underwent two or more successive cell divisions without intervening growth. These results suggest that commitment cell size contributes to determining the number of successive cell divisions. Moreover, evolutionary changes in commitment cell size probably resulted in the variation of the number of cell divisions in multiple fission cell cycle in cyanidialean red algae similar to volvocine green algae.

In order to further assess how the cellular growth is monitored in the G1 phase and decides whether the cell is committed to cell division, I examined the expression pattern of a potential sizer protein, G1 cyclin in *C. merolae.* In the budding yeast, G1 cyclin has been suggested to scale with cell size and regulate the commitment point and G1/S transition. I also found that in *C. merolae*, G1 cyclin accumulates in accord with cellular growth and decreases upon cell division. In addition, in the abnormally enlarged *C. merolae* that underwent two or more successive cell divisions without intervening cellular growth, G1 cyclin was stepwisely decreased following the successive cell divisions. When G1 cyclin was overexpressed in the G1 phase, G1/S transition was accelerated. These results suggest that the G1 cyclin level likely determines the number of successive cell divisions in cyanidialean red algae. Because the molecular mechanism of G1/S transition is widely conserved in eukaryotes, evolutionary change in this pathway may result in variation of the number of successive cell divisions in multiple fission cell cycle in cyanidialean red algae and also in other eukaryotic lineages.

Chapter 1

General introduction

Binary fission involves cells growing to twofold in size (Cavalier-Smith, 1980) and dividing into two cells. In contrast, multiple fission is characterized by cell growth of severalfold, followed by cell divisions that occur rapidly and successively for several times with little or no intervening growth (Cavalier-Smith, 1980). Early embryogenesis stage of various animals resembles multiple fission, in which stem cell grows to severalfold in cell size without any cell division at first (oogenesis), then rapid and successive cell divisions occurred without growth to form embryo (O'Farrell, 2015). This multiple fission-like stage however is only temporary and the rapid cell division cycles eventually slows down (with lengthening of S phase and introduction of G2 phase) through a transition phase known as midblastula transition and later reverts to typical binary fission-like cell cycle (with introduction of G1 phase) (O'Farrell, 2015). Other than animals, multiple fission has also been observed in some *Cyanobacteria* and *Actinobacteria,* in which multiple fission is either the sole, alternative (if induced) or part of their reproductive cycle (Angert, 2005). More commonly, multiple fission has been observed in various lineages of unicellular and colonial photosynthetic eukaryotes such as *Chlorella* and *Scenedesmus* (Donnan et al., 1985; Zachleder et al., 2002) and unicellular eukaryotic parasites such as *Trichomonas* (Kofoid and Swezy, 1915). Among them, the mode and mechanism of multiple fission cell cycle has been most well studied in the model green alga *Chlamydomonas reinhardtii* which is unicellular and undergoes multiple fission to produce 2^n cells (n = 1 to 4) by multiple fission (Craigie and Cavalier-Smith, 1982).

In animals, the cellular growth into a large size during oogenesis provides sufficient nutrients for development. However, the large size is also suggested to impose limitation on its transcription capacity (O'Farrell, 2015). The embryonic development requires the transcription of various genes from a single large diploid cell after fertilization. Thus, the multiple fission-like phase could have been adapted at this early stage as a strategy to allows a rapid burst in transcriptional capacity, which is provided by the large number of nuclei after

multiple fission (O'Farrell, 2015). The duration and the number of rapid cell divisions during animal embryogenesis however are rather invariant within species (Großhans et al., 2003; O'Farrell et al., 2004), which is different from unicellular photosynthetic eukaryotes such as *C. reinhardtii* with a variable number of successive cell divisions depending on the environment. For simpler organisms such as *C. reinhardtii,* it has been suggested that the multiple fission cell cycle evolved as a strategy to maximize their competitive fitness in certain environmental conditions. The multiple fission cell cycle offers competitive advantages compared to binary fission, in environment with either limited or temporally supplied resource (Cavalier-Smith, 1980). Temporal separation between cell growth and cell divisions in multiple fission allow cells to maximize their growth when resources are available. When resources are limited cells switch to reproductive phase, dispersing high number of daughter cells through multiple rounds of cell divisions (Cavalier-Smith, 1980). Indeed, depletion of nutrient, for example, induces multiple fission in a certain cyanobacterial species that usually undergo binary fission (Angert, 2005). For algae, their growth mainly depends on photosynthesis, which is highly influenced by the availability of light. Under diurnal condition, algae maximize their growth during daytime when light is available and proliferate during night when growth does not occur by multiple fission cell cycle (Cavalier-Smith, 1980). For motile photosynthetic algae with flagella, it is assumed that the restriction of cell division to the night was a result of adaptation to a situation in which cells must resorb their flagella prior to cell division in order to use their basal bodies to coordinate chromosome segregation and cytokinesis. During the daytime, flagella-dependent phototaxis is required to optimize light absorption to maximize photosynthesis (Cross and Umen, 2015; Koufopanou, 1994).

Studies on the multiple fission cell cycle in *C. reinhardtii* revealed the existence of a commitment point in mid G1 phase, after which cells can complete at least one round of cell division even without further cellular growth (Cross and Umen, 2015; Umen, 2018). *C. reinhardtii* cells need to grow at least twofold to pass the commitment point (Cross and Umen, 2015; Umen, 2018) (Fig. 1.1). However, cells do not enter S/M phase directly after passing commitment point as the S/M phase always delayed for certain time period until evening (Donnan and John, 1983) possibly by the circadian rhythm (Goto and Johnson, 1995). The

number of cell divisions (repetitive S/M phases) that occur after the delay was suggested to be determined by cell size attained just before G1/S transition (hence not regulated by commitment size) (Craigie and Cavalier-Smith, 1982; Cross and Umen, 2015; Donnan and John, 1983; Umen, 2018) (Fig. 1.1). Thus, the multiple fission in *C. reinhardtii* is regulated by both size-dependent and time-dependent properties of cell which are also known as sizer and timer (Donnan and John, 1983), with timer behavior regulates the timing of cell division as represented in the delay of G1/S transition until evening. On the other hand, sizer behavior involves both cell size monitoring (Facchetti et al., 2017) for the commitment to cell division during G1 phase and determination of number of cell divisions (S/M phases) depending on the cell size at the G1/S transition (Fig 1.1).

However, it has been difficult to elucidate how a cell monitors its size to coordinate cellular growth and division. Until now, most proposed mechanisms involve scaling of either DNA content or a certain protein concentration to cell size. In the budding yeast, one such protein is G1 cyclin (Cln3) which concentration is suggested to scale with cell size and regulate cell division through START at G1 phase (Litsios et al., 2019). Start in the yeast corresponds to commitment point in *C. reinhardtii* which was reported to be regulated through RB-E2F-DP pathway (Fang et al., 2006; Olson et al., 2010). However, in *C. reinhardtii,* it is still unknown how the cell size is monitored for commitment.

Although the mechanism regulating multiple fission cell cycle has been studied extensively in unicellular *C. reinhardtii,* it is still unknown how the mechanism has been modified resulting in emergence of colonial species with defined number of successive cell divisions. In the case of *C. reinhardtii*, the minimum number of cell divisions is one because the cells are committed to cell division when they grow two-fold (Umen, 2005). However, in the case of colonial algae, single mother cells in a colony must always produce four or more colonial daughter cells, and in some cases the number is fixed. For example, each cell of four-celled *Tetrabaena socialis* (a colonial relative of the unicellular *C. reinhardtii*) always divide twice to form four-celled daughter colony. Thus, one possibility is that the cells are only committed to cell division when they grow four-fold. To address this possibility, the relationship between commitment cell size and number of successive cell divisions has been examined in volvocine green algae and cyanidialean red algae which undergo different

number of successive cell divisions depending on species. The results have shown that species that undergo higher number of cell divisions are committed to cell division only when they have grown to a cell size of higher fold of their daughter cells. In addition, my study on G1 cyclin expression pattern in *C. merolae* cells implies a possibility of G1 cyclin acting as potential cell size sensing factor (sizer) to regulate the commitment point, and possibly also regulate the number of cell divisions in cyanidialean red algae. Based on these results, I will discuss what kind of changes could have occurred leading to the evolution of defined (specific) number of successive cell divisions in multiple fission cell cycle.

1.1 Figure

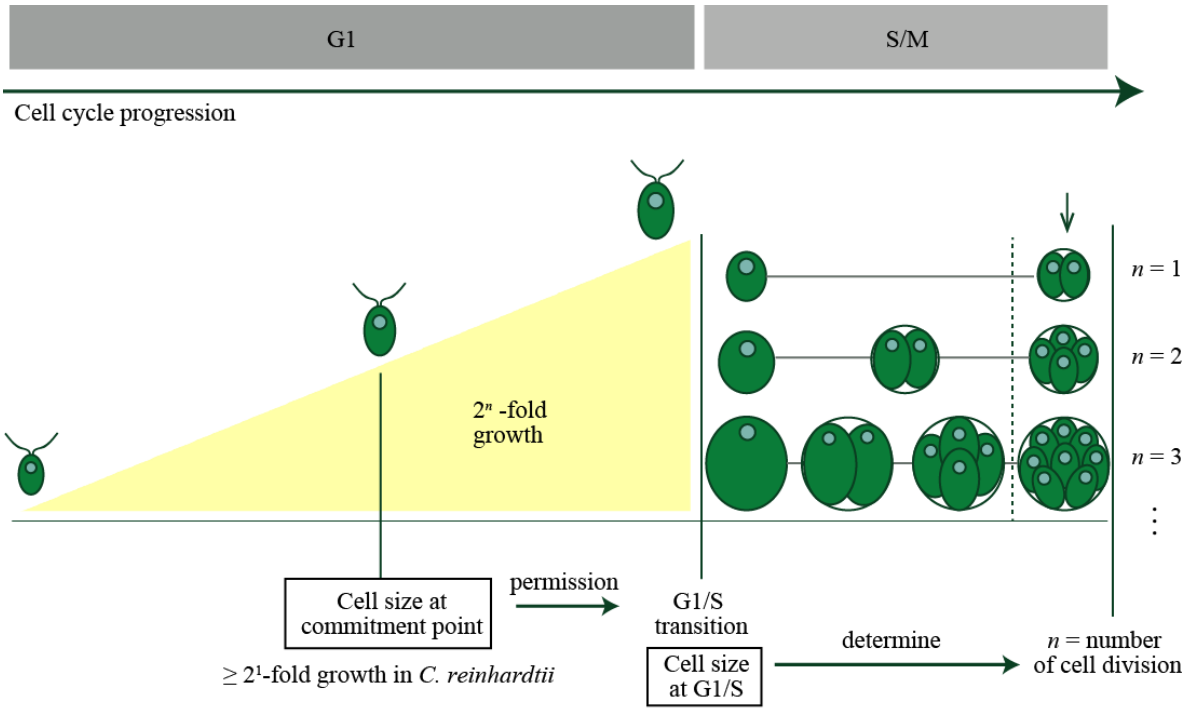

Fig. 1.1 The regulations of multiple fission cell cycle in *C. reinhardtii*. *C. reinhardtii* cell cycle is characterized by an elongated G1 phase which cell grow to severalfold (2^n-fold) in size, and then undergo multiple S/M phases without the need of intervening growth phase. A commitment point (cell size checkpoint) is located at the mid to late G1 phase, at which only cells grown beyond the commitment size (minimum 2^1-fold) are allowed to enter S/M phase later. After some delay from the commitment point which possibly regulated by the circadian rhythm (Goto and Johnson, 1995), G1/S transition occurs. The cell size at which a cell enters the first round of S phase (2^n-fold) then determines the number of cell divisions (S/M phases) and number of daughter cells produced (2^n cells, n = number of cell division) so that daughter cells of a relatively homogeneous sizes are produced. Thus, the cell size is checked at both commitment point (to determine whether or not divide) and G1/S transition (to determine number of successive cell divisions) in the multiple fission cell cycle. It has been shown that RB-E2F-DP pathway is involved in the both cell size checkpoints in *C. reinhardtii* (Cross, 2020; Cross and Umen, 2015; Umen, 2005, 2018). A recent study

suggested that amount and concentration of CDKG1 protein, which is specific to *C. reinhardtii* and its relatives, scale with cell size and is involved in the determination of number of cell divisions but not in commitment point (Li et al., 2016). However, it is still not known how the cell size is monitored at the commitment point in *C. reinhardtii*, but in the budding yeast, G1 cyclin has been suggested to scale with cell size and regulate Start (equivalent to commitment). The figure is modified from Umen (2018).

Chapter 2

Cell size for commitment to cell division and number of cell divisions in volvocine green algae

2.1 Introduction

Many eukaryotic algae belonging to diverse lineages proliferate by multiple fission events, in which cells grow to many fold of their original size and then undergo several rounds of division without intervening growth (Donnan et al., 1985; Sleigh and Sleigh, 1989) For example, a single cell of *Chlorella* spp. forms two, four, eight, 16, or occasionally 32 daughter cells in the mother cell wall by one to five rounds of successive cell division, and the daughter cells then hatch out of the mother cell wall (Donnan et al., 1985; Sleigh and Sleigh, 1989). In some cases, a defined number of multiple fission events result in a coenobium (a colony containing a fixed number of cells), as seen in *Scenedesmus* spp. and *Pediastrum* spp. (Bisova and Zachleder, 2014; Setlikova et al., 2005), and further results in more complex multicellularity, as observed in volvocine algae (Bell, 1978).

The green algal order Volvocales consist of unicellular *Chlamydomonas* and *Vitreochlamys,* and various multicellular (coenobium or colonial) species with wide ranges of cell number, size, morphology, and developmental complexity, which make these algae prominent in evolutionary study of transition from unicellular to multicellular organisms (Herron et al., 2009; Umen and Olson, 2012). The multicellular (colonial) volvocine green algae are grouped into three families, namely Tetrabaenaceae including *Tetrabaena* and *Basichlamys*, which consist of four *Chlamydomonas*-like cells surrounded by a common extracellular matrix; Goniaceae including *Gonium* with eight to 32 cells and *Astrephomene* with 32 to 64 cells; and Volvocaceae including *Pandorina*, *Eudorina* and *Pleodorina* ranging from eight to 128 cells, also highly complex *Volvox* with up to 50,000 cells consisting of somatic and differentiated reproductive cells (Arakaki et al., 2013; Herron et al., 2009; Nozaki et al., 1995). Among Volvocales, simpler multicellular organisms such as *Tetrabaena* and *Gonium* evolved earlier, in which incomplete cytokinesis results in daughter cells linked by cytoplasmic bridges before the formation of the extracellular matrix that shared by the

cells in a colony (Arakaki et al., 2013). In addition to the cell-cell connection and adhesion, species such as *Volvox* further evolved a differentiation system cells between somatic and reproductive cells.

The cell cycle of *Chlamydomonas reinhardtii* is characterized by a long G1 phase, followed by alternating S and M phases to produce 2^n newborn cells, with *n* commonly ranges from 1 to 4 (Bisova and Zachleder, 2014; Cross and Umen, 2015). The prolonged G1 phase vary from 10 to 14 h during which cell can grow more than twofold and if the condition permits, up to more than tenfold in size (Cross, 2020). At the late G1 phase, cell enters the alternating S and M phase, with each DNA replication immediately followed by a round nuclear division and cell division before the next round DNA replication begins (Bisova and Zachleder, 2014). After all cell divisions completed, daughter cells then hatch out of the mother cell and start their next cell cycle. In a typical diurnal cycle (e.g., 12-h light/12-h dark), the cell cycle becomes synchronized such that growth occurs during the light phase and cell division (S/M phases) occurs in the dark (Cross and Umen, 2015; Umen, 2005; Umen and Goodenough, 2001).

As mentioned previously (Chapter 1), the multiple fission cell cycle of *C. reinhardtii* has been shown to be controlled by the three mechanisms. Firstly, the cells are committed to cell division during mid G1 phase only they have grown at least two-fold (Cross and Umen, 2015; Li et al., 2016; Spudich and Sager, 1980; Umen, 2018). Secondly, the committed cells further grow until evening (Donnan and John, 1983) when the cells are gated to S/M phases by the circadian rhythm (Goto and Johnson, 1995). Thirdly, when the cell enters the first round of S/M phase, the number of S/M cycles (the number of successive cell division) is determined based on the cell size; large mother cells divide more times than small mother cells, so that daughter cells of a relatively uniform size distribution are always produced (Craigie and Cavalier-Smith, 1982; Donnan et al., 1985). Both the commitment point and G1/S transition in *C. reinhadrtii* have been suggested to be regulated by retinoblastoma (RB) tumor suppressor pathway (also known as RB-E2F-DP pathway) (Fang et al., 2006; Olson et al., 2010; Umen and Goodenough, 2001). RB-E2F-DP pathway has also been reported to regulate G1/S transition in animals and a similar pathway has been shown to regulate Start (equivalent to the commitment point in *C. reinhardtii*) and G1/S transition in the budding

yeast (Cooper, 2006; Malumbres and Barbacid, 2005; Umen and Goodenough, 2001). In addition, a novel volvocine-specific cyclin-dependent kinase (CDK) has been identified in *C. reinhardtii* which concentration in the nucleus correlates or scales with cell size, and suggested to regulate the number of successive cell divisions through RB-E2F-DP pathway (Li et al., 2016).

The regulations observed in *C. reinhardtii* were suggested to be conserved among volvocine green algae (Herron and Michod, 2008; Kirk, 2003, 2005). For instance, *Tetrabaena* and *Gonium* also undergo multiple fission events to form daughter colonies by keeping cells attached after multiple fissions. Each cell of a *Tetrabaena socialis* colony acts as a mother cell and undergoes two successive cell divisions that subsequently produce a four-celled colony and hatches out from the mother cell. In a similar manner, each *Gonium pectorale* cell undergoes three or four cell divisions producing an eight- or 16-celled colony. Thus, it was suggested that cell cycle regulation and cell-cell adhesion have been modified to promote multicellularity. Based on this assumption, other than the presence of cytoplasmic bridge hold the cell in colony form during incomplete cytokinesis, *T. socialis* and *G. pectorale* cells must also complete at least two and three cell divisions, respectively, before hatching out from the mother cell wall, in contrast to unicellular *C. reinhardtii* cells which can be released as unicellular cells from mother cell wall even after only one division has been completed. However, it has been unclear how the minimum number of cell divisions is defined and regulated to maintain multicellularity in *T. socialis* and *G. pectorale*.

To address this issue, I examined how *T. socialis* and *G. pectorale* cells are become committed to cell division. The results show that *T. socialis* and *G. pectorale* are committed to cell division only when the cell has grown beyond four- and eight-fold of their daughter cell size, respectively. Thus, the commitment at such cell size probably ensures two and three successive cell divisions in *T. socialis* and *G. pectorale* to produce four- and eight-celled daughter colonies, respectively. These results hence suggest that the changes in the cell size for commitment to cell division may has a prominent contribution to the emergence and evolution of multicellularity in the volvocine algae.

2.2 Materials and Methods

2.2.1 Commitment assay and commitment cell size determination

C. reinhardtii 137c, *T. socialis* NIES-571, and *G. pectorale* 2014-0520-F1-1 were used in all experiments. Cultures were first grown in an inorganic (photoautotrophic) Standard Volvox medium (SVM) in 100 mL test tubes (approximately 3 cm in diameter; containing 50 mL culture) in continuous light of 100 μmol m^{-2} s^{-1} and aeration with 0.3 L min^{-1} at 20 °C for 3 d. On the third day, 1 μl of each culture was placed on top of SVM agar (1.0% agar; approximately 2 mm thick) in separate wells of a 24-well plate. Another thin layer of agar (0.8% agar; approximately 1 mm thick) was prepared and used to cover the cultures (*T. socialis* and *G. pectorale* only) to prevent drying. The cultures were observed under light microscope and pictures were taken before transferring to dark conditions. After being kept in the dark for 24 h and 48 h at 20 °C, the cells were observed again and pictures were taken from the same areas. From the pictures, cells that divided (during the dark) were identified and the number of daughter cells produced was counted. The pictures at the 0 h (before dark incubation) were also used to measure and calculate cell volumes based on the formula $[4/3\pi(l/2)(w/2)^2]$ ("l" and "w" indicate length or longitudinal distance and width or latitudinal distance, respectively). The cell volumes at 0 h for those cells that divided later in dark are used for commitment size determination, while cell volumes after dark for those divided cells were used for daughter cell size determination.

2.2.2 Synchronous culture

T. socialis cells were precultured in SVM medium in 700 mL flat bottles (approximately 5 cm in depth; containing 500 mL culture) in the dark with an aeration with 3.0 L min^{-1} at 20 °C for more than 3 h and then synchronized by subjecting the culture to a 12-h light (130 μmol m^{-2} s^{-1}) and 12-h dark cycle. The same culture conditions were applied for synchronizing *G. pectorale* cells, except that the temperature was 25 °C.

2.2.3 Percentage determination of dividing cells and committed cells

During the third round of the light/dark cycle (LD), cells were sampled every 2 h during the light period and every 4 h during the dark period. For each sample, the numbers of dividing

and nondividing cells were counted under light microscope, and the percentage of dividing cells was calculated. To determine the percentage of committed cells, the culture samples were placed onto agar, covered with another layer of agar, as described above, and then incubated in the dark for 24 h. Cells that divided after the dark incubation was counted as committed cells and the percentage was calculated. For *T. socialis*, the percentage of committed cells was only calculated for those sampled during the light period.

2.2.4 Immunoblotting analysis to determine the expression level of an S-phase marker

Another 10 to 15 mL of cells was sampled during the third round of the LD for immunoblotting analysis. The samples were centrifuged to remove the culture medium and the cells were resuspended in SDS-PAGE sample buffer (50 mM Tris, pH 6.8, 10% glycerol, 2% SDS, 5% 2-mercaptoethanol, and 0.01% bromophenol blue). The samples were kept at -80 °C until next steps. The protein concentration in each sample was determined using an XL-Bradford protein assay kit (APRO Science, Japan). An equal amount of protein content from each sample was loaded into each well of the gel and separated by SDS-PAGE. The proteins were then transferred from the gels to polyvinylidene difluoride membranes and blocked with 5% skim milk dissolved in Tris-buffered saline (TBS) supplemented with 0.2% Tween-20 (TTBS) at room temperature. The membranes were then incubated with an anti-*C. reinhardtii* FtsZ1 antibody (Miyagishima et al., 2012) at a dilution of 1:4,000 for 30 min, washed with TTBS three times (10 min each), and then incubated with horseradish peroxidase-conjugated goat anti-rabbit antibody diluted at 1:25,000 for 30 min. The membranes were washed with TTBS three times and signals were detected using an ECL Plus Western Blotting Detection Reagents (GE Healthcare) and ImageQuant LAS400 chemiluminescent detection system (GE Healthcare).

2.3 Results

2.3.1 Number of successive cell divisions in *C. reinhardtii*, *T. socialis*, and *G. pectorale*

To determine the number of successive cell divisions that occurred after the commitment point, commitment assays were performed for *C. reinhardtii*, *T. socialis*, and *G. pectorale* (Fig. 2.1). Cells of respective species were cultured under continuous light (100 μmol m^{-2} s^{-}

[1]) with aeration of ambient air at 20 °C in a photoautotrophic (inorganic) medium. The logarithmically proliferating cells were then placed on agar plates containing medium and incubated at 20 °C in continuous dark to stop further cellular growth. It should be noted that there were two layers of agar that sandwiched the cells to prevent them from drying, especially for *G. pectorale* cells, which showed signs of drying without the top agar, and could not complete cell division properly. This observation was consistent with the previous report that *G. pectorale* cells did not grow on agar plates (Lerche and Hallmann, 2009). In this commitment assay, cells were expected to complete cell division if they had grown beyond the threshold size for cell division and passed the commitment point, before they were incubated onto the plates in the dark. In our culturing conditions, the cell divisions if initiated, always finished within 24 h in the dark on the plate and no further cell division was observed from the 24 h to 48 h after the onset of dark incubation (Fig. 2.1A–F). Thus, we examined the number of daughter cells that had been produced at 24 h after dark incubation. In our culturing conditions, approximately 70% *C. reinhardtii* cells divided, for one to three times on plates producing two to eight daughter cells. Major fraction of these cells underwent one cell division producing two daughter cells. Two or three successive divisions occurred in smaller proportions (Fig. 2.1A, D, G). On the other hand, approximately 60% *T. socialis* cells divided on the plates in dark condition, and most of the cells underwent two successive cell divisions producing four-celled daughter colonies (Fig. 2.1B, E, H). Regarding *G. pectorale*, approximately 6% of the cells divided on plates in the dark, and most of the cells underwent three successive cell divisions producing eight-celled daughter colonies (Fig. 2.1C, F, I). These results suggested that the number of cell divisions was limited to two or three in *T. socialis* and *G. pectorale*, thus always producing a four- or eight-celled daughter colony from a single mother cell, respectively. This was in contrast to *C. reinhardtii* that produced variable number of unicellular daughter cells.

2.3.2 Cell size at which commitment to cell division occurred in *C. reinhardtii*, *T. socialis*, and *G. pectorale*

In order to determine the minimal cell size beyond which cells can complete their cell cycle, cell volumes (or cell size; interchangeable) of all the three species before dark incubation on

plates were determined and the data were integrated into the results of the number of cell divisions for comparison (Fig. 2.2). Cell length and width were measured and the cell volume was calculated based on the formula for cellular ellipsoidal shape. We also determined the volume of daughter cells produced by cell division after 24-h dark incubation. The results showed that *T. socialis*, which always undergoes two successive cell divisions to produce four-celled daughter colony whenever cell division occurs, had a commitment size (the smallest size of cells that underwent cell division on plates in the dark) that was close to fourfold of the average daughter cell volume (Fig. 2.2B). Regarding *G. pectorale*, which underwent three successive cell divisions to produce eight-celled daughter colony, the commitment size was nearly equal to eightfold of the average daughter cell volume (Fig. 2.2C). In contrast to these two species, the commitment size of *C. reinhardtii* was roughly equal to twofold of the average daughter cell volume, as shown in other studies (Craigie and Cavalier-Smith, 1982; Donnan and John, 1983; Umen, 2005) (Fig. 2.2A). In addition, some of the cells that had grown beyond fourfold of the average daughter cell volume before dark incubation underwent two successive cell divisions producing four daughter cells in the dark, as shown previously (Craigie and Cavalier-Smith, 1982; Donnan and John, 1983; Umen, 2005) (Fig. 2.2A). These results indicated the correlation between the minimum number of successive cell divisions and the commitment cell size: two times the average newly born daughter cell volume for unicellular *C. reinhardtii*, four times for four-celled *T. socialis*, and eight times for eight-celled *G. pectorale*.

2.3.3 Position of the commitment point in *T. socialis* and *G. pectorale* in their cell cycle

Previous studies showed that the commitment point in *C. reinhardtii*, at which a decision to divide or not is made, lies shortly before G1/S transition (Cross and Umen, 2015; Donnan and John, 1983; Li et al., 2016; Oldenhof et al., 2007; Spudich and Sager, 1980; Umen and Goodenough, 2001). In order to examine whether this was also the case for *T. socialis* and *G. pectorale*, respective cells were synchronized by subjecting them to 12-h light/12-h dark cycle. During the third round of the LD, temporal changes in the percentage of committed cells (determined based on commitment assay described above), level of an S-phase marker protein in the culture (determined by immunoblotting), and percentage of cells in which

daughter cells were formed (initiated cell division), were examined (Fig. 2.3). A chloroplast division protein FtsZ1 was chosen as S-phase protein marker as it was expressed specifically during the S phase in eukaryotic algae including *C. reinhardtii*, shown in previous study (Miyagishima et al., 2012). In addition, the amino acid sequence of FtsZ1 is relatively highly conserved among green algae and the antibody against FtsZ1 of *C. reinhardtii* was prepared in previous study of our laboratory (Miyagishima et al., 2012). In the synchronous culture of *T. socialis*, the committed cells before cell division peaked at the 10 h (26%; Fig. 2.3C), FtsZ1 levels peaked at 12 to 16 h (Fig. 2.3C), and the cells, in which daughter cells were formed, peaked at the 16 h (Fig. 2.3A). In the synchronous culture of *G. pectorale*, the committed cells before cell division peaked at the 12 h (7.5%; Fig. 2.3D), FtsZ1 level peaked at the 16 to 20 h (Fig. 2.3D), and the cells in which daughter cells were formed (initiated cell division), peaked at the 20 h (Fig. 2.3B). In the commitment assay using cells cultured synchronously in a LD (Fig. 2.3), the number of cells in daughter colony were mostly four for *T. socialis* and eight for *G. pectorale*, which was consistent with the results obtained using asynchronous culture (Fig. 2.1). Thus, both *T. socialis* and *G. pectorale* cells are committed before S phase, as shown in *C. reinhardtii*. It was suggested that cell size is monitored in the late G1 phase to decide whether or not to enter into the S phase in these species.

2.4 Discussion

Tetrabaena and *Gonium* evolved from a *Chlamydomonas*-like unicellular ancestor earlier than other multicellular volvocine algae (Herron and Michod, 2008). The cells of both species shared a high similarity with *C. reinhardtii* and they all proliferate by a multiple fission. Here, *T. socialis* and *G. pectorale* cells were shown to pass the commitment point only when they had grown to at least four- and eight-fold in size of their daughter cell, respectively, in contrast to *C. reinhardti*i, which is committed when it has grown only beyond twofold in size. The results suggest that the larger commitment size in colonial *T. socialis* and *G. pectorale* ensures a higher minimum number of cell divisions (two and three divisions respectively) that occur later.

Various other volvocine algae which consist of a higher number of cells such as *Pandorina morum* (8 or 16 cells), *Eudorina unicocca* (32-cell) and *Volvox carteri*

(approximately 2,000 cells), have also been reported to first grow to a large maximal size and then only undergo successive cell divisions without intervening growth during their asexual reproduction phase (Hallmann, 2006). Even in *Volvox*, which produces differentiated cell types (somatic and reproductive cells), successive cell division also occurs for five rounds, during the early embryogenesis producing 32 cells of the equal size, before the onset of asymmetric cell divisions (6 to 7 rounds, also successively) and cell differentiation (Matt and Umen, 2016). As multiple fission cell cycle is shared by various volvocine green algae which all share a common *Chlamydomonas*-like unicellular ancestor (Coleman, 1999; Kirk, 2003, 2005), an evolutionary increase in commitment cell sizes as observed in *T. socialis* and *G. pectorale* could have also involved in the evolution of those species with a higher number of cells and could have contributed to the emergence of the multicellularity in volvocine algae.

As in unicellular *C. reinhardtii* (Spudich and Sager, 1980), *T. socialis* and *G. pectorale* cells were also committed to cell division during G1 phase. Thus, regulation of the commitment in these colonial algae probably involve a similar but modified mechanism of commitment in *C. reinhardtii*. In *C. reinhardtii,* The RB-E2F-DP pathway has been reported to regulate commitment size checkpoint point at mid G1 phase and the subsequent G1/S transition (Fang et al., 2006; Olson et al., 2010; Umen and Goodenough, 2001). This pathway is widely conserved among eukaryotes (Cooper, 2006; Malumbres and Barbacid, 2005). At early G1 phase, RB protein acts as transcriptional repressor by binding to and inhibiting transcriptional activity of E2F/DP complex (Fischer and Muller, 2017; Neganova and Lako, 2008). During mid to late G1 phase in animals, G1 cyclin (cyclin D) accumulates by growth factors and forms complex with CDK. Then, Cyclin D-CDK phosphorylates RB which releases it from E2F/DP thereby activating transcription of S-phase genes by E2F/DP (Cooper, 2006; Malumbres and Barbacid, 2005).

Mutations of various genes in this pathway showed to affect the commitment size in *C. reinhardtii*. Mutations in *RB* (*MAT3*) gene resulted in a decreased commitment size while those in *E2F1* and *DP1* increased commitment size (Fang et al., 2006; Olson et al., 2010; Umen and Goodenough, 2001). In addition, a comparative genomic study of unicellular *C. reinhardtii*, and multicellular species *G. pectorale* and *Volvox carteri* found a considerable variation in their primary RB structure and a higher dN/dS ratio in CYCD (G1 cyclin), a

signature of adaptive evolution (Hanschen et al., 2016). Thus, evolutionary changes in this pathway likely account for the increased commitment size of *T. socialis* and *G. pectorale* observed in this study (will be further discussed in the section of General discussion).

C. reinhardtii cells produce a variable number of daughter cells ranging from two to eight cells in this study. This variation is probably explained by the combination of commitment by at least a two-fold growth and circadian gating of S/M phase only during the (subjective) night. Even in an asynchronous culture in continuous light, the activity of each cell is under the regulation by its own circadian clock. The cell does not divide immediately even when it has passed commitment by two-fold growth and cell growth continues until a subjective evening, when the cell is permitted to undergo the S/M cycle. In this case, there will be a variation in cell size among post-committed cells. During the (subjective) night, larger cells undergo two or more rounds of S/M phases depending on their cell size to produce a relatively uniform-sized population of daughter cells.

In contrast to *C. reinhardtii*, in this study, I observed only two successive cell divisions in *T. socialis*, even though a certain population had grown by more than eight-fold before cell division. In a similar manner, in the *G. pectorale* strain that was used in this study, four-celled (observed in our culturing condition) or eight-celled colonies have been observed (Hanschen et al., 2016) but 32 (or more)-celled colonies have never been observed. Thus, the third and fifth cell divisions are inhibited in *T. socialis* and *G. pectorale*, respectively. However, it is theoretically likely that, for example in *T. socialis*, a cell undergoes four successive cell divisions to produce four four-celled colonies (16 cells in total), if cellular growth during subjective daytime can be accelerated by changing the cultivating condition.

Regarding the mechanism that determines the number of successive cell divisions depending on cellular size, a recent study in *C. reinhardtii* showed that the potential "sizer" protein CDKG1 accumulated at a higher level in larger mother cell and suggested CDKG1 was consumed in a stepwise manner by successive cell divisions until the level became insufficient for a further round of cell division (Li et al., 2016). Given this information in *C. reinhardtii*, the threshold CDKG1 level for a further round of cell division also likely changed during the evolution of four-celled *Tetrabaena* and eight- or 16-celled *Gonium* from unicellular *Chlamydomonas*-like ancestors. CDKG1 however was suggested not to involve

in the regulation of commitment. As the recent study also suggested that CDKG1 acts though the RB and G1-cyclin (cyclin D) pathway (Li et al., 2016), the evolutionary changes in G1 cyclin and RB proposed previously were likely the cause of a change in the control of the number of successive cell divisions besides that in commitment sizes.

Other than volvocine algae, many other algae with a coenobium structure proliferate by a defined number of divisions in a multiple fission cell cycle. In addition, some other unicellular algae, such as cyanidialean red algae, produce at least four or eight daughter cells in mother cells before hatching out of the mother cell wall and the minimum number of cell divisions varies depending on the strain (Miyagishima et al., 2018). Thus, characterization of the mechanisms that restrict the minimum number of multiple fissions in other lineages will also be important to understand the evolution of a multiple fission cell cycle in eukaryotes, which will be addressed in Chapter 3.

2.5 Figures

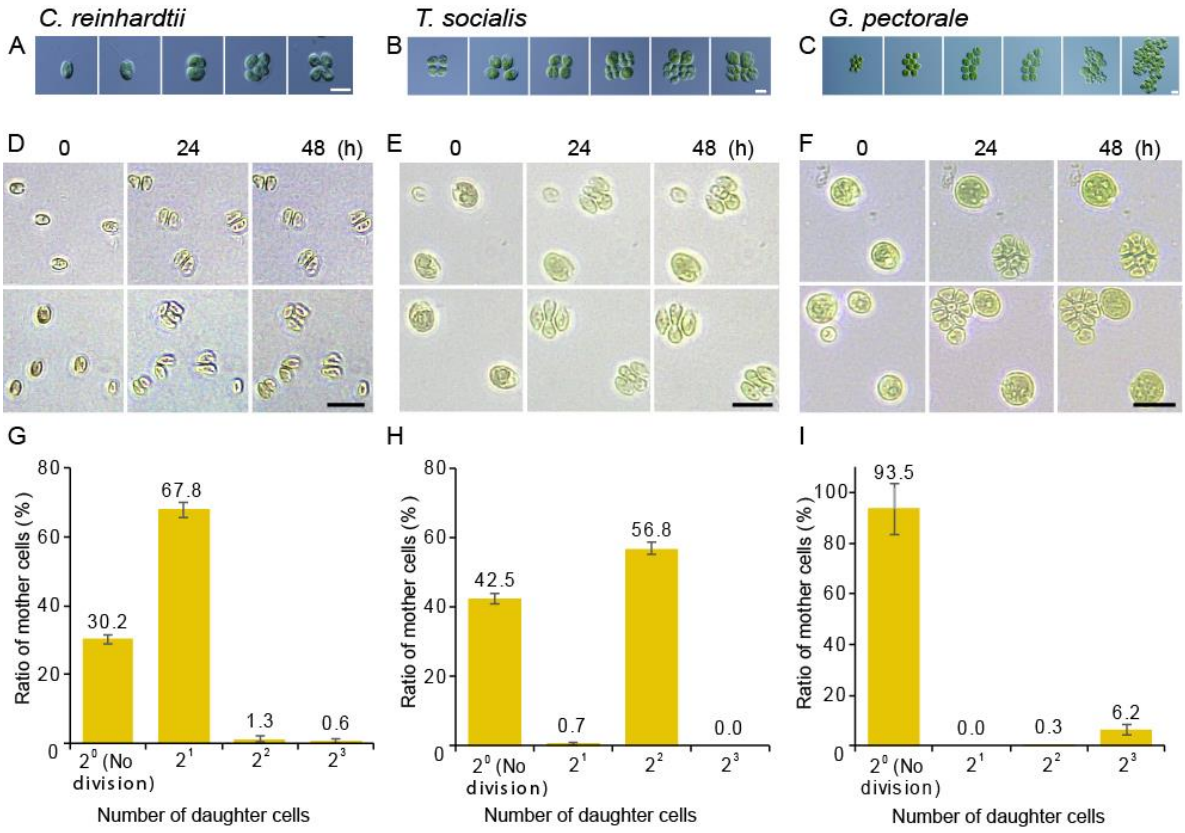

Figure 2.1. Number of successive cell divisions in *C. reinhardtii*, *T. socialis*, and *G. pectorale*. Microscopic images of cells showing processes in which mother cells grow and later divide, producing a defined number of daughter cells: two or four daughter cells in *C. reinhardtii* (A), four daughter cells in *T. socialis* (B), and eight daughter cells in *G. pectorale* (C). To determine the number of successive cell divisions, log phase cells cultured in an inorganic medium, asynchronously under continuous light were plated on agar containing medium and incubated in the dark to stop cell growth while allowing committed cells to divide. The images of the cells just before dark (0 h), and at the 24 h and 48 h after dark incubation on plates are shown for *C. reinhardtii* (D), *T. socialis* (E), and *G. pectorale* (F). The number of daughter cells produced (number of cell divisions) was counted 24 h after the dark incubation on plates. The results for *C. reinhardtii* (G), *T. socialis* (H), and *G. pectorale* (I) are shown. The error bar indicates the standard deviation of three biological replicates. Scale bars represent 10 μm (A, B, C) and 20 μm (D, E, F) respectively.

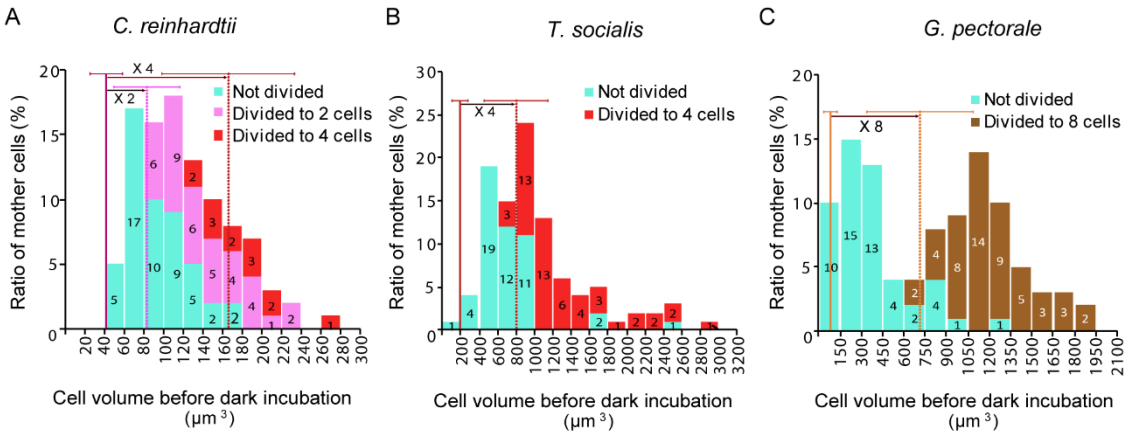

D

Species	Average daughter cell volume (μm³ ± S.D.)	Smallest volume of mother cell that divided during dark incubation (μm³)	
C. reinhardtii	41.5 ± 17.0	One cell division	82.5
		Two cell division	127.4
T. socialis	199.9 ± 86.7	705.3	
G. pectorale	89.6 ± 47.6	675.7	

Figure 2.2. Relationship between cell size and the number of successive cell divisions in *C. reinhardtii*, *T. socialis*, and *G. pectorale*. The experimental conditions were the same as in Fig. 2.1. Cell volumes before dark incubation on plates were determined (n = 100 for each) and are presented in the histogram. Different colored bars used to differentiate cells that did not divide, divided once producing two daughter cells, divided twice producing four daughter cells, and divided three times producing eight daughter cells. On each histogram, the average size of daughter cells after cell division is also shown as a straight vertical line with the standard deviation, and the dotted line indicates the expected twofold, fourfold, or eightfold of the daughter cell size (A–C). The average size of daughter cells after cell division and the smallest size of mother cells that divided during dark incubation are also summarized in the table (D).

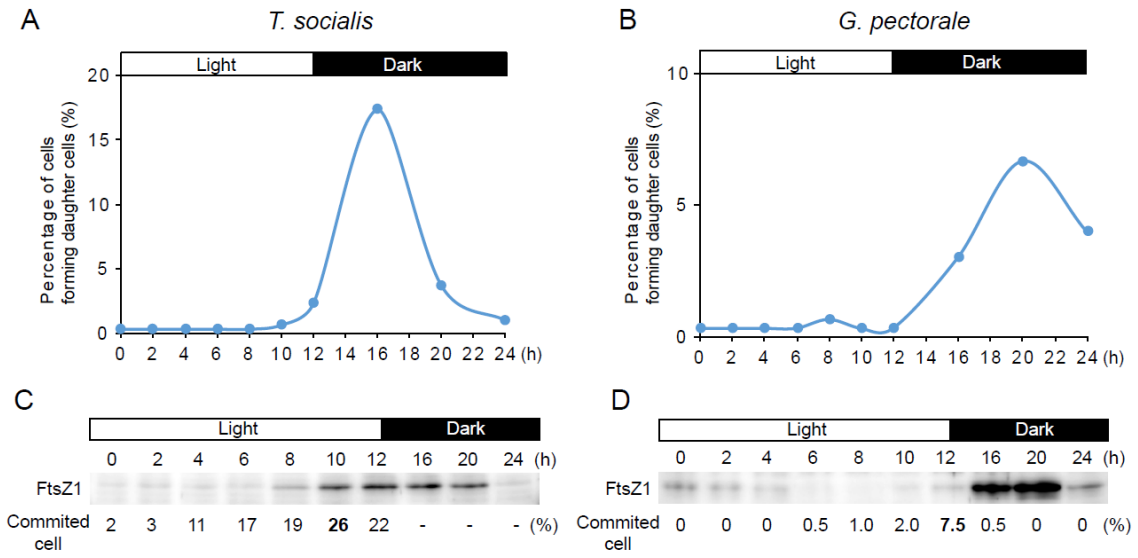

Figure 2.3. Changes in percentage of committed cells, level of an S-phase marker protein FtsZ1, and percentage of cells in which daughter cells were formed (initiated cell division) in *T. socialis* and *G. pectorale*. Both *T. socialis*, and *G. pectorale* were synchronized by a 12-h light/12-h dark cycle and the onset of the third round of the LD is defined as the 0 h. The percentages of cells in which daughter cells were formed, during the LD, are shown for *T. socialis* (A) and *G. pectorale* (B). The S-phase protein marker, FtsZ1, in the cultures collected throughout LD, was detected by the immunoblotting analyses for *T. socialis* (C) and *G. pectorale* (D). The percentage of committed cells in cultures collected at the indicated timings are shown below the immunoblot result for *T. socialis* (C) and *G. pectorale* (D).

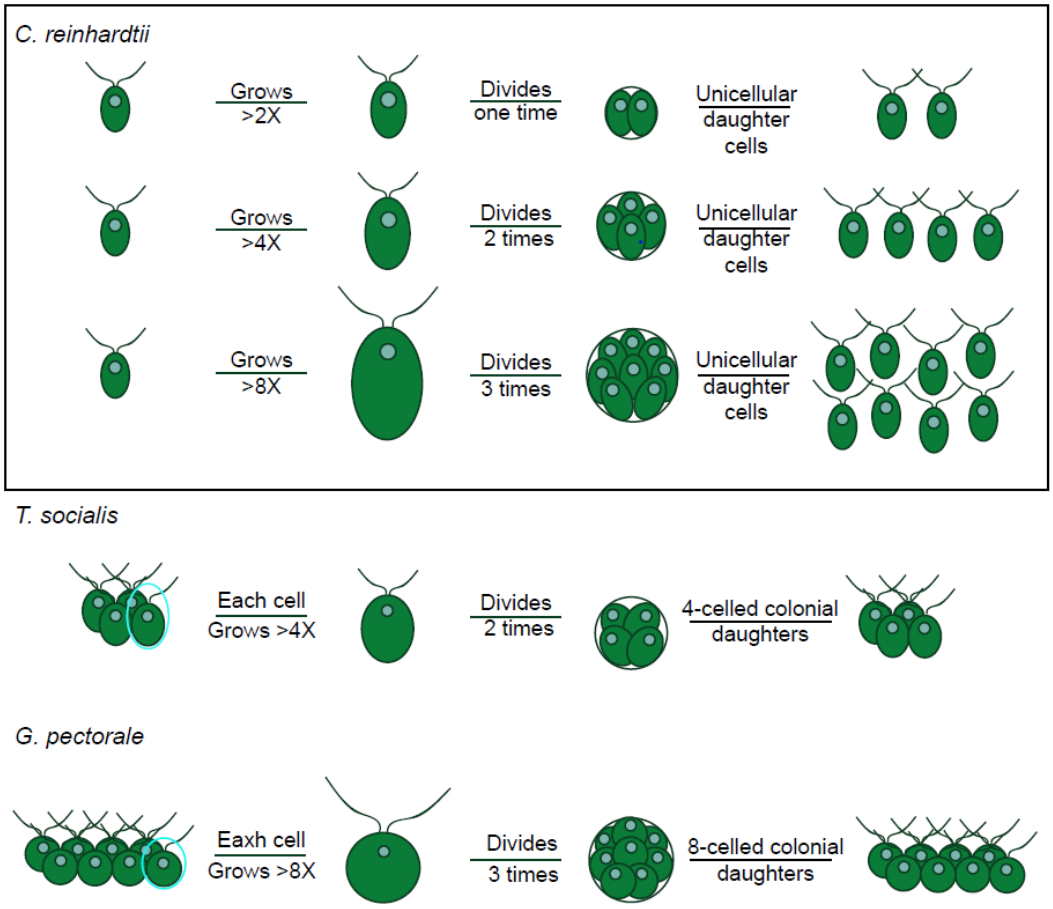

Figure 2.4. Schematic diagram of the progression of cell divisions in *C. reinhardtii*, *T. socialis*, and *G. pectorale* which depends on their cell sizes. In order to perform cell division, *C. reinhardtii*, *T. socialis*, and *G. pectorale* have to grow at least twofold, fourfold, and eightfold, respectively, during G1 phase. Depending on the mother cell size, *C. reinhardtii* undergoes two or more rounds of cell division, thus ensuring a relatively uniform-sized population of daughter cells. For *T. socialis* and *G. pectorale*, the cell division illustrated is only for one cell in each mother colony.

Chapter 3

Cell size for commitment to cell division and number of successive cell divisions in cyanidialean red algae

3.1 Introduction

My study on three volvocine green algal species – *C. reinhardtii, T. socialis* and *G. pectorale*, which undergo multiple fission, determined the cell size for commitment to cell division among the species (twofold, fourfold, and eightfold growth respectively). These sizes correlate with their minimum number of successive cell divisions (one, two and three respectively) suggesting that the evolutionary change in the commitment cell sizes likely increased the minimum number of successive cell divisions and resulted in multicellularity in volvocine green algae (Chapter 2). Other than volvocine green algae, multiple fission has also been observed in various lineages of eukaryotic algae (Cavalier-Smith, 1980). For example, in the two related unicellular red algal genera, *Cyanidium* and *Galdieria*, two or more successive cell divisions occurring to produce four to 32 autospores in a mother cell wall (Albertano et al., 2000; Merola et al., 2009), which later hatch out of mother cell as unicellular daughter cells (here, the divided cells inside mother cell walls are referred to as autospores and the cells that hatched out are referred as daughter cells). Both *Cyandium* and *Galdieria* belong to the order Cyanidiales. Cyanidiales also includes another genus *Cyanidioschyzon* which proliferates by binary fission and does not possess cell wall unlike *Cyandium* and *Galdieria* (Albertano et al., 2000; Merola et al., 2009). It is unclear whether the suggested evolution changes in commitment size as in volvocine green algae also occurred in this or any other algal lineages to regulate their number of cell divisions.

Both green and red algae diverged relatively early in eukaryotic evolution. The first eukaryotic alga with chloroplast was established by an endosymbiotic event between a cyanobacterial endosymbiont and a non-photosynthetic eukaryotic host more than 1.5 billion years ago (BYA) (Parfrey et al., 2011; Yoon et al., 2004). After the split between red and green algae, the common ancestor of the order Cyanidiales was suggested to have split from other red algae at 1.3 to 1.4 BYA based on molecular clock inference and fossil evidence of

the first multicellular red alga (Yoon et al., 2006; Yoon et al., 2004). As in other eukaryotic algae, the cell cycle of *Cyanidioschyzon merolae* is regulated by circadian rhythm and it can be synchronized with diurnal cycle in which cells grow during the light period and divide during the dark period. In motile (flagellated) green algae such as volvocine green algae, the day/night separation of cell growth and division has been suggested as an adaptation to use flagella during the daytime for phototaxis to optimize photosynthesis, and delaying cell division to dark in which cell must resorbs flagella to use their basal bodies to coordinate chromosome segregation and cytokinesis (Cross and Umen, 2015; Koufopanou, 1994). Although the cyanidialean red algae do not possess flagella, the day/night separation of cell growth and division has been suggested to reduce the risks of nuclear DNA damage during S phase by photosynthetic oxidative stress (Miyagishima et al., 2014).

Among the unicellular cyanidialean red algae, *C. merolae* is genetically tractable and various genetic modification protocols have been developed (Kuroiwa et al., 2018). As in the unicellular green alga *C. reinhardtii* (Umen and Goodenough, 2001), the RB-E2F-DP pathway was also shown to be involved in the commitment and G1/S transition in *C. merolae* (Miyagishima et al., 2014). The commitment size checkpoint and the RB-E2F-DP pathway hence likely also regulates the number of cell divisions in *C. merolae* and other Cyanidiales. These features of cyanidialean red algae will facilitate the studies on their cell cycle and demonstrate their suitability to investigate on whether the evolutionary change in the commitment cell sizes as suggested in volvocine green algae also occurred in other algal lineages.

To examine this possibility, the cell sizes at which various cyanidialean red algae committed to cell division were examined in this study. The results show a correlation between the commitment cell size and the number of successive cell divisions in cyanidialean red algae. Twofold, fourfold, and sevenfold growth of newly born daughter cells respectively, is required for commitment to cell division(s) for *C. merolae* which proliferates by binary fission, *Cyanidium caldarium* which produces four autospores and *Galdieria sulphuraria* which produces four or eight autospores. In addition, abnormally enlarged, genetically altered *C. merolae* cells were shown to undergo two or more successive cell divisions without intervening growth. These results suggest commitment cell sizes to involve in determination

of the number of successive cell divisions, and that the evolutionary changes in commitment cell size likely resulted in a variation of the number of cell divisions in the multiple fission cell cycle in cyanidialean red algae as previously suggested in volvocine green algae.

3.2 Materials and Methods

3.2.1 Algal strains and culture

C. merolae 10D (NIES-3377) was cultured in 2 × Allen's medium (an inorganic medium) (Allen, 1959). *Cy. caldarium* RK-1 (NIES-2137) and *G. sulphuraria* 074W (Oesterhelt et al., 2008) were cultured in modified Allen's medium (MA2 medium; an inorganic medium) (Minoda et al., 2004). *C. merolae* A-type cyclin-dependent kinase (*CDKA*) conditional knockdown line (*CDKA*-cKD) had been generated previously by inserting *C. merolae* nitrate reductase (*NR*) promoters, and an *HA*-coding sequence into the chromosomal *CDKA* locus of *C. merolae* 10D (Fujiwara et al., 2020). *C. merolae CDKA*-cKD was maintained in MA2-NO_3 medium, in which NH_4^+ (in MA2 medium) was replaced with the same concentration of NO_3^- as the sole nitrogen source (20 mM $NaNO_3$, 20 mM Na_2SO_4, 8 mM H_2KPO_4, 4 mM $MgSO_4$, 1 mM $CaCl_2$, 2.8 μM $ZnCl_2$, 16 μM $MnCl_2$, 7.2 μM Na_2MoO_4, 1.28 μM $CuCl_2$, 0.68 μM $CoCl_2$, 100 μM $FeCl_3$, 72 μM EDTA-2Na; pH 2.3, adjusted with H_2SO_4) (Fujiwara et al., 2020). Stock cultures of these strains were kept at 40 ˚C under light (20 μmol photons m^{-2} s^{-1}) and agitated with a shaker.

All of the above strains were inoculated into 50 mL of the above-mentioned media unless otherwise indicated, and cultured in 100 mL test tubes with aeration of ambient air (0.4 L min^{-1}) at 42 °C with or without light (100 μmol photons m^{-2} s^{-1}) as indicated. For the synchronous culture, cells were pre-cultured in the dark for 4 h (unless otherwise indicated), and then subjected to 12-h light/12-h dark cycle. *C. merolae*, *Cy. caldarium*, and *G. sulphuraria* cells were inoculated to give an initial OD750 of 0.1, 0.25, and 0.25, respectively, except for the commitment assay of *G. sulphuraria* in which the cells were inoculated to give an OD750 of 0.1.

3.2.2 Commitment assay

For the commitment assay of *C. merolae*, culture was collected at the 9 h of second LD, while for *Cy. caldarium* and *G. sulphuraria*, culture was collected at the 8 h and 5.5 h of third LD respectively. For the commitment assay of *Cy. caldarium*, 1 μL of the collected culture was placed on a gellan gum-solidified MA2 plate (1.0 % gellan gum; approximately 4 mm thick). A section of the gellan gum with the cells was dissected and placed onto a glass bottom dish (with grid; 3922-035; IWAKI, Japan), with the cells facing the dish so that the cells were immobilized by sandwiching between the gellan gum and the glass. Then, the cells were observed under an inverted microscope (IX71; Olympus), and micrographs were taken. After being incubated at 42 ˚C in the dark for 24 h, the cells that were identical to those observed before the 24-h dark incubation were viewed and micrographs were taken again.

For the commitment assay of *C. merolae* and *G. sulphuraria*, 400 μL of respective collected culture was transferred into a chamber (100 mm^2) of an 8-well chambered polymer slide (μ-slide; ibidi GmbH, Germany). The chambered polymer slide was maintained at 42°C by a Thermo Plate (Tokai-hit, Japan) connected to the stage of an inverted microscope (IX71; Olympus). To immobilize the cells, the chambered slide was left for 30 min in order for cells to sediment and stick to the bottom of dish, and then micrographs of the cells were taken. After being incubated in the dark at 42˚C for 24 h, micrographs of the same areas were taken again and the identical cells were observed. The occurrence of cell division was determined based on the comparisons of cell micrographs before and after the 24-h dark incubation on the chambered polymer slide. Cell volume before and after cell division was calculated as an ellipsoid volume [$4/3\pi(l/2)(w/2)^2$; l = length; w = width].

3.2.3 DAPI staining and microscopy

To visualize nuclei, 500 μL of culture was fixed by the addition of glutaraldehyde to give a final concentration of 0.35%, then incubated at room temperature for 10 min. The fixed cells were stained with 1 μg mL^{-1} DAPI, and observed by an epifluorescence microscope (BX51; Olympus).

3.2.4 Analysis of cell size and cell number

The method for determination of cell volumes from micrograph for the commitment assay was described above. For other assays, cells were first fixed with 0.35% glutaraldehyde and then cell number and cell volume were analyzed with a Coulter Counter (Z2, Beckman Coulter).

3.2.5 Quantitative reverse transcription PCR (qRT-PCR).

Cells were harvested from the 5-mL culture by centrifugation at 1,000 *g* for 5 min at 4°C and then stored at –80˚C until RNA extraction. To extract RNA, the cell pellet was resuspended in 700 µL of SDS-EB (50 mM Tris-HCl, pH 8.0, 5 mM EDTA, 0.5 % SDS). The same volumes of PCI (phenol: chloroform: isoamyl alcohol, 25: 24: 1) and glass beads (425–600 µm) were then added and homogenized by vigorous shaking at 4 °C for 10 min. After centrifugation at 10,000 *g* for 5 min at 4 °C, the aqueous phase was collected, and the same volume of PCI was added. After another vigorous shaking for 2 minutes, the homogenate was centrifuged, the aqueous phase was collected and mixed with the same volume of chloroform. After centrifugation, the aqueous phase was collected once more, and mixed with the equal volume of isopropanol. Another centrifugation at 15,000 *g* was carried out for 15 min to collect pellet, which was washed with 70 % ethanol, dried, and resuspended in RNase-free water. The sample was further treated with DNase I (2270A; Takara Bio) according to manufacturer instruction.

The qPCR amplification of *MCM2* (accession number: XM_005708777.1) and *PCNA* (accession number: XM_005705453.1) were performed with an 1/500 aliquot of cDNA prepared from 1 µg of total RNA for each sample and *DRP3* (accession number: XM_005706881.1) was utilized as an internal control. Power SYBR Green PCR Master Mix (Applied Biosystems) was used in a real-time PCR system (StepOne Plus; Applied Biosystems). The primers used are listed in Table 3.1.

3.2.5 Immunoblot analyses

Cells were harvested from 2 mL of culture by centrifugation at 1,000 *g* for 5 min at 4˚C and then stored at –80 ˚C until next step. The harvested cells were resuspended in SDS-PAGE

sample buffer (50 mM Tris-HCl, pH 6.8, 10% glycerol, 2% SDS, 5% 2-mercaptoethanol, 0.01 % bromophenol blue) and protein concentration was determined with an XL-Bradford protein assay kit (APRO Science, Japan). For *Cy. caldarium*, cells resuspended in the SDS-PAGE sample buffer were homogenized with the same volume of glass beads (425–600 μm) in a bead crusher (3,200 r min^{-1}, 1 min, 4°C; μT-12; Titec, Japan) to disrupt cell walls before the protein assay. Total cellular protein of 3 μg for each sample was separated in different lanes by SDS-PAGE and then transferred onto a polyvinylidene difluoride (PVDF) membrane (Immobilon; Millipore). Membrane blocking, antibody reactions, and signal detection were performed as previously described (Fujiwara et al., 2020). An anti-HA monoclonal antibody (1 μg mL^{-1}; clone 16B12, BioLegend) was used to detect HA-CDKA protein. An anti-alpha-tubulin monoclonal antibody (1 μg mL^{-1}; clone B-5-1-2, Sigma), an anti-histone H3 phosphorylated at serine 10 (H3S10ph) polyclonal antibody (1 μg/mL; 06-570, Millipore), and an anti-FtsZ2-1 polyclonal antibody (0.1 μg mL^{-1}; raised against *C. merolae* FtsZ2-1) (Sumiya et al., 2016) were used as the primary antibodies for detection of cell cycle markers.

3.3 Results

3.3.1 Properties of *G. sulphuraria* synchronous culture

In order to examine the minimum number of cell divisions without intervening cell growth and the cell size for commitment to cell division in *C. merolae*, *Cy. caldarium* and *G. sulphuraria*, commitment assays were performed, similar to those applied in the green algae *C. reinhardtii* (Fang et al., 2006; Umen and Goodenough, 2001), *T. socialis*, and *G. pectorale* (Chapter 2) at first. During the commitment assays, cells that grown in light by photosynthesis in an inorganic photoautotrophic medium were immobilized on either gellan gum or chambered polymer slide and moved to the dark to stop further cellular growth. During the dark incubation, cells were expected to complete cell division if they had grown beyond the threshold size for cell division and passed the commitment point, before they were incubated in the dark. However, in my initial trial, very few *G. sulphuraria* cells underwent cell division during dark incubation, thus its threshold cell size for commitment or the minimum number of successive cell divisions could not be reliably determined. To

overcome this issue, synchronous culture was prepared for the commitment assay of all analyzed species, in order to enrich the cells around the commitment point.

The cell cycle of several species of algae is synchronized under 24-h light and dark cycle (Johnson, 2010). Previous studies have also shown that the cell cycles of *C. merolae* and *Cy. caldarium* can be synchronized with a 12-h light/12-h dark cycle. Under the LD, *C. merolae* cells predominantly divide during the dark period (Miyagishima et al., 2014). *Cy. caldarium* cells while predominantly undergo the first cell division late in the light period producing two autospores and followed by the second cell division occurs predominantly during the dark period producing four autospores in mother cells (Takahara et al., 2000). However, the cell cycle synchronization in *G. sulphuraria* has not yet been reported. Thus, *G. sulphuraria* was cultured in an inorganic medium under the LD in this study to first assess the cell cycle synchronization.

Throughout the LD, majority (85~90%) of *G. sulphuraria* cells were in the one-cell stage and only 10 to 15 % of the cells contained two to eight autospores (2- to 8-cell stages; Fig. 3.1A). The term autospores refer to divided cells formed within a mother cell wall and have not yet hatch out, while the terms daughter cells generally refer those hatched out from the mother cell (or produced by binary fission as in *C. merolae*). *G. sulphuraria* cells with 16 autospores were occasionally observed, but the percentage was much lower than those of two to eight autospores. Although the overall percentage of cells with autospores was relatively low throughout the LD, the progression of successive cell divisions in *G. sulphuraria* can be implied from temporal changes in the percentage. The percentage of cells with eight autospores (8-cell stage) decreased during the 0 h to 12 h (onset of the light period is defined as the 0 h), while no increase in the percentage of cells with 16 autospores (16-cell stage) observed during the same period, and instead those in one-cell stage increased (Fig. 3.1A), indicating the cells with eight autospores should have hatched out as unicellular daughter cells during this light period from the 0 h to 12 h. On the other hand, the percentage of cells with two autospores (2-cell stage) which refers to cells that initiated their first round of successive cell divisions peaked around the 16 h to 20 h and decreased afterward. As the percentage of cells with two autospores decreased, the cells with eight autospores which completed three rounds of successive cell division while showed to increase and reached the

highest percentage at the 24 h (Fig. 3.1A), suggesting the cells with two autospores progressed into eight autospores with successive cell divisions (Fig. 3.1A). In addition, the qRT-PCR showed that the S-phase marker genes, *PCNA* and *MCM2*, exhibited a 24-h periodic expression pattern with the highest level observed from the 8 h to 16 h of the LD (Fig. 3.1B). Collectively, these observations suggest a certain portion (10 to 15%) of *G. sulphuraria* cells cultured in inorganic medium under the LD, synchronously underwent successive cell divisions, mostly forming four or eight autospores, although majority of the cells did not divide and stayed in the one-cell stage throughout the LD. For the small portion of cells (which did not stay in one-cell stage), the cell division likely started before the 16 h and completed before the 24 h.

3.3.2 Number of cell divisions in *C. merolae, Cy. caldarium,* and *G. sulphuraria* after commitment

To examine the number of (successive) cell divisions and the commitment cell size in *C. merolae, Cy. caldarium* and *G. sulphuraria*, commitment assays were performed using cells collected from synchronous culture prepared under LD. Timings at which the cells collected were different among species, with most cells were at G1 phase when they are collected and the timings were approximately 2 h before most cell divisions occur (based on preliminary analysis), at the 8 h, 9 h, and 5.5 h of LD respectively for *C. merolae, Cy. caldarium* and *G. sulphuraria* (Fig. 3.2). Hence, majority of cells collected were in pre-cell division stage but had grown under light (for some time). The collected cells were immobilized on gellan gum or chambered polymer slide as described below and subjected to 24-h dark incubation to stop further cellular growth. The identical areas were observed before and after the 24-h dark incubation by microscopy to determine whether individual cells divided during the dark incubation.

To immobilize *Cy. caldarium*, the cells were sandwiched between a glass bottom dish and a piece of thin gellan gum containing the inorganic medium (Fig. 3.2A). As a result, the cells stopped cellular growth in the dark and some cells successfully completed cell division. When the same procedure was applied to *G. sulphuraria*, the cells however continued to grow even in the dark unlike the *Cy. caldarium.* This growth under dark was

also observed when agar was used instead of gellan gum. At this point, it is unclear on how the *G. sulphuraria* cells grew in the dark on the gellan gam or agar solidified inorganic medium. Both *C. merolae* and *Cy. caldarium* are obligate photoautotroph, however *G. sulphuraria* is capable of heterotrophic growth and can assimilate more than 50 different carbon sources such as sugars and sugar alcohols (Gross and Oesterhelt, 1999; Gross and Schnarrenberger, 1995; Rigano et al., 1977; Rigano et al., 1976), hence *G. sulphuraria* cells likely have grown heterotrophically by assimilating gellan gum and agar in this assay. Regarding *C. merolae* cells sandwiched between the glass and gellan gum, the cell division was arrested at various stages before completion, likely caused by its lack of cell wall compared to the other two species (Albertano et al., 2000; Kuroiwa et al., 2018) and the pressure of being sandwiched could have damaged the cells. Due to these limitations, *G. sulphuraria* and *C. merolae* cells were immobilized by settling down and sticking to the bottom of chambered polymer slide containing inorganic liquid medium, and the chambered slide was incubated in the dark on the stage of an inverted microscope. Under these conditions, *G. sulphuraria* and *C. merolae* cells which successfully completed cell division without cell growth in the dark, were observed. However, most daughter cells of *G. sulphuraria* flowed away after they hatched out as from the mother cell and for the small proportion of daughter cells that remained in place they usually surrounded or attached with the remaining mother cell wall (Fig. 3.2A), while *C. merolae* cells mostly stayed in place after they settled down to the bottom of the slide whether they divide in the dark.

C. merolae cells that were pre-cell division at the onset of the dark incubation either did not divide or divided into two daughter cells, after the 24-h dark incubation (Fig. 3.2A). *Cy. caldarium* cells in one-cell stage (i.e. before the first cell division) at the onset of the dark incubation either stayed in this stage, or produced four autospores after the dark incubation (Fig. 3.2A). In the case of *G. sulphuraria*, one-cell stage cells at the onset of the dark incubation either stayed in one-cell stage, or produced four or eight autospores after the dark incubation (Fig. 3.2A). After the dark incubation, no cell with two autospores was observed in both *Cy. caldarium* and *G. sulphuraria*, indicating they always underwent two or more successive cell divisions without intervening cellular growth whenever cell division initiated.

In the commitment assays of *Cy. caldarium* performed on gellan gum, the daughter cells stayed in place after hatching out of the mother cell (indicated by arrows in Fig. 3.2A). In contrast, in the case of *G. sulphuraria*, most of the daughter cells flowed away upon hatching, as described above. In some cases, one or two daughter cells were remained in place as trapped by the remnants of mother cell wall (indicated by the arrow in Fig. 3.2A, different from autospores which have smooth round mother cell wall). For this reason, the number of cell divisions which *G. sulphuraria* underwent during the dark incubation was determined based on the number of autospores formed in cells that remained in place, omitting the hatched-out cells.

3.3.3 Cell size for commitment to cell division in *C. merolae, Cy. caldarium,* and *G. sulphuraria*

In order to determine the cell sizes at which cells are committed to cell division, the volumes of *C. merolae, Cy. caldarium* and *G. sulphuraria* cells before the 24-h dark incubation of commitment assays were first determined. Among these cells, those that committed to cell division during dark (arrowheads in Fig. 3.2A) were identified from the micrograph and their average cell volumes of was calculated as committed cell volumes (Fig. 3.2C). The volumes of daughter cells produced by cell division after the dark incubation were also determined (for *Cy. caldarium,* and *G. sulphuraria,* the volumes of daughter cell were determined from unicellular cells that hatched out from the mother cell during the dark) (Fig. 3.2C). Cell volumes of the same number (n = 100 each) of committed cells and non-committed cells were measured and shown in the histogram (Fig. 3.2C). It should be noted that the histograms did not represent the overall distribution of cell volumes or the actual percentage of committed cells in each culture.

The results showed that *C. merolae* had a commitment cell size that was close to twofold of the average daughter cell volume (2.4-fold; Fig. 3.2B, C). In contrast, *Cy. caldarium* which always underwent two successive cell divisions to produce four autospores whenever cell division initiated, had a commitment cell size that was roughly equal to fourfold of the average daughter cell volume (3.6-fold; Fig. 3.2B, C). On the other hand, *G. sulphuraria* which always underwent two or three successive cell divisions to produce four

or eight autospores whenever cell division occurs, committed to cell division at cell size that was about sevenfold of the average daughter cell volume (6.7-fold; Fig. 3.2B, C). These results indicate that there is a correlation between the number of (successive) cell divisions, and the commitment cell size among cyanidialean red algae: two times the average newly born daughter cell volume for *C. merolae* which proliferates by binary fission, four times for *Cy. caldarium* producing four autospores, and approximately 7 times for *G. sulphuraria* producing four or eight autospores.

3.3.4 *C. merolae* and *Cy. caldarium* commit to cell division at late G1 phase

Previous studies have shown that the commitment point lies before the G1/S transition in the volvocine green algae, *C. reinhardtii* (Cross and Umen, 2015; Umen, 2018), *T. socialis* and *G. pectorale* (Chapter 2). In order to examine whether this is also the case for cyanidialean red algae, *C. merolae* and *Cy. caldarium* cells were synchronized by subjecting them to the LD. Temporal changes in the percentage of committed cells (by the commitment assay described above), and levels of S- and M-phase marker proteins in the culture (by immunoblotting) were determined (Fig. 3.3). This analysis was not performed for *G. sulphuraria* since very little cells underwent cell divisions under the LD (Fig. 3.1), and thus the changes in the percentage of committed cell for this species was not able to be determined reliably.

In the synchronous culture of *C. merolae* under the LD, the percentage of committed was highest at the 10 h (~50%; Fig. 3.3A). The levels of alpha-tubulin, which is expressed specifically during the S and M phases in *C. merolae* (Fujiwara, Tanaka, et al., 2013), and the M-phase marker H3S10ph (Fujiwara, Tanaka, et al., 2013), while peaked at the 14 h (Fig. 3.3C). On the other hand, the committed cells were at the highest percentage at the 10 h in the synchronous culture of *Cy. caldarium* under the LD (5–7%; Fig. 3.3B). To examine the cell cycle progression in *Cy. caldarium*, the expression pattern of FtsZ, a chloroplast division protein expressed specifically during the S phase in eukaryotic algae, was determined (Miyagishima et al., 2012), instead of H3S10ph. This difference was due to the limitation of H3S10ph antibody, which did not show a clear band in the immunoblotting of *Cy. caldarium* total proteins. The levels of FtsZ and alpha-tubulin peaked at the 12 h and 14 h respectively

of the LD for *Cy. caldarium* (Fig. 3.3D). Thus, both in *C. merolae* and *Cy. caldarium,* the commitment point is earlier than G1/S transition as in volvocine green algae.

3.3.5 Abnormally enlarged *C. merolae* cells undergo two or more cell divisions without intervening cellular growth

The results above suggest that the difference in the number of successive cell divisions without intervening cellular growth probably resulted from the difference in the cell size at which cell commits to first round of cell division. In addition, our results suggest that cell size is monitored (committed) late in G1 phase in *C. merolae* and *Cy. caldarium*. Based on these considerations, we experimentally tested whether cell size is a major determining factor for the onset of cell division and the number of cell divisions that occur. If this assumption is correct, then a *C. merolae* cell with a twofold of its usual cell size for division should undergoes two successive cell divisions without intervening growth, as in *Cy. caldarium*, as long as the cell has grown more than fourfold in size during G1 phase.

In order to generate such abnormally enlarged G1 cells of *C. merolae*, we used a previously generated *CDKA*-cKD line in which the endogenous *CDKA* transcription is turned on or off by replacing the inorganic nitrogen source in the medium (Fujiwara et al., 2020). In mammalian cells, the complex of G1 cyclin and CDK regulates the G1/S transition (Lim and Kaldis, 2013). Similarly, in plants and eukaryotic algae, the G1 cyclin and CDKA complex is responsible for the G1/S phase transition (Vandepoele et al., 2002). In the *CDKA*-cKD strain, nitrate reductase (*NR*) promoter was inserted to the chromosomal *CDKA* locus so that *CDKA* transcription, and thus G1/S transition (but not cellular growth) was inhibited in the presence of NH_4^+ in the medium (Fujiwara et al., 2020) (Fig. 3.4A). To detect CDKA protein with an anti-HA antibody, an *HA*-coding sequence was also inserted just after the start codon of *CDKA* (Fujiwara et al., 2020) (Fig. 3.4A).

When *CDKA*-cKD cells of a stock culture maintained in the NO_3^- medium (*NR* promoter on) (Fig. 3.4B-I, stage i) were inoculated into the NH_4^+ medium (*NR* promoter off) and cultured under light for 3 days (Fig. 3.4B-I, stage ii), CDKA protein was mostly depleted from the cells, and the M-phase marker H3S10Ph was no longer detected (Fig. 3.4C, stage ii). In addition, the cells were abnormally enlarged with their average cell size reached

approximately elevenfold of the average cell size before *CDKA* knockdown (Fig. 3.4D-F, stage i to ii; 4.4 to 47.9 μm^3). These enlarged cells contained single cup-shaped chloroplasts, which indicates that the cells are at G1 phase (Fujiwara, Tanaka, et al., 2013) (Fig. 3.4D, stage ii). Although the cells were enlarged, the intensity and size of the DAPI-stained nucleus after CDKA depletion (Fig. 3.4E, stage ii) was equivalent to those before CDKA depletion (Fig. 3.4E, stage i). These observations indicate abnormally enlarged *CDKA*-cKD cells that were arrested at G1 phase, were successfully obtained.

The enlarged CDKA-depleted cells were transferred to the NO_3^- medium (*NR* promoter on; cells in the NH_4^+ medium was centrifuged and the cell pellets were resuspended in the same volume of the NO_3^- medium) and cultured for 12 h under light to re-express CDKA protein (Fig. 3.4B-I, stage iii). After the 12-h light (Fig. 3.4 stage ii to iii), CDKA and the M-phase marker H3S10ph proteins accumulated in the culture (Fig. 3.4C, stage iii), and some cells contained a dividing chloroplast or two already-divided chloroplasts, which are indicative of the S and M phases, respectively (Fujiwara, Tanaka, et al., 2013; Miyagishima et al., 2012) (Fig. 3.4D, stage iii). During this CDKA-recovery phase (Fig. 3.4B, stage ii to iii), the cell number increased for approximately twofold (Fig. 3.4G, stages ii to iii), suggesting the cells underwent one round of cell division on average. Even though the average cell size was reduced due to cell division, it was still 6.4-fold larger than the average cell size before CDKA depletion (Fig. 3.4D and F, iii vs. i).

The enlarged *CDKA*-cKD cells, in which CDKA had been re-expressed in the light (Fig. 3.4B-I, stages iii), were then transferred to the dark to stop further cellular growth and cultured for 24 h (Fig. 3.4B-I, stages iii to iv). During the 24-h dark, no cellular growth occurred, as evidenced by the no increase in the total cellular protein concentration of the culture was observed (Fig. 3.4I, stages iii to iv), and the cell number increased 3.3-fold, while the mean cell size decreased (Fig. 3.4F, G, stages iii to iv). After the 24-h dark, CDKA level substantially decreased, and the M-phase marker, H3S10ph almost disappeared in the culture (Fig. 3.4C, stage iv). The cells became nearly equal in size to the cells before *CDKA* knockdown (Fig. 3.4D, F, stages iv vs. i), and most of the cells contained single, cup-shaped chloroplasts (Fig. 3.4D, stage iv), which is indicative of the G1 phase. Thus, the cells completed cell division by the end of the 24-h dark (Fig. 3.4B-I, stage iv).

The 3.3-fold increase in cell number without cellular growth during the 24-h dark (Fig. 3.4F, G, stages iii to iv) suggests that a certain portion of the cells underwent two rounds of cell divisions, without intervening cellular growth. During the preceding stage of CDKA recovery, the total cellular proteins in the culture increased approximately 1.2-fold by photosynthetic cellular growth under the 12-h light, (Fig 3.4I, stages ii to iii), and this level was sustained during the subsequent 24-h dark (Fig 3.4I, stages iii to iv). The cell number, whereas increased approximately 6.8-fold during the 12-h light and the subsequent 24-h dark (Fig 3.4B, F, ii to iv), suggesting a certain portion of the cells even underwent three rounds of cell divisions, accompanied with approximately 1.2-fold cellular growth. Thus, these results suggest (i) *C. merolae* cells undergo cell division (enter S phase) if the cell size is sufficient, regardless of prior growth history (i.e., light or dark in photoautotrophic conditions), and (ii) *C. merolae* cells with a cell size of more than fourfold or eightfold of the daughter cells divide two or three times respectively, without intervening cellular growth.

In this assay, the total cell volume in the culture decreased slightly during the 24-h dark period (Fig. 3.4H, stages iii to iv), accompanied with little change in the level of total protein (Fig. 3.4I, stages iii to iv). This decrease in total cell volume was probably due to the consumption of starch granules in cells as an energy source in the dark (Edmundson and Huesemann, 2015; Vitova et al., 2011).

3.3.6 Comparison on progression of successive cell divisions between *Cy. caldarium* and abnormally enlarged *C. merolae* cells

The abnormally enlarged *C. merolae* cells underwent two or more rounds of cell divisions without intervening growth, which resembles the cell division of *Cy. caldarium*. The time-course of successive cell divisions was compared between *Cy. caldarium* and the abnormally enlarged *C. merolae.* To this end, *C. merolae CDKA*-cKD cells were inoculated into the NH_4^+ medium and cultured for three days in the light same as previous assay to deplete CDKA, then incubated in the dark for 12 h, before transferring to the NO_3^- medium for CDKA recovery, and cultured under the LD to synchronize cell cycle progression (Fig. 3.5A, C, E). For comparison, *Cy. caldarium* was also cultured in the same conditions (Fig. 3.5B, D, F).

Under the LD, the cell number of *C. merolae CDKA*-cKD predominantly increased during the dark period (Fig. 3.5C). *Cy. caldarium* cultured in LD while exhibited a 24-h rhythm in the percentages of cells with two autospores (2-cell stage) and four autospores (4-cell stage) (Fig. 3.5G). Both observations indicate the cell cycle progression was successfully synchronized in these cultures. In the *Cy. caldarium* LD culture, the cell number increased during the light period (Fig. 3.5D; cell number was determined with a Coulter Counter). Since the cells with autospores in a mother cell (e.g. 2-cell and 4-cell stage) were as counted one cell, the observed increase in cell number indicated the autospores predominantly hatched out early in the light period, as in the case of *G. sulphuraria* (Fig. 3.1A).

In the *C. merolae CDKA*-cKD LD culture, the cell number increased approximately 2.6-fold during the first dark period (Fig. 3.5C; in both the two independent cultures performed on different days), indicating that a certain portion of the cells underwent two rounds of cell division during this time period, without further cellular growth. In a similar manner, *Cy. caldarium* cells with two autospores (2-cell stage as in Fig. 3.5G) peaked around the end of light period (12–16 and 26–40 h), while those with four autospores (4-cell stage as in Fig. 3.5G) peaked late in the dark period (20–24 and 44–48 h) in each round of LD (Fig. 3.5C). Thus, *Cy. caldarium* also completed two rounds of cell divisions within one round of LD. Although the cells completed two successive cell divisions during one round of LD, the increase in cell number was 1.53/1.81-fold and 1.91/2.16-fold during the first and second LD respectively (replicate 1/replicate 2; two independent cultures performed on different days), which both were less than fourfold (Fig. 3.5D). This observation probably indicates some cells were not committed to cell division and likely stayed at one cell stage throughout the entire round of LD, as was observed in the *G. sulphuraria* LD culture (Fig. 3.1), because their cell size did not reach the commitment size for cell division.

In the *C. merolae CDKA*-cKD LD culture, the mean cell size at the end of the first round of LD was still more than twofold of the initial cell size before the *CDKA* knockdown (Fig. 3.5A), and the mean cell size again decreased during the second round of LD, to a cell size that was almost equal to the initial cell size (Fig. 3.5A). Thus, the cells might not perform all possible (permitted) rounds of cell divisions within the first round of LD. However, as the mean cell volume in the *Cy. caldarium* culture, which completed two cell divisions during

every round of LD, also continually decreased in the culture (Fig. 3.5B). Thus, possibility that the decrease in cell volume was not solely attributable to cell division, but also due to the change of the inorganic nitrogen source from NH_4^+ to NO_3^- in the cultures, cannot be completely ruled out.

3.4 Discussion

In this study, when *C. merolae* cells in the G1 phase were abnormally enlarged, they later underwent two or three rounds of cell division as in *Cy. caldarium* and *G. sulphuraria* (Figs. 3.4 and 3.5). These observations suggest that the mechanism of successive cell division is also conserved in *C. merolae*, and the number of successive cell divisions is regulated by cell size in *C. merolae*, as in the green alga *C. reinhardtii* (Craigie and Cavalier-Smith, 1982; Donnan and John, 1983). The cyanidialean red algae *C. merolae*, *Cy. caldarium* and *G. sulphuraria* were shown to divide into 2 cells, 4 cells (autospores), and 4 or 8 cells (autospores) respectively, and these species were committed to cell division when they reached a cell size of two-, four- and seven-fold of their daughter cells, respectively. These results suggest that the evolutionary changes in the commitment size for cell division probably resulted in the variation in number of successive cell divisions in cyanidialean red algae. Similar evolution was suggested to have occurred in volvocine green algae (Chapter 2), in which a *Chlamydomonas*-like unicellular ancestor evolved into multicellular species. Thus, regardless of unicellular (cyanidialean red algae) or multicellular (volvocine green algae) organisms, the evolutionary changes in commitment cell size, suggested to have occurred independently and resulted in variation of number of successive cell divisions.

Based on the topology of evolutionary trees, *Galdieria* spp. and *Cyanidium spp.* branched first in Cyanidiales, and the *C. merolae* emerged from a member of *Cyanidium spp.* (Toplin et al., 2008; Yoon et al., 2006). Thus, it is most likely that a reduction in commitment cell size, and number of cell divisions occurred in the evolution of *C. merolae*, which contrasts with the volvocine green algae, in which the commitment cell size increased during the course of evolution (Chapter 2). However, there is no information available to deduce how the common ancestor of Cyanidiales proliferated, and thus it is still unclear how the commitment cell size could have changed in the overall evolution of cyanidialean red algae.

In this study, *G. sulphuraria* 074W was cultured in an inorganic liquid medium, and majority of the cells produced four or eight autospores. Cells with 16 autospores were rare (Figs 3.1A and 3.2). This result contrasts with previous reports in which *Galdieria* spp. produce up to 32 autospores (Albertano et al., 2000; Merola et al., 2009). In another study using *G. sulphuraria* M-8, majority of the cells produced 16 autospores in an inorganic liquid medium (Kuroiwa et al., 1989). At this point, the reason for this difference in the number of autospores is unclear. It is likely due to differences in the strains of *Galdieria* spp. used, given that many strains have diverged during the last ~1 billion years (Toplin et al., 2008). In addition, *Galdieria* spp. are capable of mixotrophic and heterotrophic growth which different from *Cyanidium* spp. and *C. merolae* (Gross, 1999; Gross and Schnarrenberger, 1995; Rigano et al., 1977; Rigano et al., 1976), and hence their commitment cell size are likely to change depending on environment, and intracellular physiological state, as more 16-cell stage of *G. sulphuraria* cells were observed on gellan gum solidified medium than in the liquid medium.

In the synchronous cultures under the LD, the percentage of cells that underwent cell division was lowest in the *G. sulphuraria* culture, followed in order, by *Cy. caldarium* and *C. merolae* (Figs. 3.1 and 3.5). This observation can be explained by the differences in the commitment cell size among these three species, and the circadian regulation of the G1/S transition. In order to undergo the first round of cell division, a *C. merolae* cell only needs to grow until it becomes two-fold larger than its original cell size, while *Cy. caldarium* and *G. sulphuraria* need to grow until reaching four- and seven-fold in size respectively. The cellular growth rates of these three species were similar in the applied culture conditions using an inorganic medium; their cell sizes became approximately twofold in *C. merolae*, and 1.5-fold for *Cy. caldarium* and *G. sulphuraria* during the 12-h light (based on increase in total protein in each culture). Thus, the duration for a newly born (hatched out) daughter cell to grow to the commitment cell size should have been the longest for the *G. sulphuraria* culture, followed by *Cy. caldarium*, and then *C. merolae*. Under the LD, G1/S transition was inhibited early and in the middle of the light period (Miyagishima et al., 2014). Under this regulation, only cells that have reached the commitment cell size during the preceding light period underwent cell division during the dark period, and other cells stayed in the G1 phase

throughout that round of the LD. Thus, the duration of G1 phase under the LD is expected the longest for *G. sulphraria*, which corresponds to at least three rounds of LD plus another light period (based on 1.5-fold growth during one light period, and the requirement of sevenfold growth for the first cell division). In the case of *Cy. caldarium*, the estimated G1 period is at least two rounds of LD and another light period (based on 1.5-fold growth during one light period and the requirement of fourfold growth for the first cell division). In contrast, the estimated duration of G1 phase under the LD in *C. merolae* cells is approximately 12-h light (based on twofold growth during one light period, and the requirement of twofold growth for the first cell division).

The effects of both commitment cell size and circadian rhythm on cell division also explain, at least partly, the variation of cell sizes among G1 cells which have passed commitment in the three species of cyanidialean red algae, and the number of autospores formed in *G. sulphuraria* (i.e., four or eight) (Fig. 3.2). For example, under the LD, a certain cell reached the commitment size early in the light period, but stays in G1 phase with additional cell growth until the circadian gating of G1/S around evening. Another cell reached the commitment size late in the light period and immediately starts cell division during the dark period. Some other cells grown in size during the light period, but did not reached the commitment cell size, hence staying in the G1 phase during the subsequent dark period. The cell size is sustained during the dark period, and increases again during the next light period. Thus, cells can reach the threshold cell size anytime during the light period, but the timing of the first round of G1/S transition is limited to evening under the LD, resulting in variations in the duration of additional cell growth after commitment until the G1/S transition.

The multiple fission cell cycle allows a much greater temporal separation between the cell growth and cell division phases, and increases cell size variations in a population when compared to than binary fission (Cavalier-Smith, 1978). In this regard, growth phase durations and size variations decrease, in the order of *G. sulphuraria*, *Cy. caldarium*, and then *C. merolae*. Among the Cyanidiales, the most notable and distinct feature of *Galdieria* spp. is their ability to assimilate more than 50 different organic carbon sources, and grow both heterotrophically and mixotrophically in contrast to the obligate photoautotrophic

Cyanidium spp. and *C. merolae* (Barbier et al., 2005; Gross, 1999; Gross and Schnarrenberger, 1995; Oesterhelt et al., 1999; Rigano et al., 1977; Rigano et al., 1976). Cells of *Galdieria* spp. and *Cyanidium* spp. are surrounded by a rigid cell wall, which must be broken upon hatching of autospores (Albertano et al., 2000; Merola et al., 2009). In contrast, *C. merolae* cells lack cell walls (Albertano et al., 2000; Merola et al., 2009) and its genome does not encode extensive membrane transporters as in *G. sulphuraria* which likely help with regulation of osmotic pressure (Barbier et al., 2005). Although it is still unknown at present, the structural and physiological differences described might be related to the diversification of the modes of cell division among cyanidialean red algae.

For *C. merolae* and *Cy. caldarium* which undergoes binary fission and multiple fission respectively, the commitment point for cell division was suggested to be in the late G1 phase (Fig. 3.3). This is similar to the situation of various volvocine green algae that perform multiple fission in which cells are committed to cell division in the middle of or late in the G1 phase (Umen and Goodenough, 2001) (Chapter 2). In *C. reinhardtii*, there is a time lag of several hours between the commitment point and the G1/S transition (Umen, 2018). This was also the case for *C. merolae* and *Cy. caldarium* although the time lag was shorter than that in green alga *C. reinhardtii* (Fig. 3). As in *C. reinhardtii* (Olson et al., 2010; Umen, 2018), the RB-E2F-DP pathway was suggested to be involved in both the commitment and G1/S transition in *C. merolae* (Miyagishima et al., 2014). Because the artificial increase in the cell size at G1 phase was shown to be sufficient for *C. merolae* cells to perform two successive cell divisions, the mechanism for regulating commitment and G1/S transition based on the RB-E2F-DP pathway is a strong candidate for factors that could have been modified during evolution which resulted in the variation of number of successive cell divisions among cyanidialean red algae. This point is further discussed in the section of General discussion.

3.5 Figures and table

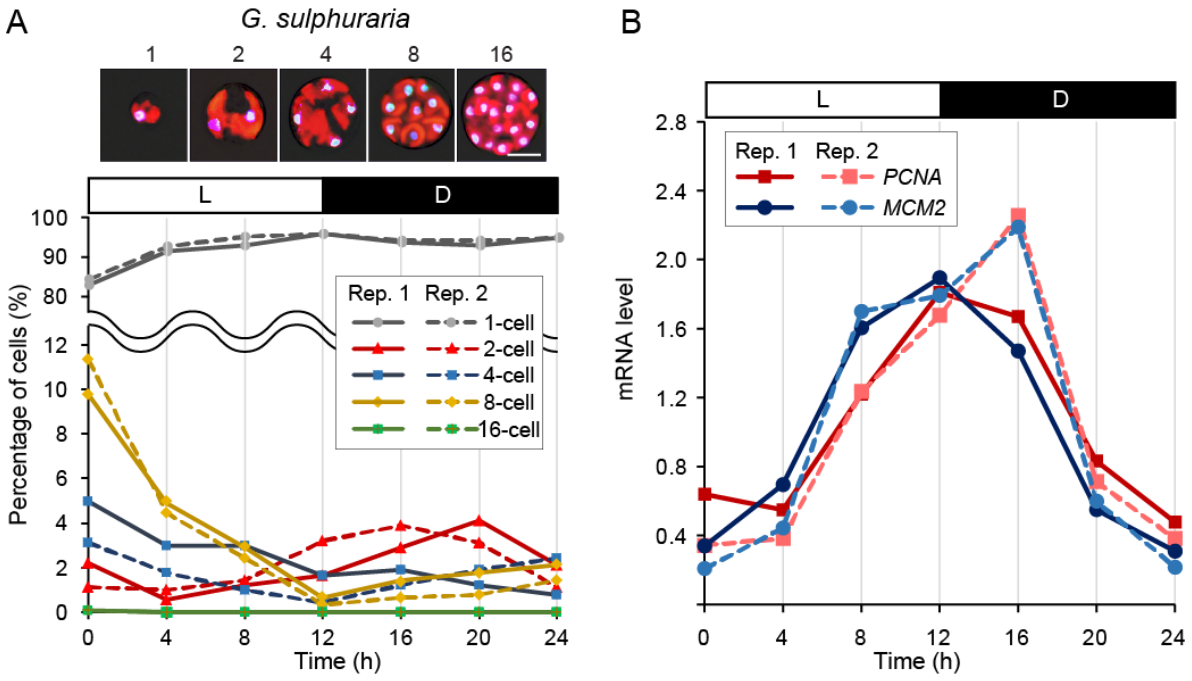

Figure 3.1. Evaluation of the synchrony of the *G. sulphuraria* cell cycle under the LD. *G. sulphuraria* cells cultured in an inorganic medium were subjected to the LD, and cells were examined during the third round of the LD. Cells were collected every 4 h (during the third round of LD; the onset of the light period was defined as the 0 h). Two independent analyses were carried out on cells cultured on different days under same condition and the results are shown as Rep.1 and Rep. 2. **(A)** Change in percentages of cells in respective stages (n = 300 cells for each time point). Cells were classified into five stages: 1, 2, 4, 8, and 16-cell stages, with 1-cell stage represents unicellular cells, and 2- to 16-cell stages represent two to 16 autospores in a mother cell respectively. Examples of images of DAPI-stained cells in respective stages are shown above the graph. Red is for chlorophyll fluorescence, and blue fluorescence is DAPI-stained DNA. Bar = 5 µm. **(B)** qRT-PCR analyses showing the change in mRNA levels of S-phase marker genes *PCNA* and *MCM2*. The values of *PCNA* and *MCM2* were normalized with that of an internal control *DRP3*.

A

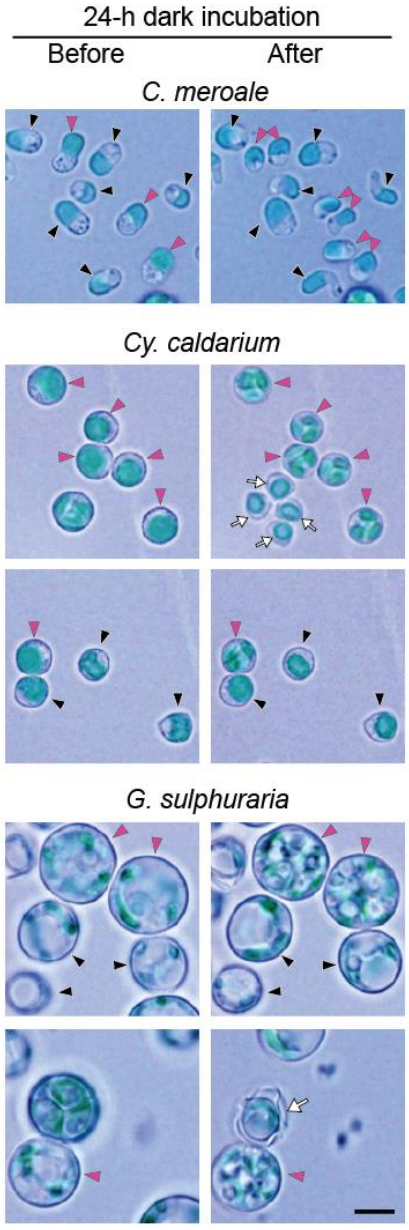

B

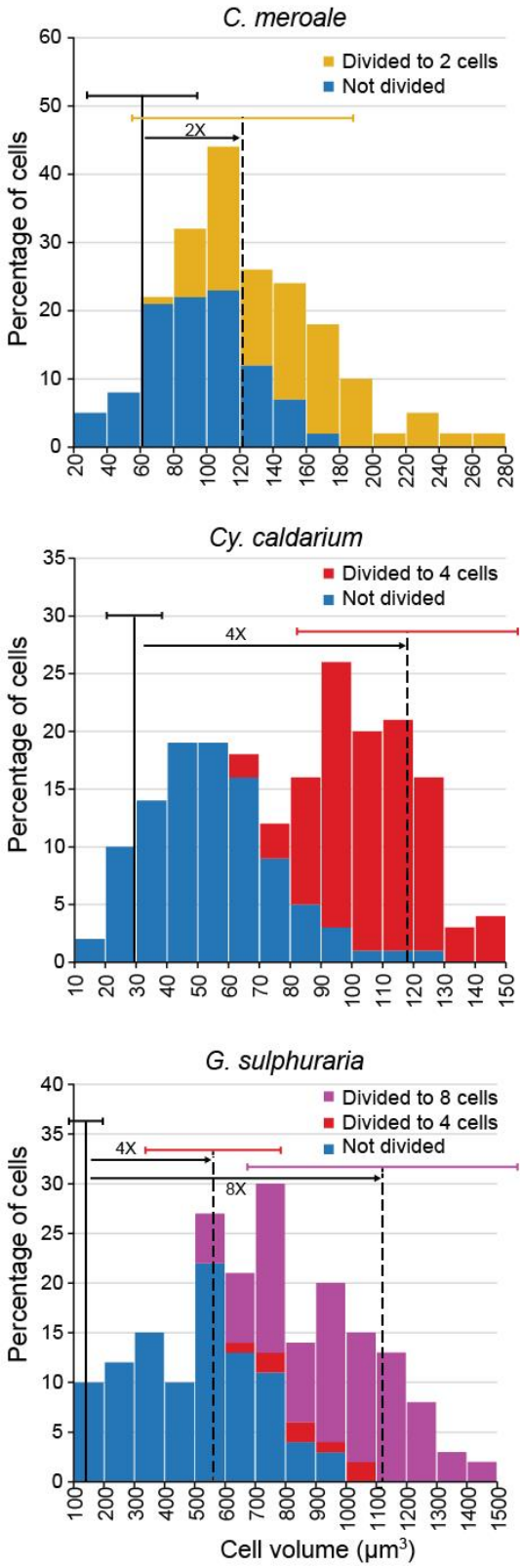

C

Species	*C. merolae*	*Cy. caldarium*	*G. sulphuraria*
Number of daughter cells (or autospores)	2	4	4 or 8 (7.7 ± 1.0)
Daughter cell volume (μm^3)	60.9 ± 33.2	29.5 ± 9.0	140.0 ± 55.8
Comitted cell volume (μm^3)	149.2 ± 44.5	107.2 ± 19.8	974.4 ± 311.9
Ratio	2.4	3.6	6.7

Figure 3.2. The relationship between the number of successive cell divisions and the ratio of cell size at commitment to cell size of newly produced daughters, in *C. merolae*, *Cy. caldarium* and *G. sulphuraria*. To determine the number of successive cell divisions, synchronized cells in an inorganic medium were collected at the 9 h of second round of LD for *C. merolae*, at the 8 h of third round of LD for *Cy. Caldarium*, and at the 5.5 h of the third round of LD for *G. sulphuraria.* The synchronous cultures of respective species at the indicated time points mainly contained G1 phase cells. The collected cells were subjected to 24-h dark incubation in a chambered polymer slide (µ-Slide; ibidi GmbH, Gräfelfing, Germany) for *C. merolae* and *G. sulphuraria*, or on a glass bottom dish covered with gellan gum containing the inorganic medium for *Cy. caldarium*. After immobilization, identical cells were observed by differential interference contrast microscopy before and after the 24-h dark incubation. **(A and B)** The sizes of cells before cell division (indicated by black and magenta arrowheads in **A**) were determined based on the microscopic images taken before the 24-h dark incubation, and are presented in the histogram **(B)**. Cells divided (black arrowheads in **A**) or not divided (magenta arrowheads in **A**) after the 24-h dark incubation are also determined and classified in the histogram **(B)**. The percentage of divided cells and the percentage of cells did not divide are calculated separately with each sum up to a hundred percent. For *Cy. caldarium* and *G. sulphuraria*, the white arrows indicate daughter cells that hatched out of from mother cell containing autospores. In the case of *Cy. caldarium,* hatched-out daughter cells remained in place, whereas, in the case of *G. sulphuraria*, majority of the daughter cells flowed away after hatching, and only a few daughter cells remained in place. The cell sizes after cell division(s) (shown as daughter cell volumes) were determined based on the microscopic images of cells that either hatched out of the mother cell in *Cy. caldarium* and *G. sulphuraria*, or divided in *C. merolae* (*n* = 100 cells for each species). Bar = 10 µm. **(C)** The average size of daughter cells and average size of committed cell (mother cells that divided after the dark incubation) are summarized. The number of daughter cells (autospores in the case of *Cy. caldarium* and *G. sulphuraria*) produced after the dark incubation and the cell size ratio of committed cell to daughter cell are also shown.

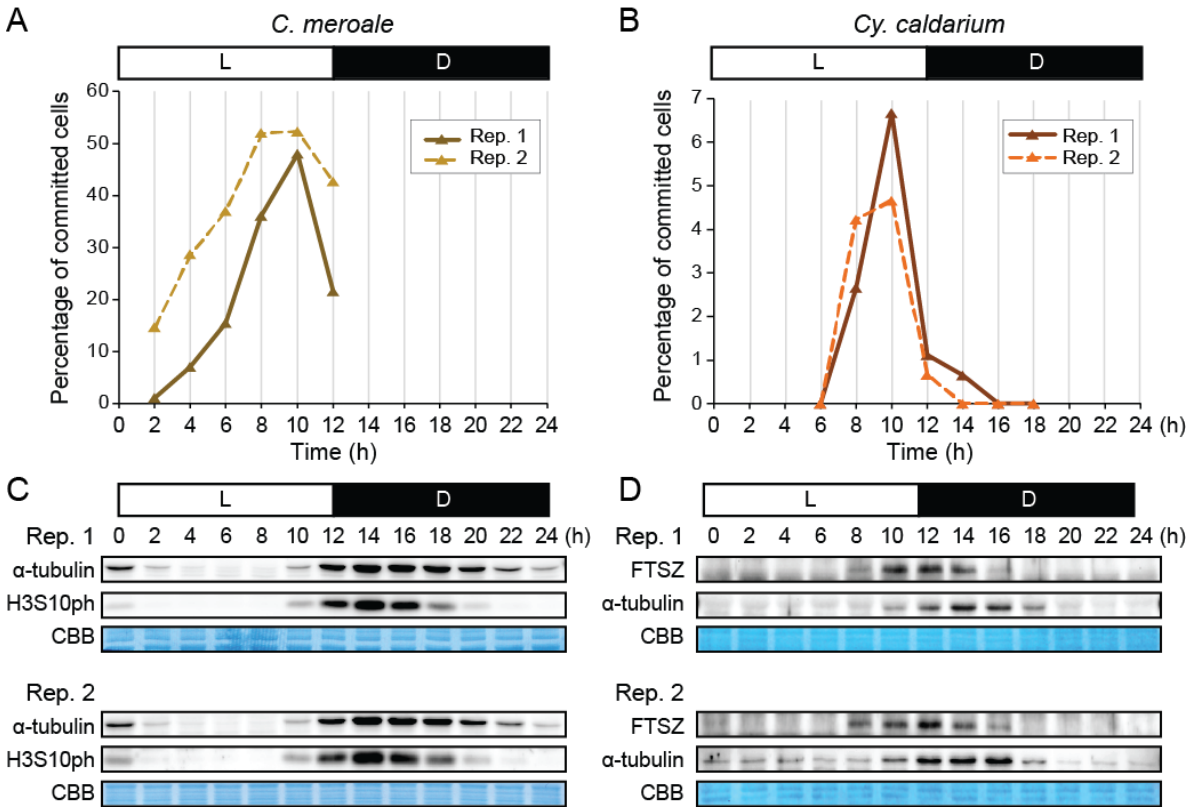

Figure 3.3 Changes in the percentage of committed cells, levels of S- and M-phase marker proteins in synchronous cultures of *C. merolae* and *Cy. caldarium* under the LD. The onset of the second and third round of the LD is defined as the 0 h in *C. merolae* and *Cy. caldarium*, respectively. The results of two independent analyses carried out on cells cultured on different days (Rep. 1 and Rep. 2) are shown. **(A and B)** Changes in the percentage of committed cells are indicated for *C. merolae* **(A)** and *Cy. caldarium* **(B)**. **(C** and **D)** Immunoblot analyses showing the change in the levels of the chloroplast division protein FtsZ2-1 (expressed specifically in S phase) (Miyagishima et al., 2012), alpha-tubulin (expressed specifically during S and M-phases in *C. merolae*) (Fujiwara, Tanaka, et al., 2013) and an M-phase marker H3S10ph (Fujiwara, Tanaka, et al., 2013) in *C. merolae* **(C)** and *Cy. caldarium* **(D)**. Gels stained with Coomassie Brilliant Blue (CBB) are shown as loading controls.

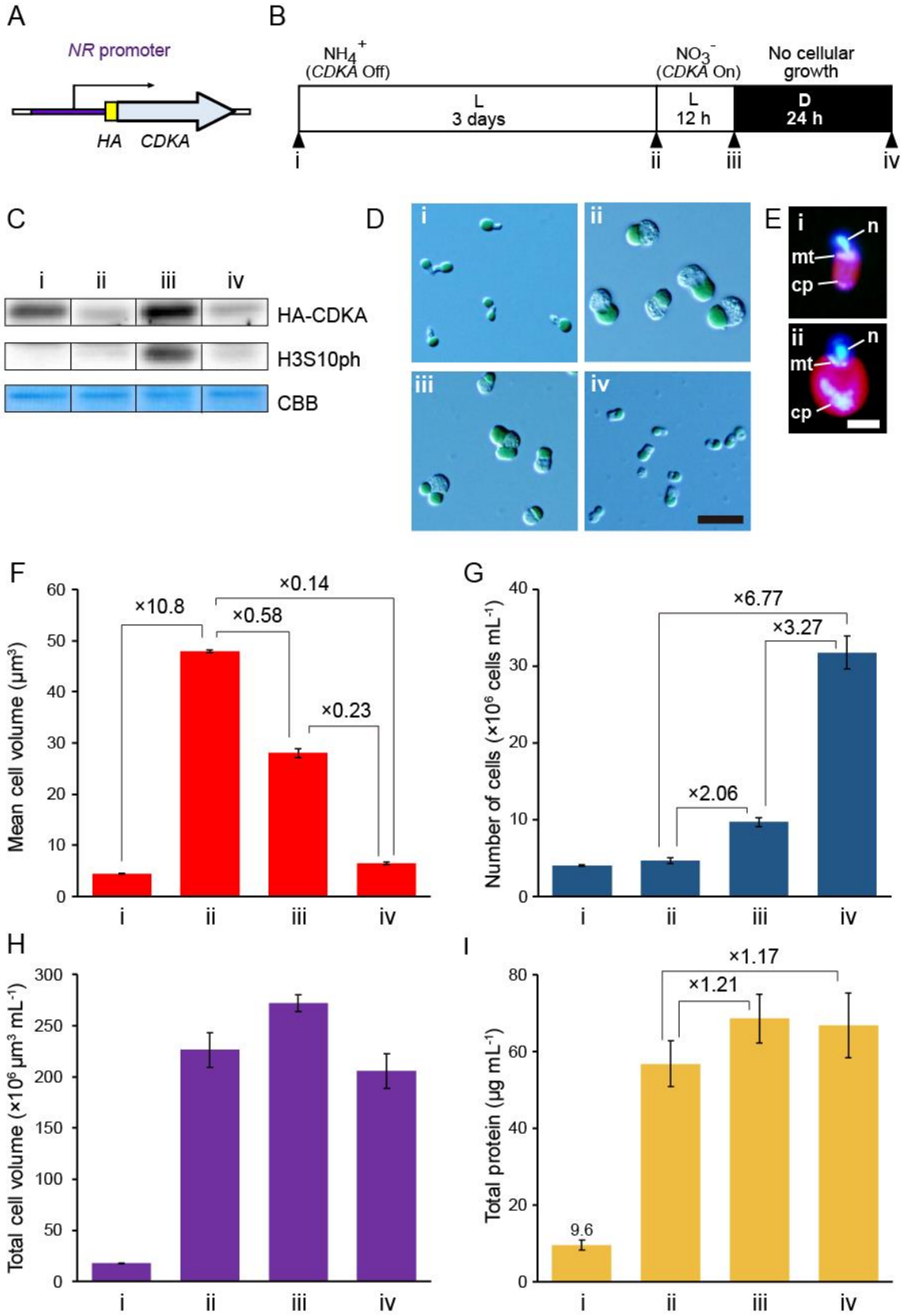
A
NR promoter
HA CDKA
B
NH4+ (CDKA Off)
NO3- (CDKA On)
No cellular growth
L 3 days
L 12 h
D 24 h
i
ii
iii
iv
C
i ii iii iv
HA-CDKA
H3S10ph
CBB
D
i
ii
iii
iv
E
i
n
mt
cp
ii
n
mt
cp
F
Mean cell volume (μm3)
×10.8
×0.58
×0.14
×0.23
i ii iii iv
G
Number of cells (×10^6 cells mL-1)
×6.77
×3.27
×2.06
i ii iii iv
H
Total cell volume (×10^6 μm3 mL-1)
i ii iii iv
I
Total protein (μg mL-1)
×1.17
×1.21
9.6
i ii iii iv

Figure 3.4. Multiple cell divisions without intervening cellular growth in abnormally enlarged *C. merolae* cells. To prepare a population of enlarged *C. merolae* cells, the G1/S transition was blocked while maintaining the cellular growth under conditional knockdown of *CDKA*. **(A)** A schematic illustration of the chromosomal *CDKA* locus in the *C. merolae CDKA*-cKD strain. A 3 × HA epitope–coding sequence and *NR* promoter were inserted to into the chromosomal *CDKA* locus, under which *HA-CDKA* expression could be activated or inactivated by the absence or presence of NH_4^+ in the medium (Fujiwara et al., 2020). **(B)** A schematic illustration of the culture conditions of *CDKA*-cKD cells and the timings at which cells were collected for the analyses shown in C and D. In order to support cellular growth in the absence of NH_4^+, the NH_4^+-depleted medium was supplemented with NO_3^- as an inorganic nitrogen source. A stock of *CDKA*-cKD cells cultured in an inorganic NO_3^- medium (*NR* promoter on) (i) was inoculated into the NH_4^+ medium (*NR* promoter off), and cultured in the light for 3 days to knock down *CDKA*, but allow the cells to keep growing without cell division (ii). To recover CDKA in the abnormally enlarged *CDKA*-cKD cells, the cells were transferred to the NO_3^- medium, and cultured in the light for 12 h (iii). Then, to stop cellular growth, the cells were transferred to the dark and cultured for 24 h (iv). **(C)** Immunoblot analyses showing the change in the levels of HA-CDKA and an M-phase marker, H3S10ph, during the culture. A gel stained with Coomassie Brilliant Blue (CBB) is shown as a loading control. **(D)** Differential interference contrast images of *CDKA*-cKD cells showing the change in the cellular size during the culture. Bar = 10 μm. **(E)** Fluorescent micrographs of DAPI-stained cells at time points (i) and (ii). Red is chlorophyll fluorescence, and blue fluorescence is DAPI-stained DNA. *n*, *mt* and *cp* indicate nuclear, mitochondrial and chloroplast DNA, respectively. Bar = 2 μm. **(F–I)** Changes in the mean cell volume **(F)**, cell density in the culture **(G)**, total cell volume in the culture **(H)**, and total cellular protein concentration in the culture **(I)** are shown. The cell volume and cell number were determined by Coulter Counter Z2. The bar represents the standard deviation of the three cultures prepared at the same time and cultured under same condition.

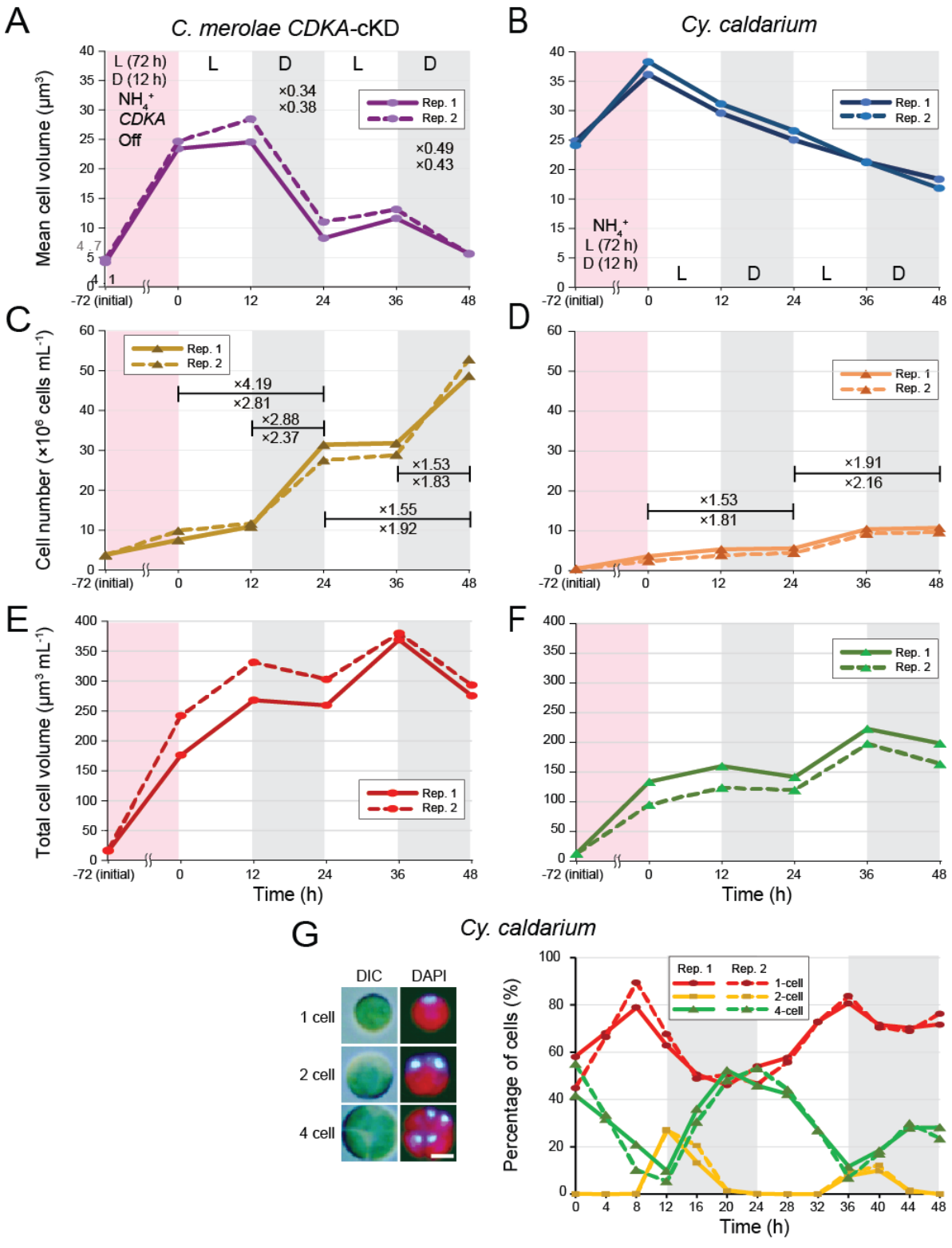
A
C. merolae CDKA-cKD
L (72 h)
D (12 h)
NH4+
CDKA
Off
L
D
L
D
×0.34
×0.38
×0.49
×0.43
Rep. 1
Rep. 2
Mean cell volume (μm3)
B
Cy. caldarium
NH4+
L (72 h)
D (12 h)
C
Cell number (×10^6 cells mL-1)
×4.19
×2.81
×2.88
×2.37
×1.53
×1.83
×1.55
×1.92
D
×1.53
×1.81
×1.91
×2.16
E
Total cell volume (μm3 mL-1)
F
-72 (initial)
Time (h)
G
Cy. caldarium
DIC
DAPI
1 cell
2 cell
4 cell
Percentage of cells (%)
1-cell
2-cell
4-cell

Figure 3.5. Comparison on progression of successive cell divisions between the abnormally enlarged *C. merolae* and the wild-type *Cy. caldarium*. **(A, C, E)** Progression of successive cell divisions in the abnormally enlarged *C. merolae* cells. *C. merolae CDKA*-cKD stock culture in the NO_3^- medium was inoculated into the NH_4^+ medium and cultured in the light for 3 days to knock down *CDKA*, and then subjected to dark for 12 h. The cells were later transferred to the NO_3^- medium to recover CDKA, and subjected to the LD. The changes in the mean cell volume **(A)**, cell number **(C)**, and total cell volume **(E)** are shown. **(B, D, F, G)** Progression of successive cell divisions in *Cy. caldarium*. *Cy. caldarium* was also cultured the same condition as *C. merolae CDKA*-cKD in **A**. The changes in the mean cell volume **(B)**, cell number **(D),** and total cell volume **(F)** are shown. The changes in percentages of cells in 1-, 2- and 4-cell stages in *Cy. caldarium* culture are also shown (n = 300 cells for each time point), representing unicellular cell, mother cell with two autospores and mother cell with four autospores respectively **(G)**. Examples of differential interference contrast (DIC) and DAPI-stained images of *Cy. caldarium* cells in respective stages are shown beside the graph. Red is chlorophyll fluorescence, and blue fluorescence is DAPI-stained DNA. Bar = 2 µm. The cell volume and cell number were determined by Coulter Counter Z2. For both *C. merolae CDKA*-cKD and *Cy. caldarium*, results of two independent cultures prepared on different days (Rep. 1 and Rep. 2) are shown.

Table 3.1

Primers used for qRT-PCR for *G. sulphuraria* in this study

Gene	Direction	Sequence (5’ to 3’)
PCNA	Forward	ACGTCTCTTTGGTTTCCATGGT
	Reverse	TCTTTGACAACGGAACATTTCG
MCM2	Forward	CGATATCAAAGGCTGGAATTGTT
	Reverse	GGGTTCGCTGCAGCTATTACA
DRP3	Forward	CAACGGGTCGTCCTTCCTT
	Reverse	TGAGGACCACTTCCAGTAGCATT

Chapter 4

Potential of G1 cyclin as a sizer protein in *C. merolae*

4.1 Introduction

How cell growth and cell division are coordinated, and how the cell growth or cell size is actually monitored are still mostly unknown. Three mechanisms (or behaviors) that are involved in cell size homeostasis however have been proposed – timer, sizer and adder (mainly observed in bacteria), which are mainly based on studies on binary fission cell cycle (Facchetti et al., 2017). To regulate cell size, cell division is suggested to occur at a defined timing in the timer model; or after achieving a critical size or commitment size in the sizer model, or after a fixed amount of cell growth in the adder model (Facchetti et al., 2017; Willis and Huang, 2017). The cell size homeostasis in multiple fission however need to consider also the influence of number of cell divisions. The number of cell divisions in multiple fission cell cycle was reported to either depend or correlate with cell size in green alga *C. reinhardtii* (Craigie and Cavalier-Smith, 1982; Donnan et al., 1985), and this phenomenon was also observed in various volvocine green algae and cyanidialean red algae in this study (Chapters 2 and 3). The timer behavior has also been reported in regulation of multiple fission (circadian gating of G1/S transition), however as cells are committed to cell division at different time points before the circadian gating of G1/S when the cells have grown to a certain threshold size (Chapters 2 and 3), sizer behavior is more prominent in regulation of multiple fission cell cycle in volvocine green algae and cyanidialean red alge.

Sizer behavior, in general involves cell-size sensing (Facchetti et al., 2017). Many studies have proposed that a cell monitors its size either through DNA content or concentration of a certain protein, although it is still difficult to elucidate how this actually works. One famous concept is nucleocytoplasmic (NC) ratio which generally considered as the ratio between nuclear size (or DNA content) and cell size. NC ratio was proposed to be constant in a cell type (Wilson, 1928) and this constancy has been observed in various unicellular and multicellular organisms (Cantwell and Nurse, 2019; Cavalier-Smith, 1978; Gregory, 2001). Cell size was suggested to scale positively with genome size with cells of

higher genomic size or DNA content generally have larger cell size (Cavalier-Smith, 1978; Gregory, 2001), as in polypoid cells with larger size. NC ratio has been shown to involve in cell size homeostasis as it regulates the termination of rapid cell divisions (multiple-fission-like cell cycle) during early embryogenesis of animals such as *Xenopus* (Newport and Kirschner, 1982) and *Drosophila* (Edgar et al., 1986), but the actual mechanisms are still unclear. NC ratio regulates the length of S phase probably through control of DNA replication (Murphy and Michael, 2013) and was shown to be able affect transcription of genes in different modes during embryogenesis (Syed et al., 2020). If this role of NC ratio is applicable to typical binary and multiple fission cell cycle, it may regulate the protein expression level to scale with cell size.

The scaling of cell size to concentration of certain proteins has also been suggested, which directly or indirectly involved in regulation of cell division. In the fission yeast, cell size checkpoint for cell division in G2 phase. In this case, the local concentrations of membrane protein Pom1 and/or Cdr2 at medial cortex, which correlate with cell length or surface area, have been proposed to promote cell division only when cells grow to a certain size (Bahler and Pringle, 1998; Bhatia et al., 2014; Facchetti et al., 2017; Martin and Berthelot-Grosjean, 2009; Pan et al., 2014). In the budding yeast, the cell size while is monitored in G1 phase for cell division. In this case, the progression into S phase has been suggested to be regulated through concentration of Cln3 (G1 cyclin) that scales with the cell size (Litsios et al., 2019). Cln3 is involved in the regulation of G1 progression through Start (commitment point) in the budding yeast, during which the complex of G1 cyclin Cln3 and a cyclin dependent kinase (Cdc28) phosphorylates/inactivates Whi5. This phosphorylation releases Whi5 from a transcription factor SBF, allowing transcription of S-phase genes by SBF to occur (Cooper, 2006; de Bruin et al., 2004).

Whi5, Cln3 and SBF in the budding yeast are believed to be functional homologs of RB and D-type cyclin (G1 cyclin), and E2F-DP transcription factor in animals (Cooper, 2006). RB, G1 cyclin and E2F-DP are also well conserved in other eukaryotic lineages and these factors were also shown to be involved in G1/S transition in the green alga *C. reinhartii* (Umen and Goodenough, 2001). Similar to *whi5* mutation in the budding yeast which led to smaller commitment size (Jorgensen et al., 2002), *rb* (*mat3*) mutation in *C. reinhardtii*

resulted in reduced commitment size (Umen and Goodenough, 2001). In addition, the mutation also increased number of cell divisions and hence RB suggested to involve in both the commitment point (mid G1 phase) and regulation of number of cell divisions (during S/M phase) in the multiple fission cell cycle of *C. reinhardtii* (Umen and Goodenough, 2001). However, whether the concentration of G1 cyclin scales with cell size in *C. reinhardtii* has not yet been examined. Instead, a protein known as CDKG1 has been suggested in a recent study, to function as a sizer in determining the number of successive cell divisions based on cell size of *C. reinhardtii*, probably through the RB-E2F-DP pathway (Li et al., 2016). CDKG1 is synthesized at late G1 phase (after commitment) and reached the highest level just prior to the S/M phase, with its concentration scales with the mother cell size (Li et al., 2016). It is suggested to be consumed in a stepwise manner by successive cell divisions until its level becomes insufficient for a further round of cell division (Li et al., 2016). However, this CDKG1 is specific to volvocine green algae and was shown to regulate only the number of successive cell divisions, but not to commitment point (Li et al., 2016), hence it is still unclear whether protein of similar function exists to regulate commitment and/or number of cell divisions among cyanidialean red algae.

The red alga *C. merolae* genome encodes homologs of RB, E2F, DP and potential G1 cyclin (CYCLIN 1; CYC1) (Miyagishima et al., 2014). A previous study showed that depletion of RB in *C. merolae* leads to small cell phenotype as in the green alga *C. reinhardtii* (Miyagishima et al., 2014). Thus, the RB-E2F-DP pathway in *C. merolae*, in which G1 cyclin-CDK complex phosphorylates RB, is probably involved in regulation of the commitment to cell division as in *C. reinhardtii*. Hence, CYC1 is a candidate for sizer protein in *C. merolae*. In this chapter, I have examined the changes in CYC1 level in *C. merolae* and showed that CYC1 protein accumulated during G1 phase when cell growth occurring in the light period of the 12-h light/12-h dark (LD) synchronous culture. My results also showed that, in the genetically modified abnormally enlarged *C. merolae* cells, CYC1 is likely degraded stepwisely along with the successive cell divisions. In addition, CYC1 overexpression during G1 phase resulted in earlier G1/S transition, similar to Cln3 overexpression in the budding yeast (Wijnen et al., 2002). These results strengthen the

possibility of CYC1 as a sizer regulating both commitment to cell division and number of successive cell divisions after G1/S transition.

4.2 Materials and methods

4.2.1 Algal culture

C. merolae transformants *CAT* (Fujiwara et al., 2015), *FLAG-CYC1*, HSp*FLAG-CYC1* were cultured in 2 × Allen's medium (an inorganic medium) (Allen, 1959). *FLAG-CYC1/CDKA*-cKD strain was maintained in MA2-NO_3, in which NH_4^+ was replaced with the same concentration of NO_3^- as the sole nitrogen source (20 mM $NaNO_3$, 20 mM Na_2SO_4, 8 mM H_2KPO_4, 4 mM $MgSO_4$, 1 mM $CaCl_2$, 2.8 μM $ZnCl_2$, 16 μM $MnCl_2$, 7.2 μM Na_2MoO_4, 1.28 μM $CuCl_2$, 0.68 μM $CoCl_2$, 100 μM $FeCl_3$, 72 μM EDTA-2Na; pH 2.3, adjusted with H_2SO_4) (Fujiwara et al., 2020). For *CDKA* knockdown assay, *FLAG-CYC1/CDKA*-cKD and the *FLAG-CYC1* (as a control) were inoculated into MA2-NH_4^+ medium (Minoda et al., 2004). The culture conditions for *CDKA* knockdown and CDKA recovery were same as in Chapter 2.3.1. Stock cultures of *C. merolae* 10D and *FLAG-CYC1/CDKA*-cKD were kept at 40°C in the light (20 μmol photons m^{-2} s^{-1}) and agitated with a shaker. Stock cultures of other transformants were kept in CO_2 (2%) incubator in the light at 40 ˚C with the exception of HSp*FLAG-CYC1* which was kept at 38°C.

All of the above strains were inoculated into 50 mL of the above-mentioned media unless otherwise indicated and cultured in 100 mL test tubes with aeration of ambient air (0.4 L min^{-1}) at 42 °C with or without light (100 μmol photons m^{-2} s^{-1}). For synchronous cultures, cells were pre-cultured in the dark for 4 h (unless otherwise indicated), and then subjected to 12-h light/12-h dark cycle (LD). For heat shock assay to overexpress CYC1 in HSp*FLAG-CYC1* strain, the cells were cultured at 40 °C and subjected to heat shock at 50 °C for twice during the 4 h to 5 h and 6 h to 7 h of the second round of LD. Cells were inoculated to give an OD750 of 0.2, except for the *CDKA* knockdown assay in which the cells were inoculated to give an OD750 of 0.1.

4.2.2 Plasmid construction and the preparation of the *C. merolae* transformants

The primers used are listed in Table 4.1. To produce *FLAG-CYC1* strain, plasmid p*FLAG-CYC1* was first prepared. pUC19 vector was amplified as a linear DNA by primer set No. 1/2. DNA fragment of *CYC1* (CML219C) 1,500-bp upstream genomic sequence, *CYC1 orf* with 200-bp downstream genomic sequence, *CYC1* 1,900-bp downstream genomic sequence and *APCC* (*CMO250C*) promoter (600-bp), was amplified from *C. merolae* genomic DNA using primer sets No. 3/4, No. 5/6, No.7/8 and No.9/10, respectively. A DNA fragment encoding the chloroplast transit peptides (60 amino acids) of APCC which was fused with *Staphylococcus aureus* chloramphenicol acetyltransferase (McAteer et al., 1985) and *C. merolae* β-tubulin terminator (200 bp; βt3') were amplified by PCR with the primer set No. 11/12 and pCDKA (Fujiwara et al., 2017) as the template. PCR fusion was then performed to prepare three DNA fragments; the first one included pUC19 vector and *CYC1* 1,900-bp downstream genomic sequence; second one included 4×FLAG-encoding sequence (ATGGACTATAAGGATCACGATGGCGACTACAAAGACCATGACGGTGATTATA AAGATCATGACATCGATTACAAGGATGACGATGACAAG) and *CYC1 orf* (with the 200-bp downstream genomic sequence); third one included *APCC* promoter, the chloroplast transit peptide of APCC, *CAT orf* and the βt3', each prepared by primer set No.13/6, No.9/8 and No.1/4 respectively. These DNA fragments were fused with InFusion Cloning Kit (TAKARA), producing p*FLAG-CYC1*.

To produce *FLAG-CYC1/CDKA*-cKD strain, plasmid p*FLAG-CYC1/CDKA*-cKD was prepared. This plasmid was prepared by replacing the *APCC* promoter region of p*FLAG-CYC1* with *CPCC* (*CMP166C)* promoter sequence for a stronger selection. The vector without *APCC* promoter was amplified from p*FLAG-CYC1* with the primer set No.14/15 and *CPCC* promoter was amplified from *C. merolae* genomic DNA with the primer set No.16/17. The DNA fragment were then cloned into the vector by InFusion Cloning Kit (TAKARA).

To produce HSp*FLAG-CYC1* strain, plasmid pHSp*FLAG-CYC1* was prepared. A DNA fragment consisting of a pQE80 vector and *CMD184C orf* with its 1.9-kb downstream sequence (a genomic-neutral locus) was amplified by PCR with the primer sets No. 18/19 and pD184 (Fujiwara, Ohnuma, et al., 2013) as the template. A DNA fragment encoding 4×FLAG was amplified from p*FLAG-CYC1* with the primer set No.20/21. *CMJ101C*

promoter (a heat shock promoter; 250-bp), and *CYC1 orf* with 426-bp downstream genomic sequence were amplified from *C. merolae* genomic DNA with the primer sets No.22/23 and No.24/25, respectively. A DNA fragment consisting of *APCC* promoter region, the chloroplast transit peptides of APCC, *CAT orf* and βt3' was amplified from p*FLAG-CYC1* was fused by PCR with *CYC1 orf* with 426-bp downstream genomic sequence with the primer set No.24/12. This fragment was fused by PCR with 4×FLAG-encoding sequence with the primer set No.20/12. To prepare pHSp*FLAG-CYC1*, the resulting DNA fragment and *CMJ101C* promoter were cloned into the prepared pQE80 vector with *CMD184C orf* by InFusion Cloning Kit (TAKARA).

For transformation of *C. merolae*, a linear DNA was amplified from above mentioned vectors with the primer set No.26/27. A total of 3–5 μg of the PCR product was used for the transformation. The transformation and the transformant selection were performed as previously described (Fujiwara et al., 2017). *FLAG-CYC1* and HSp*FLAG-CYC1* strains were prepared by transformation of *C. merolae* 10D. *FLAG-CYC1/CDKA*-cKD strain was prepared by transformation of *C. merolae CDKA*-cKD strain (Fujiwara et al., 2020). For the preparation of *FLAG-CYC1/CDKA*-cKD, the culture medium used for transformation was MA2-NO_3 medium instead of MA2 medium which was used for all other transformations.

4.2.3 Immunoblot analyses

Cells were harvested from 2 mL of culture by centrifugation of 2,000 *g* for 5 min at 4˚C and then stored at –80 ˚C until next step. The cells were resuspended in SDS-PAGE sample buffer (50 mM Tris-HCl, pH 6.8, 10% glycerol, 2% SDS, 5% 2-mercaptoethanol, 0.01 % bromophenol blue) and the protein concentration was determined with XL-Bradford protein assay kit (APRO Science, Japan). 3 μg of total cellular protein was separated in each lane by SDS-PAGE and then transferred onto a polyvinylidene difluoride (PVDF) membrane (Immobilon; Millipore). Membrane blocking, antibody reactions, and signal detection were performed as previously described (Fujiwara et al., 2020). An anti-HA monoclonal antibody (0.5 μg mL^{-1}; clone 16B12, BioLegend) and anti-FLAG monoclonal antibody (1 μg mL^{-1}; clone M2, Sigma) were used as the primary antibodies to detect HA-CDKA and FLAG-CYC1 proteins, respectively. An anti-alpha-tubulin monoclonal antibody (1 μg mL^{-1}; clone

B-5-1-2, Sigma) and an anti-histone H3 phosphorylated at serine 10 (H3S10ph) polyclonal antibody (1 μg mL^{-1}; 06-570, Millipore) were also used as the primary antibodies. The antibodies against *C. merolae* RB and E2F raised in rabbits using the respective recombinant proteins which were prepared in a previous study (Miyagishima et al., 2014) were used as primary antibodies to detect RB (anti-RB, 0.3 μg mL^{-1}) and E2F (anti-E2F, 0.3 μg mL^{-1}). A goat anti-mouse IgG-HRP (for anti-HA, anti-FLAG, anti-GFP and anti-alpha-tubulin) and a goat anti-rabbit IgG-HRP (for anti-H3, anti-RB and anti-E2F) were used as secondary antibodies at dilution of 1:25,000.

4.2.4 Cell size and cell number determination

Cells were fixed with 0.35% glutaraldehyde and the cell number and cell volume were analyzed with Coulter Counter (Z2, Beckman Coulter).

4.3 Results

4.3.1 G1 cyclin accumulated with cell growth in *C. merolae* cells

To assess the potential of G1 cyclin (CYC1) as a sizer protein in *C. merolae*, the changes in CYC1 protein level (concentration) in the LD synchronous culture was examined. To detect CYC1 protein, *FLAG-CYC1* strain was first prepared in which 4×FLAG-encoding sequence was inserted into the chromosomal *CYC1* locus to express FLAG-CYC1 protein by *CYC1* promoter. *FLAG-CYC1* was synchronized under LD and cells were collected every 2 h during the second round of LD (onset of this light period was defined as the 0 h; Fig 4.1). Immunoblot analysis was then performed to detect the level (concentration) of FLAG-CYC1 and other cell cycle markers in the (same amount of) total cellular protein. Under the LD, the phosphorylation of RB (the band shift of RB) was observed from the 6 h to 12 h (Fig 4.1). Alpha-tubulin (S/M-phase marker in *C. merolae*) and histone H3 phosphorylated at serine 10 (H3S10ph; an M-phase marker) while were strongly detected from the 12 h to 18 h (Fig 4.1). FLAG-CYC1 shown to accumulate during the light period when photosynthetic dependent cellular growth occurred, with its level (concentration) peaked at the 8 h which corresponding to the timing at which RB phosphorylation highly detected (Fig 4.1). After the 8 h, FLAG-CYC1 started to decrease and almost no FLAG-CYC1 was detected at the 16 h (Fig 4.1).

Thus, CYC1 accumulates in G1 phase along with cellular growth and degraded upon entering S phase.

4.3.2 G1 cyclin accumulated to a higher level in abnormally enlarged *C. merolae* cells and degraded in a stepwise manner during the successive cell divisions

To further examine the scaling of CYC1 protein level with cell size, the level of FLAG-CYC1 was also determined in abnormally enlarged *C. merolae* cells. For this assay, *C. merolae FLAG-CYC1/CDKA*-cKD strain was first generated (Fig 4.2A). To this end, 4×FLAG-encoding sequence was inserted into the chromosomal *CYC1* locus of the previously generated *CDKA*-cKD strain (Fujiwara et al., 2020) (Chapter 3, Fig 3.4). As in Chapter 3, *CDKA* was knocked down first by culturing *FLAG-CYC1/CDKA*-cKD strain in NH_4^+-containing medium which turn off expression of *CDKA* by nitrate reductase (*NR*) promoter, and the CDKA was later recovered by transferring the cells into NO_3^--containing medium (Fig. 4.2A). As a control, *FLAG-CYC1* strain was also cultured under the same condition and *CDKA* knockdown not occurring in this control strain (Fig. 4.2A). Cultures were collected at various timepoints (Fig. 4.2A) to analyze their cell size (Fig. 4.2B) and immunoblot analyses were performed to detect protein concentrations of HA-CDKA, FLAG-CYC1 and few cell cycle markers (Fig. 4.2C).

CDKA was depleted in *FLAG-CYC1/CDKA*-cKD cells after cultured in NH_4^+ medium for three days under the light (Fig. 4.2C, stage ii). No further phosphorylation was detected for RB protein after the *CDKA* knockdown and M-phase marker H3S10ph was no longer detected, hence showing the cells were successfully arrested at G1 phase (Fig. 4.2C, stage ii). During this continuous light of three days, G1-arrested cells grew in size to approximately ninefold of their initial cell size (Fig. 4.2B, stages i to ii). The concentration of FLAG-CYC1 protein also increased (Fig. 4.2C, stages i to ii) together with the cell size, again showing a correlation between CYC1 accumulation and cell growth. In contrast to *FLAG-CYC1/CDKA*-cKD, cell divisions occurred normally in the control *FLAG-CYC1* cells when cultured in NH_4^+ medium as no *CDKA* knockdown occurred, and only small increase in the mean cell volume observed after cultured three days under the light (Fig. 4.2B, stages i to ii). The concentration of FLAG-CYC1 protein in *FLAG-CYC1* culture after *CDKA*

knockdown was similar to those before *CDKA* knockdown (Fig. 4.2C, stages i to ii) and it was significantly lower than the concentration of FLAG-CYC1 detected in the abnormally enlarged *FLAG-CYC1/CDKA*-cKD (Fig. 4.2C, stage ii), showing that the larger cells generally contained higher concentration of CYC1.

After exchange into NO_3^- medium, *CDKA* was re-expressed in *FLAG-CYC1/CDKA*-cKD cells (Fig. 4.2C, stages iii to v) and G1/S transition started within 6 h after medium exchange which is evidenced from the detected phosphorylation of RB and appearance of the M-phase marker H3S10ph (Fig. 4.2C, stage iv). The cell division should have occurred at a rate faster than the cellular growth as suggested from the decrease in the mean cell volume (Fig. 4.2B, stages iii to iv and v). Along with the cell divisions, the FLAG-CYC1 concentration decreased (Fig. 4.2C, stages iii to iv). The cells were then transferred to the dark to stop the cell growth, during which the cell continued to divide (Fig. 4.2B and C, stages v to ix). *FLAG-CYC1/CDKA*-cKD cells completed cell division between 12 to 18 h after dark shift (Fig. 4.2B and C, between stages vii to viii) while the control *FLAG-CYC1* finished cell division between 6 h to 12 h after dark shift (Fig. 4.2B and C, between stages vi to vii). FLAC-CYC1 protein decreased along with successive cell divisions in *FLAG-CYC1/CDKA*-cKD and was longer detected at 18 h after dark shift (Fig. 4.2C, stages viii). In contrast, FLAC-CYC1 protein was undetectable at 12 h after dark shift in *FLAG-CYC1* cells (Fig. 4.2C, stages viii), which was earlier that those in *FLAG-CYC1/CDKA*-cKD. These results suggest that CYC1 is consumed stepwisely along with successive cell divisions in *FLAG-CYC1/CDKA*-cKD cells. This stepwise decrease resembles the properties of potential sizer protein in *C. reinhardtii* – CDKG1, which has been suggested to inhibit further round of cell division when it dropped to a certain level. However, it is unfeasible to determine CYC1 level in each cell by immunoblotting. Thus, further studies at a single cell level (e.g. by microscopic observation of fluorescent protein-tagged CYC1) will be required in future, to examine whether CYC1 is actually consumed stepwisely in a single cell with each round of the successive cell divisions.

4.3.3 Overexpression of G1 cyclin accelerates G1/S transition in *C. merolae*

To further examine the role of CYC1 in *C. merolae*, FLAG-CYC1 protein was overexpressed in *C. merolae*. A heat shock inducible gene expression system has been developed in *C. merolae* utilizing promoter of *CMJ101C* gene (referred to as *HS* gene) which encodes small heat shock protein and its promoter is able to overexpress proteins only under high temperature (Sumiya et al., 2014). A DNA fragment including *HS* promoter, *FLAG-CYC1 orf*, *CAT* selectable marker was introduced into a genomic-neutral locus (Fujiwara, Ohnuma, et al., 2013) in *C. merolae*, and this strain is referred to as HSp*FLAG-CYC1* (Fig. 4.3A). HSp*FLAG-CYC1* strain was cultured at 40°C under 12-h light/12-h dark cycle (LD) to synchronize their cell cycle. During the second round of LD, the cells were subjected to heat-shock treatment at 50°C between the 4 h to 5h and 6 h to 7 h (the onset of the second light period is defined as the 0 h) (Fig. 4.3B). These timings were selected in order to overexpress FLAG-CYC1 before the 8 h, when CYC1 level was detected at the highest in the *FLAG-CYC1* strain (Fig. 4.1), corresponding to late G1 phase. *C. merolae CAT* strain with only *CAT* selectable marker introduced into the same genomic-neutral locus, was also cultured under the same condition as a control. Cultures were collected every 4 h during the second round of LD, and total proteins were prepared from the collected cultures.

The immunoblot analyses showed a high level of FLAG-CYC1 protein was successfully expressed in HSp*FLAG-CYC1* upon two rounds of heat shocks while it was hardly detected in the culture without heat shock treatments [Fig. 4.3B (i)]. The concentration of FLAG-CYC1, however, rapidly reduced to basal level at the 16 h, upon G1/S transition [Fig. 4.3B (i)]. By examining the expression patterns of cell cycle makers, the heat shock at 50°C alone, without any protein overexpression (as in *CAT* strain) shown to delay the timing of S/M phase [Fig. 4.3B (ii)]. Both α-tubulin (an S/M-phase marker) and H3S10ph (an M-phase marker), started to be detected at the 12 h and reached highest level at the 16 h in *CAT* LD culture without any heat shock treatment [Fig. 4.3B (ii)]. In contrast, the appearance and the peak of these cell cycle markers delayed for about 4 hours under heat shock treatment [Fig. 4.3B (ii)]. The higher temperature may have temporarily arrested the cell cycle progression, as reported previously in green algae *C. reinhardtii* (Zachleder et al., 2019). On the other hand, no delay of cell cycle progression upon the heat shock treatment was observed

in HSp*FLAG-CYC1* culture with both α-tubulin and H3S10ph detected at the highest level at the 16 h regardless of heat shock treatment, suggesting that the overexpression of CYC1 accelerates G1/S transition in *C. merolae* (while the effect on number of cell divisions still unclear at this point).

4.4 Discussion

In the budding yeast, Cln3 protein (G1 cyclin) has been reported to exhibit sizer behavior with its concentration increases with cell growth to regulate Start (commitment) and G1/S transition (Litsios et al., 2019). In a similar manner, CYC1 accumulated during the light period in *C. merolae* when cultured under LD, during which cell grows in size. CYC1 concentration reached peak at the late G1 phase and then decreased upon G1/S transition. Based on the overexpression assay, high CYC1 level is suggested to accelerate the G1/S transition in *C. merolae*. In this case, the high level of CYC1 could form complex with CDKA in *C. merolae* to phosphorylate and inactive RB protein at a faster rate, which allows for earlier progression through G1/S transition. This is consistent with the overexpression of Cln3 in budding yeast which also reported to result in earlier progression through Start and G1/S (Nash et al., 1988). These results suggest that CYC1 possibly act as sizer to regulate commitment, in a similar manner as Cln3 in budding yeast. However, the effect of heat shock in this study, complicated the interpretation on the results of CYC1 overexpression. The heat shock delayed G1/S transition while the overexpressed CYC1 should have accelerated it. To overcome this issue, other inducible expression system, which does not utilize heat shock promoter, has to be employed for further analyses.

To act as a potential sizer protein in multiple fission, the protein level is proposed to scale with cell size to regulate commitment and decrease upon cell divisions to regulate number of cell divisions. In this study, CYC1 level was shown to decrease at a slower rate with cell divisions in the abnormally enlarged *C. merolae* cells, when compared to the control strain (binary fission), hence suggesting CYC1 level likely decreased in a stepwise manner with successive cell divisions similar to CDKG1 level in *C. reinhardtii*, which was suggested to regulate number of cell divisions (Li et al., 2016). However, to verify this assumption,

further analyses are required to examine whether CYC1 is actually consumed stepwisely on a single cell level.

The immunoblot analyses in this study were performed using protein samples of the same amount of total cellular protein, each prepared from a population of *C. merolae* cells in which there was variation in cell sizes, timing and number of cell divisions. Due to these limitations, direct visualization of G1 cyclin protein in *C. merolae* cells, for example by preparing *C. merolae* transformant expressing a fluorescent protein-tagged G1 cyclin, is required to examine G1 cyclin concentration, also the timing and number of successive cell divisions, at a single cell level. To this end, time lapse imagining will be required to track G1 cyclin concentration, in the abnormally enlarged *C. merolae* which undergoes successive cell divisions and compare it with normal(-sized) *C. merolae*. Alternatively, fluorescent immunostaining as reported in the *C. reinhardtii* (Li et al., 2016) and budding yeast (Verges et al., 2007; Wang et al., 2009) can be performed to quantify the FLAG-tagged G1 cyclin in *C. merolae* transformants *FLAG-CYC1* and *FLAG-CYC1/CDKA-cKD* (abnormally enlarged).

G1 cyclin degradation upon G1/S transition is expected to be not only modulated through a single mechanism but various different mechanisms redundantly as demonstrated in the budding yeast (Landry et al., 2012; Tyers et al., 1992), and also supported by the presence of more than one ubiquitin ligases that may be involved in CYC1 degradation in *C. merolae* (Kobayashi et al., 2011). In the budding yeast, these various controls on Cln3 have been suggested to be important for coupling of cell division and cellular growth (Gallego et al., 1997; Landry et al., 2012; Tyers et al., 1992), which may also be true for *C. merolae*. During the evolution of cyanidialean red algae with different modes of cell cycle (binary or multiple fission), the modification on G1 cyclin accumulation or degradation mechanisms may have occurred. In this regard, further comparative analyses on G1 cyclin among cyanidialean red algae will give important insights into the evolution of multiple fission cell cycle.

4.5 Figures and tables

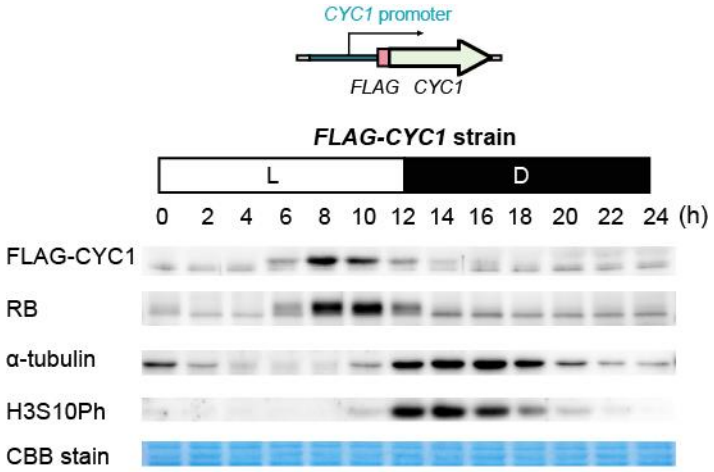

Figure 4.1 Changes in the levels (concentration) of CYC1 and other cell cycle marker proteins in the synchronous culture of *C. merolae*. To detect CYC1 by an anti-FLAG antibody, 4×FLAG-encoding sequence was inserted into the chromosomal *CYC1* locus (*FLAG-CYC1* strain). *FLAG-CYC1* cells were cultured in an inorganic medium under the LD. During the second round of LD, cultures were collected every 2 h from the onset of light (defined as the 0 h), from which protein samples were prepared. Immunoblot analyses were performed using protein samples with the same amount of total protein content (3 μg) to examine the changes in the levels of FLAG-CYC1, RB, α-tubulin (an S/M-phase marker), and H3S10ph (an M-phase marker). A gel stained with Coomassie Brilliant Blue (CBB) is shown as a loading control.

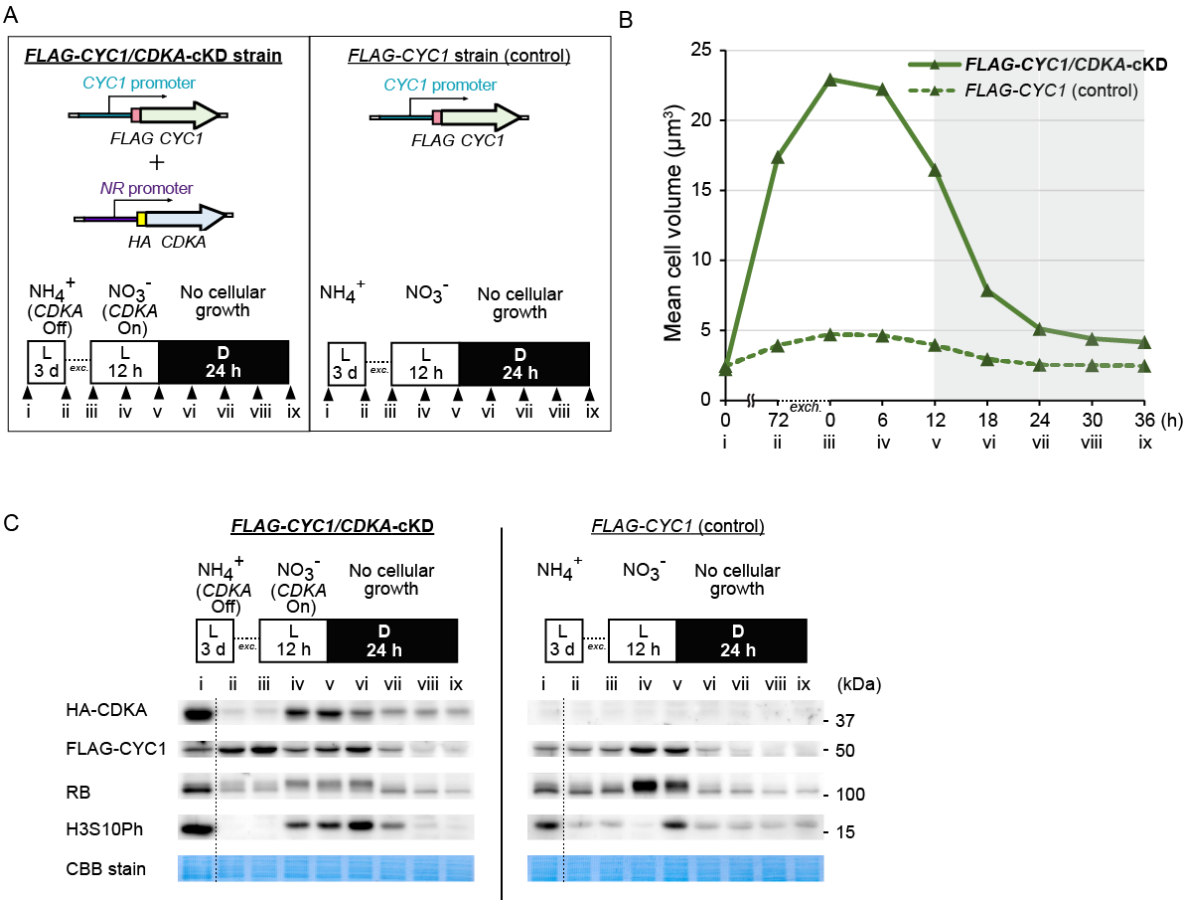

Figure 4.2 Changes in the levels of FLAG-CYC1 and other cell cycle marker proteins in abnormally enlarged *C. merolae FLAG-CYC1/CDKA*-cKD and control *FLAG-CYC1*. The abnormally enlarged *C. merolae* cells were prepared by conditional knockdown of *CDKA* which block G1/S transition while maintaining cellular growth under the light. **(A)** A schematic illustration of the chromosomal *CYC1* locus in the both strains and *CDKA* locus in the *FLAG-CYC1/CDKA*-cKD strain are shown. A 4×FLAG-encoding sequence was inserted to into the chromosomal *CYC1* locus in the both strains. A 3×HA-encoding sequence and *NR* promoter were inserted into the chromosomal *CDKA* locus in *FLAG-CYC1/CDKA*-cKD strain, in order to activate or inactivate *HA-CDKA* expression with the absence or presence of NH_4^+ in the culture medium (Fujiwara et al., 2020). Stock culture of *FLAG-CYC1/CDKA*-cKD which was maintained in an inorganic NO_3^- medium (NH_4^+ was replaced with NO_3^- as an inorganic nitrogen source; *NR* promoter on), was inoculated into the NH_4^+

medium (*NR* promoter off), and cultured in the light for three days to knock down *CDKA*, allowing the cells to grow in size without entering G1/S transition. To recover CDKA, the abnormally enlarged *FLAG-CYC1/CDKA*-cKD cells were transferred to the NO_3^- medium and cultured in the light for 12 h. The cells were later shift to dark condition for 24 h to stop cellular growth. As a control *FLAG-CYC1* cells were also cultured under the same condition. Cells were collected before and after culturing for three days in NH_4^+ medium under the light. After exchange into NO_3^- medium, cells were collected every 6 h, from the onset of 12-h light till the end of 24-h dark. **(B)** The changes in the mean cell volumes of both strains were examined by Coulter Counter Z2. **(C)**. The changes in the levels of HA-CDKA, FLAG-CYC1, RB, and H3S10Ph (an M-phase marker) was examined by immunoblot analyses of the cellular total proteins. A gel stained with Coomassie Brilliant Blue (CBB) is shown as a loading control.

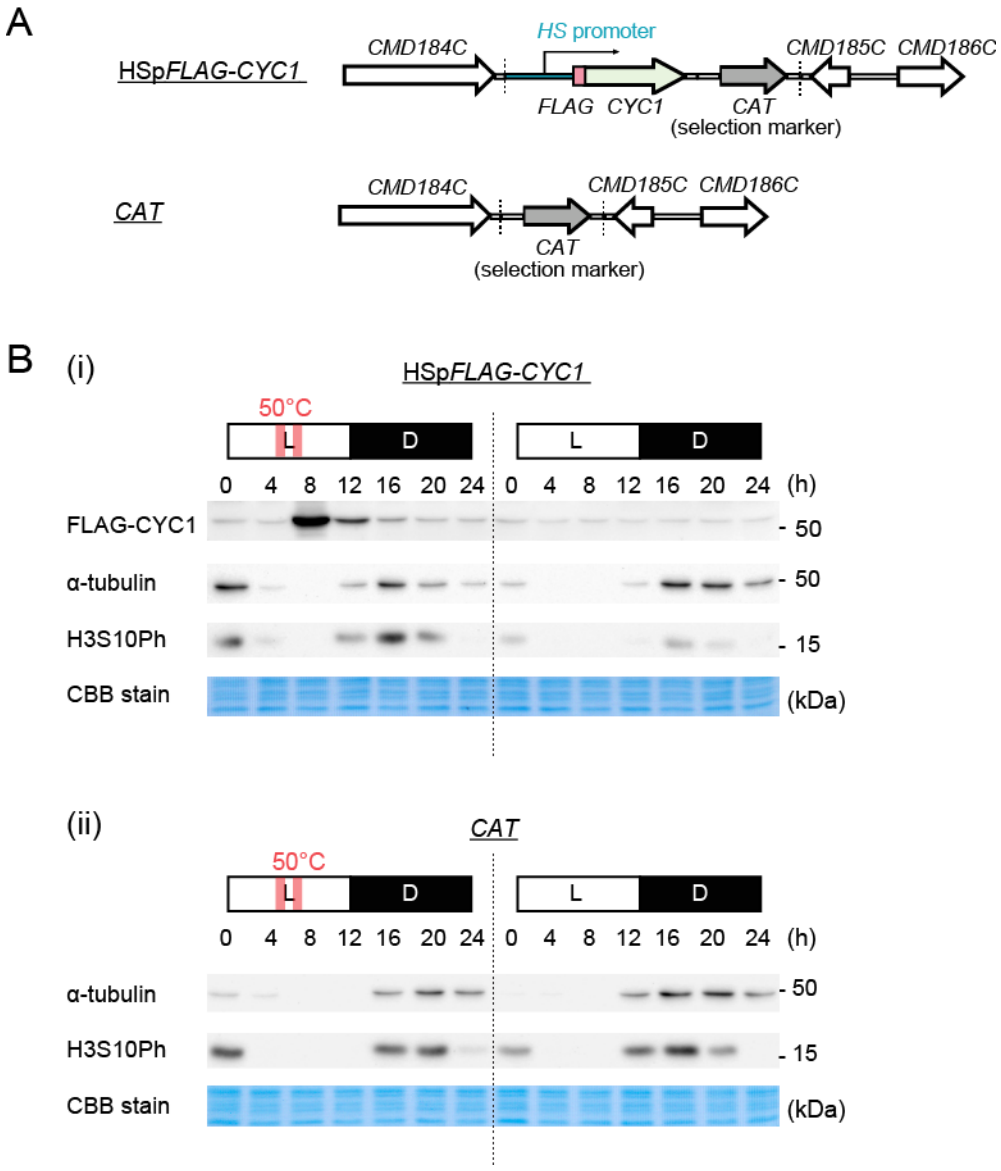

Figure 4.3 Effect of CYC1 overexpression on the cell cycle progression in *C. merolae*. *HS* promoter, 4×FLAG-coding sequence together with a selection marker *CAT* were inserted to into a genomic-neutral locus to overexpress *CYC1* with two rounds of heat shock treatments (HSp*FLAG-CYC1* strain). *CAT* strain in which only *CAT* was inserted into the locus, was used as a control. **(A)** A schematic illustration of the genomic-neutral locus in both strains are shown. Both the strains were cultured in an inorganic medium at 40°C under the LD. During the second round of the LD, the cultures were subjected to two rounds of 1-

h heat shocks (50°C) between the 4 h and 5 h and between the 6 h and 7 h. Cells were collected every 4 h during the second round of the LD from the onset of light (defined as the 0 h). Both the strains were also cultured without any heat shock treatment for comparison (heat shock control). **(B)** The changes in the levels of FLAG-CYC1, RB, α-tubulin (an S/M-phase marker) and H3S10Ph (an M-phase marker) were examined by immunoblot analyses of the cellular total proteins for both (i) HSp*FLAG-CYC1* and (ii) *CAT* strains. A gel stained with Coomassie Brilliant Blue (CBB) is shown as a loading control.

Table 4.1

No.	Primers	Sequence 5' to 3'
	Primers used in cloning and transformation	
1	pUC(264)F	GATCCCCGGGTACCGAGCTCGAATTCACT
2	pUC(263)R	CTCTAGAGTCGACCTGCAGGCATGCAAGCT
3	CYC1(-1500)pucF	AGGTCGACTCTAGAGGCTCGAATACACTCACTTGAGAGCT
4	CmCYC1(-1)R	GACCACTCGATCCACGACAGAA
5	CYC1(4)flagF	GATGACGATGACAAGCTGGTTGAAACGAAGGGATCTGAATG
6	CYC1(+200)apccpR	TATACGTTCTCGTCGTTCGATGAGGTCTGGTGGCGGG
7	CYC1(+201)btF	GCAGGCAAAAAGTGTCTCGAACGCATGTGCTCGGATA
8	CYC1(+2100)pucR	CGGTACCCGGGGATCCGGATGTAGTTTGAGGCTGTAAAGTTCA
9	APCC(-600)F	CGACGAGAACGTATAAGGAGTGC
10	APCC(-1)R	GGTCAACGAAC GAAGAAACACAG
11	CAT(1)apccpF	CTTCGTTCGTTGACCATGTTCGTTCAGACCAGTTTCTTTGG
12	bt(+200)R	ACACTTTTTGCCTGCACAAG
13	FLAG(1)cycF	GTGGATCGAGTGGTCATGCTGGTTGAAACGGACTATAAGGATCACGATGGCGACTAC
14	APCC(1)cpccpF	TAAAGCACTTCTGATATGTTCGTTCAGACCAGTTTCTTTGGAACAGGTGTTAAGGC
15	CYC1(+200)cpccR	TTCACCGGACTAGTGTTCGATGAGGTCTGGTGGCGGGGC
16	CPCC(-500)F	CACTAGTCCGGTGAACTCGG
17	CPCC(-1)R	ATCAGAAGTGCTTTACGAGGAAC
18	D184(+28)btF	GCAGGCAAAAAGTGTGAAACCGCTCAGCGACCAAGC
19	D184(+25)R	CGTCACCCTCGGGACTTG
20	FLAG-CYC1(1)HSpF	GAGAACCAGGGATTCATGCTGGTTGAAACGGACTATAAGGA
21	FLAG(90)R	CTTGTCATCGTCATCCTTGTAATCG
22	FLAG(90)cycR	GATCCTTGTCATCTACTTGTCATCGTCATCCTTGTAATCGATGT
23	HS(-1)flagR	ATCCTTATAGTCCATGAATCCCTGGTTCTCTCACAGG
24	CYC1(+1)cycF	CTGGATGACGCGTTGTAGATGACAAGGATCGTGAACCAAGG
25	CYC1(+426)apccpR	TATACGTTCTCGTCGACGCGATTTATCGTACTGTAGTTGGC
26	pUC(193)F	ACAATTTCACACAGGAAACAGCTATGAC
27	pUC(310)R	CGTTGTAAAACGACGGCCAGT
	Primers for checking homologous recombination	
28	CYC1(-1800)F	CCTCTTGCAACTTTTCCCTGC
29	CYC1(+2199)R	ATACACTCGAACAGGCCCTC
30	D184(771)F	TTTGGTTGACGCGCGGTAATC
31	D184(+1967)R	GAGTGCTCCCTTGGCATCAG
	Primers used for qRT-PCR	
29	CYC1(271)F	CTGGCGAGCGCGTGTAT
30	CYC1(325)R	GGTCGCTCTCCGTCTCTTCA
31	DRP3(1656)F	CGCGAAAGCTGCGAACA
32	DRP3(1713)R	GTTGCTCTCTTTCGGTGCACTA

Underlined sequences are adaptor sequences for InFusion reaction (or PCR fusion)

Chapter 5

General discussion

Several eukaryotic cell lineages proliferate by multiple fission cell cycles, during which cells grow to severalfold of their original size and then undergo several rounds of cell division without intervening growth. Although the mechanism of multiple fission cell cycle has been well studied in the unicellular volvocine green alga *C. reinhardtii,* yet how the mechanism of multiple fission could have been modified during the evolution of various species which undergo different numbers of successive cell divisions, has not been examined. I have shown that volvocine green algae *C. reinhardtii, T. socialis* and *G. pectorale* are committed to cell division when they have grown to two-, four- and eight-fold of their daughter cell size, respectively. These commitment sizes correlate with the minimum number of successive cell divisions in these species; one, two, three cell divisions, respectively (Chapter 2; Fig. 5.1). In a similar manner, I have shown that cyanidialean red algae *C. merolae*, *Cy. caldarium* and *G. sulphuraria* are committed to cell division at the cell size of two-, four- and seven-fold of their daughter cell, respectively, and undergo one (binary fission), two, and two or three cell divisions (Chapter 3; Fig. 5.1). These correlations suggest that the evolutionary changes in commitment cell size resulted in the variations in the number of cell divisions, which occurred independently in two different algal lineages regardless of unicellular (cyanidialean red algae) or multicellular (volvocine green algae) species. This phenomenon likely has also occurred in other eukaryotic lineages.

Multiple fission cell cycle in *C. reinhardtii* is suggested to be regulated through three main mechanisms; (1) the cell size is checked during mid G1 (commitment) and only cells that have grown two-fold in size are committed to S/M phase, (2) however, the committed cells have to wait for S/M phases which possibly regulated by circadian gating, and (3) the number of cell divisions (number of S/M phases) that occurs depend on the cell size at G1/S transition (Heldt et al., 2020; Umen, 2005). Molecular genetic studies have shown that both the commitment and G1/S transition are regulated by RB-E2F-DP pathway. In addition, CDKG1 which is specific to volvocine green algae, has been suggested as a sizer that

determines the number of cell divisions at G1/S transition (but not involve in commitment) in *C. reinhardtii*. However, the sizer for regulating commitment in *C. reinhardtii* is still unknown.

In animal cells, RB protein binds and represses E2F/DP complex in G1 phase (Fischer and Muller, 2017; Neganova and Lako, 2008). During mid to late G1 phase, G1 cyclin (cyclin D), which synthesis is stimulated by growth factors, forms complex with CDK to phosphorylate RB. This phosphorylation releases RB from E2F/DP, allowing E2F/DP to start transcribing S-phase genes (Cooper, 2006; Fischer and Muller, 2017; Neganova and Lako, 2008). In this study, I have shown that the colonial volvocine algae (*T. socialis* and *G. pectorale*) and the cyanidialean red algae (*C. merolae* and *Cy. caldarium*) also commit to cell division at G1 phase (Chapters 2 and 3), as in the unicellular volvocine green alga *C. reinhardtii*. Also, the RB-E2F-DP pathway reported to involve in the commitment and G1/S transition in *C. merolae* (Miyagishima et al., 2014), agreeing with those in *C. reinhardtii* (Fang et al., 2006; Olson et al., 2010; Umen and Goodenough, 2001). In addition, this pathway is widely conserved among eukaryotes (Cross et al., 2011) and although appeared to have lost in yeasts, yet they possess functional homologs of RB-E2F-DP (Cooper, 2006; Cross et al., 2011). Hence, the RB-DP-E2F pathway likely also involved in those studied algal species and evolutionary modification of this pathway could have resulted in the evolution and variation of multiple fission cell cycle, as discussed later.

A comparative genomic study involving unicellular *C. reinhardtii*, and multicellular (colonial) species *G. pectorale* and *Volvox carteri* has reported some evidences on the evolution of cell cycle controls among volvocine green algae (Hanschen et al., 2016). Considerable variations in their primary RB structure were reported, which potentially affect their binding with E2F/DP (Hanschen et al., 2016). In addition, Dr. Shunsuke Hirooka in our laboratory has recently found that the typical *Cyanidium* sp. cells, which possess cell wall and produce four autospores by two successive cell divisions, are diploid. Under certain condition, the diploid *Cyanidium* sp. cells produce haploid cells which lack cell wall and undergo binary fission like the *C. merolae* (unpublished results). Moreover, he also found that different paralogs of E2F are expressed in diploid and haploid cells (unpublished results), suggesting that changes in RB-E2F-DP pathway result in alternation between binary fission

and multiple fission in the same strain depending on its nuclear (haploid or diploid) phase. Besides RB protein, the previously mentioned comparative genomic study in volvocine green algae also showed that the cyclin D (G1 cyclin) exhibited a high dN/dS ratio, signature of adaptive evolution (Hanschen et al., 2016). In this study, G1 cyclin shown to accumulate during cell growth and accelerate G1/S transition when highly expressed in *C. merolae* (Chapter 4), implying the G1 cyclin acts as a potential sizer to regulate commitment as in budding yeast, and likely also determine number of cell divisions (suggested from step wise decrease in G1 cyclin as in Chapter 4 or regulated at commitment).

Theoretically, if the rate at which G1 cyclin accumulates accord with cellular growth (balance between translation and degradation) decreases due to certain evolutionary change, more cellular growth will be required to be committed to cell division and thus number of successive cell divisions increases (Fig. 5.2, scenario 1). Alternatively, if the affinity between G1 cyclin and CDK or between G1 cyclin-CDK complex and RB weakened by an evolutionary change, further G1 cyclin accumulation and thus more cell growth will be required for the cell to commit to cell division (Fig. 5.2, scenario 2). Hence, the number of successive cell divisions also increases (Fig. 5.2, scenario 2). In addition to the regulation of commitment, if G1 cyclin is consumed step wisely with each round of successive cell division like suggested in volvocine CDKG1 protein (Li et al., 2016), previously mentioned possible evolutionary changes also lead to the change in the determination of number of cell divisions upon G1/S transition (i.e. slower consumption of G1 cyclin with each round of successive cell divisions, or lower G1 cyclin level required for a further round of successive cell division to occur, can result in the higher number of successive cell divisions).

Regarding the molecular basis of evolution of multiple fission cell cycle, further comparative analyses of G1 cyclin and RB-E2F-DP pathways are required. For example, characterization of G1 cyclin in algal species that undergo multiple fission, and swapping of G1 cyclin, RB-E2F-DP, or related factors between related species that undergo different number of successive cell divisions. As these proteins (or their functional homologs) are well conserved in eukaryotes and the multiple fission cell cycle have evolved many times independently in eukaryotes, further studies should yield significant insights into evolution of the cell cycle in eukaryotes.

5.1 Figures

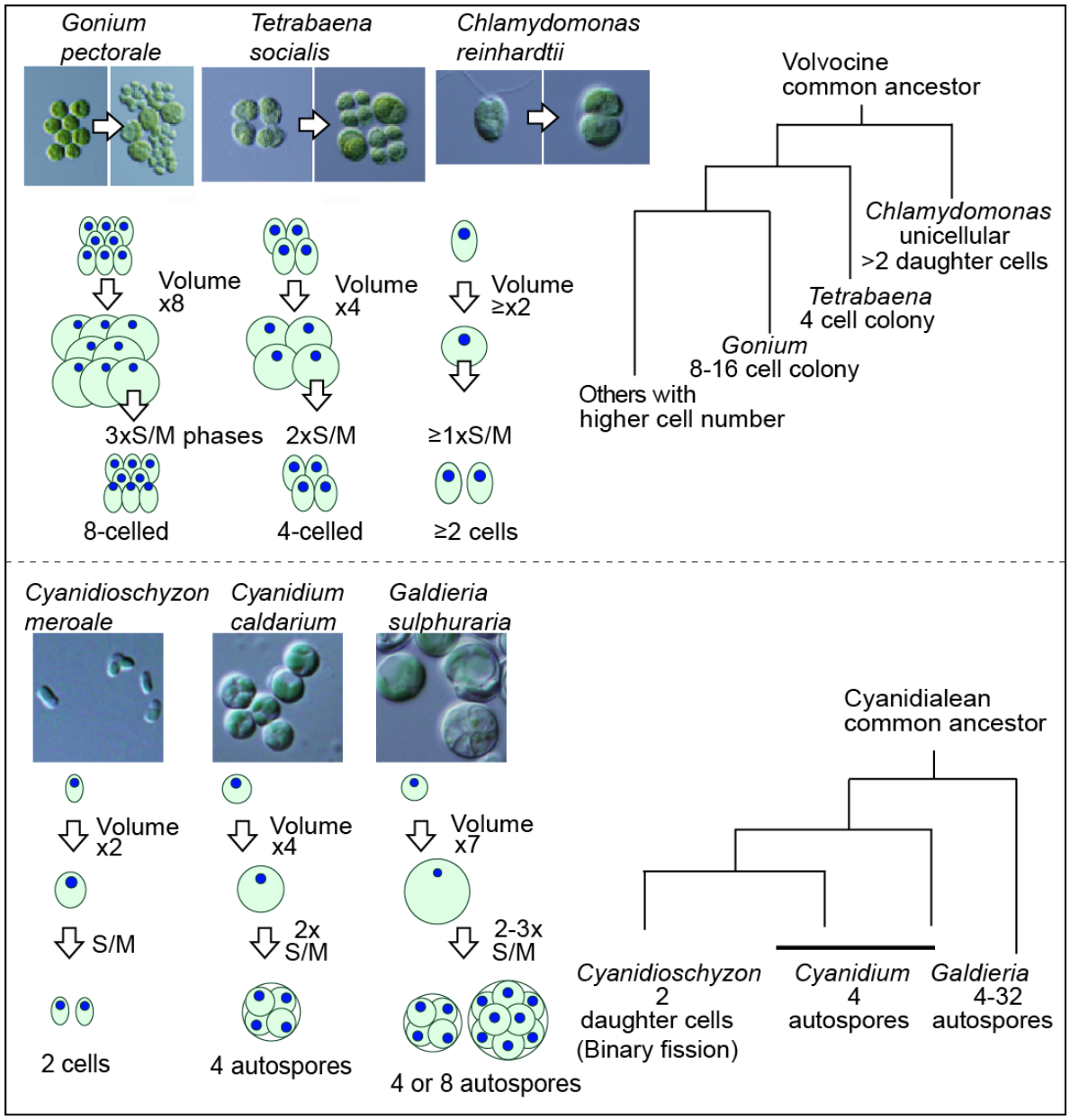

Fig 5.1 Comparison of various volvocine green algae and cyanidialean red algae that undergo different modes of cell division. In this study, three volvocine green algal species *C. reinhardtii* (unicellular), *T. socialis* (four-celled colony) and *G. pectorale* (eight-celled colony) are shown to commit to cell division when they have grown to at least two- four- and eight-fold of their daughter cell size, respectively. Under this regulation, each cell in the

colonial *T. socialis* and *G. pectorale* produced four- and eight-celled colony, respectively. In comparison, three cyanidialean red algal species *C. merolae, Cy. caldarium* and *G. sulphuraria* are shown to produce two, four and four or eight daughter cells in each cell cycle, respectively. *C. merolae* undergoes binary fission, while *Cy. caldarium* and *G. sulphuraria* undergo multiple fission producing autospores in a mother cell wall before hatch out as unicellular daughter cells. These species are shown to commit to cell division at the cell size of two-, four- and seven-fold of their daughter cells. In both the volvocine green algal species and cyandialean red algal species studied, the correlations between the commitment cell size and number of successive cell divisions were observed. These results suggest that the evolutionary changes in commitment cell size likely contributed to the variations in the number of cell divisions.

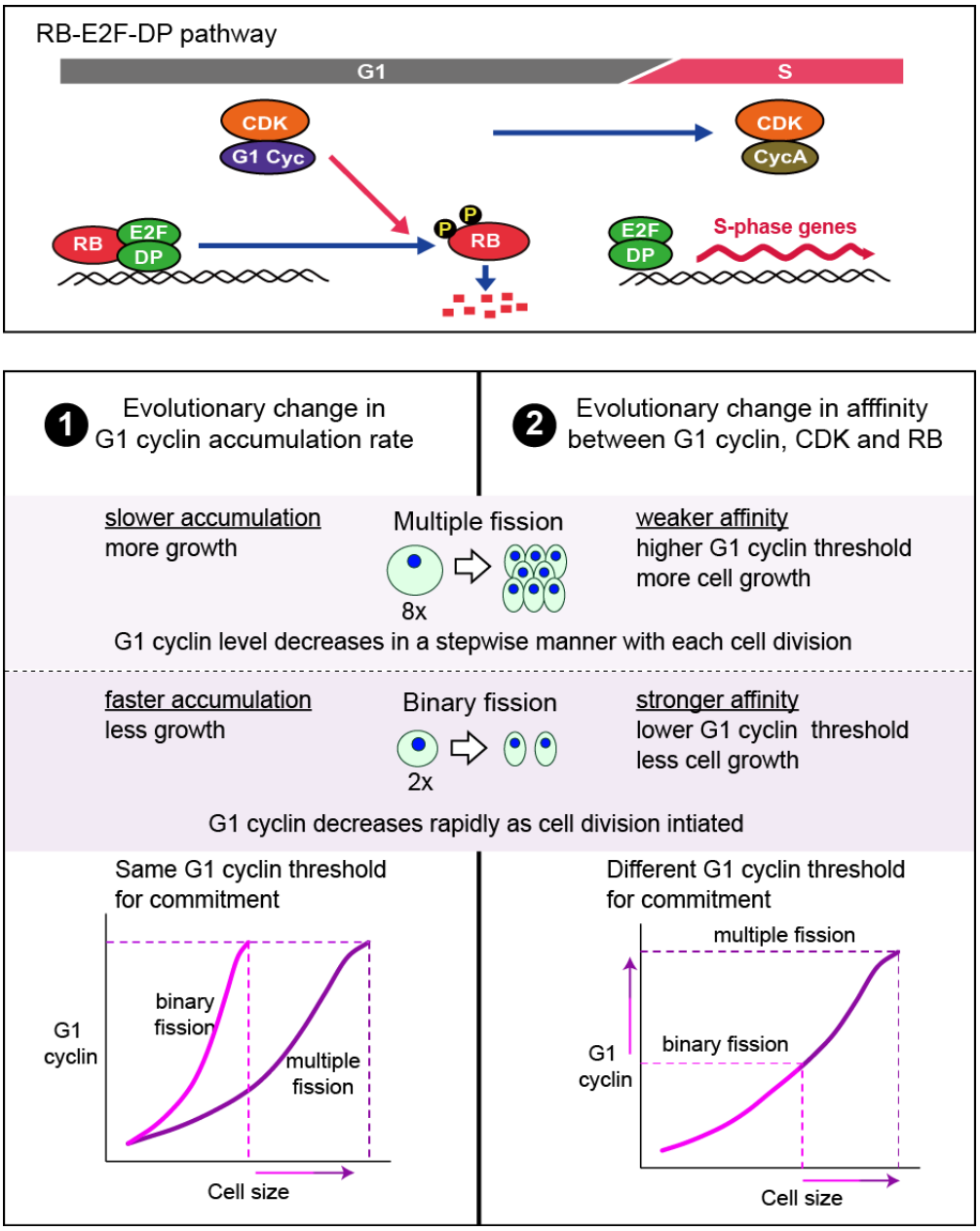

Fig. 5.2 A model on cell cycle regulation at commitment and G1/S transition, and scenarios of evolutionary changes that can possibly resulted in changes of commitment cell size and number of cell divisions. During G1 phase, G1 cyclin accumulates with cellular growth and binds to CDK. When G1 cyclin-CDK level exceeds a certain threshold, it phosphorylates and inactivate RB, releasing it from E2F-DP. E2F-DP then activates the transcription of the S-phase genes. This RB-E2F-DP pathway regulates both the commitment

and G1/S transition, but how they are separately regulated are still unknown at this point. G1/S transition likely requires an additional factor such as E2F phosphorylation which was shown to be regulated by the circadian rhythm in *C. merolae* (Miyagishima et al., 2014). The increase in the commitment size and thus the increase in number of successive cell divisions may resulted from a slower accumulation of G1 cyclin relative to cell growth (scenario 1) or a higher threshold of G1 cyclin for commitment (scenario 2). When accumulation rate of G1 cyclin relatives to cell growth decreases due to an evolutionary change, the cell needs to grow to a larger cell size to accumulate a certain level of cyclin in order to commit to cell division (scenario 1). Alternatively, if the affinity between G1 cyclin and CDK/RB becomes weaker due to an evolutionary change, higher level of accumulated G1 cyclin and thus a larger cell size will be required for the commitment. These kinds of evolutionary changes would result in increase in the number of successive cell divisions. If G1 cyclin is consumed step wisely with each round of successive cell division like suggested in volvocine CDKG1 protein to regulate number of cell divisions (Li et al., 2016), those mentioned evolutionary changes will also affect the determination on the number of cell divisions (in a more direct manner).

References

Albertano, P., Ciniglia, C., Pinto, G., & Pollio, A. (2000). The taxonomic position of *Cyanidium*, *Cyanidioschyzon* and *Galdieria*: an update. *Hydrobiologia, 433*(1/3), 137-143. doi:10.1023/a:1004031123806

Allen, M. B. (1959). Studies with *Cyanidium caldarium*, an anomalously pigmented chlorophyte. *Arch Mikrobiol, 32*(3), 270-277. doi:10.1007/BF00409348

Angert, E. R. (2005). Alternatives to binary fission in bacteria. *Nat Rev Microbiol, 3*(3), 214-224. doi:10.1038/nrmicro1096

Arakaki, Y., Kawai-Toyooka, H., Hamamura, Y., Higashiyama, T., Noga, A., Hirono, M., . . . Nozaki, H. (2013). The simplest integrated multicellular organism unveiled. *PLoS One, 8*(12), e81641. doi:10.1371/journal.pone.0081641

Bahler, J., & Pringle, J. R. (1998). Pom1p, a fission yeast protein kinase that provides positional information for both polarized growth and cytokinesis. *Genes Dev, 12*(9), 1356-1370. doi:10.1101/gad.12.9.1356

Barbier, G., Oesterhelt, C., Larson, M. D., Halgren, R. G., Wilkerson, C., Garavito, R. M., . . . Weber, A. P. (2005). Comparative genomics of two closely related unicellular thermo-acidophilic red algae, *Galdieria sulphuraria* and *Cyanidioschyzon merolae*, reveals the molecular basis of the metabolic flexibility of *Galdieria sulphuraria* and significant differences in carbohydrate metabolism of both algae. *Plant Physiol, 137*(2), 460-474. doi:10.1104/pp.104.051169

Bell, G. (1978). The evolution of anisogamy. *J Theor Biol, 73*(2), 247-270. doi:10.1016/0022-5193(78)90189-3

Bhatia, P., Hachet, O., Hersch, M., Rincon, S. A., Berthelot-Grosjean, M., Dalessi, S., . . . Martin, S. G. (2014). Distinct levels in Pom1 gradients limit Cdr2 activity and localization to time and position division. *Cell Cycle, 13*(4), 538-552. doi:10.4161/cc.27411

Bisova, K., & Zachleder, V. (2014). Cell-cycle regulation in green algae dividing by multiple fission. *J Exp Bot, 65*(10), 2585-2602. doi:10.1093/jxb/ert466

Cantwell, H., & Nurse, P. (2019). Unravelling nuclear size control. *Curr Genet, 65*(6), 1281-1285. doi:10.1007/s00294-019-00999-3

Cavalier-Smith, T. (1978). Nuclear volume control by nucleoskeletal DNA, selection for cell volume and cell growth rate, and the solution of the DNA C-value paradox. *J Cell Sci, 34*(1), 247-278.

Cavalier-Smith, T. (1980). *r*- and *K*-tactics in the evolution of protist developmental systems: cell and genome size, phenotype diversifying selection, and cell cycle patterns. *Biosystems, 12*(1-2), 43-59. doi:10.1016/0303-2647(80)90037-4

Coleman, A. W. (1999). Phylogenetic analysis of "Volvocacae" for comparative genetic studies. *Proc Natl Acad Sci U S A, 96*(24), 13892-13897. doi:10.1073/pnas.96.24.13892

Cooper, K. (2006). Rb, whi it's not just for metazoans anymore. *Oncogene, 25*(38), 5228-5232. doi:10.1038/sj.onc.1209630

Craigie, R. A., & Cavalier-Smith, T. (1982). Cell volume and the control of the *Chlamydomonas* cell cycle. *J Cell Sci, 54*(1), 173-191.

Cross, F. R. (2020). Regulation of multiple fission and cell-cycle-dependent gene expression by CDKA1 and the Rb-E2F pathway in *Chlamydomonas*. *Curr Biol, 30*(10), 1855-1865 e1854. doi:10.1016/j.cub.2020.03.019

Cross, F. R., Buchler, N. E., & Skotheim, J. M. (2011). Evolution of networks and sequences in eukaryotic cell cycle control. *Philos Trans R Soc Lond B Biol Sci, 366*(1584), 3532-3544. doi:10.1098/rstb.2011.0078

Cross, F. R., & Umen, J. G. (2015). The *Chlamydomonas* cell cycle. *Plant J, 82*(3), 370-392. doi:10.1111/tpj.12795

de Bruin, R. A., McDonald, W. H., Kalashnikova, T. I., Yates, J., 3rd, & Wittenberg, C. (2004). Cln3 activates G1-specific transcription via phosphorylation of the SBF bound repressor Whi5. *Cell, 117*(7), 887-898. doi:10.1016/j.cell.2004.05.025

Donnan, L., Carvill, E. P., Gilliland, T. J., & John, P. C. L. (1985). The Cell Cycles of *Chlamydomonas* and *Chlorella*. *New Phytologist, 99*(1), 1-40. doi:10.1111/j.1469-8137.1985.tb03634.x

Donnan, L., & John, P. C. (1983). Cell cycle control by timer and sizer in *Chlamydomonas*. *Nature, 304*(5927), 630-633. doi:10.1038/304630a0

Edgar, B. A., Kiehle, C. P., & Schubiger, G. (1986). Cell cycle control by the nucleo-cytoplasmic ratio in early *Drosophila* development. *Cell, 44*(2), 365-372. doi:10.1016/0092-8674(86)90771-3

Edmundson, S. J., & Huesemann, M. H. (2015). The dark side of algae cultivation: Characterizing night biomass loss in three photosynthetic algae, *Chlorella sorokiniana*, *Nannochloropsis salina* and *Picochlorum* sp. *Algal Res, 12*, 470-476. doi:10.1016/j.algal.2015.10.012

Facchetti, G., Chang, F., & Howard, M. (2017). Controlling cell size through sizer mechanisms. *Curr Opin Syst Biol, 5*, 86-92. doi:10.1016/j.coisb.2017.08.010

Fang, S. C., de los Reyes, C., & Umen, J. G. (2006). Cell size checkpoint control by the retinoblastoma tumor suppressor pathway. *PLoS Genet, 2*(10), e167. doi:10.1371/journal.pgen.0020167

Fischer, M., & Muller, G. A. (2017). Cell cycle transcription control: DREAM/MuvB and RB-E2F complexes. *Crit Rev Biochem Mol Biol, 52*(6), 638-662. doi:10.1080/10409238.2017.1360836

Fujiwara, T., Hirooka, S., Ohbayashi, R., Onuma, R., & Miyagishima, S. Y. (2020). Relationship between cell cycle and diel transcriptomic changes in metabolism in a unicellular red alga. *Plant Physiol, 183*(4), 1484-1501. doi:10.1104/pp.20.00469

Fujiwara, T., Kanesaki, Y., Hirooka, S., Era, A., Sumiya, N., Yoshikawa, H., . . . Miyagishima, S. Y. (2015). A nitrogen source-dependent inducible and repressible gene expression system in the red alga *Cyanidioschyzon merolae*. *Front Plant Sci, 6*, 657. doi:10.3389/fpls.2015.00657

Fujiwara, T., Ohnuma, M., Kuroiwa, T., Ohbayashi, R., Hirooka, S., & Miyagishima, S. Y. (2017). Development of a double nuclear gene-targeting method by two-step transformation based on a newly established chloramphenicol-selection system in the red alga *Cyanidioschyzon merolae*. *Front Plant Sci, 8*, 343. doi:10.3389/fpls.2017.00343

Fujiwara, T., Ohnuma, M., Yoshida, M., Kuroiwa, T., & Hirano, T. (2013). Gene targeting in the red alga *Cyanidioschyzon merolae*: single- and multi-copy insertion using authentic and chimeric selection markers. *PLoS One, 8*(9), e73608. doi:10.1371/journal.pone.0073608

Fujiwara, T., Tanaka, K., Kuroiwa, T., & Hirano, T. (2013). Spatiotemporal dynamics of condensins I and II: evolutionary insights from the primitive red alga *Cyanidioschyzon merolae*. *Mol Biol Cell, 24*(16), 2515-2527. doi:10.1091/mbc.E13-04-0208

Gallego, C., Garí, E., Colomina, N., Herrero, E., & Aldea, M. (1997). The Cln3 cyclin is down-regulated by translational repression and degradation during the G1 arrest caused by nitrogen deprivation in budding yeast. *EMBO J, 16*(23), 7196-7206. doi:10.1093/emboj/16.23.7196

Goto, K., & Johnson, C. H. (1995). Is the cell division cycle gated by a circadian clock? The case of *Chlamydomonas reinhardtii*. *J Cell Biol, 129*(4), 1061-1069. doi:10.1083/jcb.129.4.1061

Gregory, T. R. (2001). Coincidence, coevolution, or causation? DNA content, cell size, and the C-value enigma. *Biol Rev Camb Philos Soc, 76*(1), 65-101. doi:10.1017/s1464793100005595

Gross, W. (1999). *Revision of comparative craits for the acido- and thermophilic aed algae Cyanidium and Galdieria*.
Gross, W., & Oesterhelt, C. (1999). Ecophysiological studies on the red alga *Galdieria sulphuraria* isolated from southwest iceland. *Plant Biol, 1*(6), 694-700. doi:10.1111/j.1438-8677.1999.tb00282.x
Gross, W., & Schnarrenberger, C. (1995). Heterotrophic growth of two strains of the acido-thermophilic red alga *Galdieria sulphuraria*. *Plant and Cell Physiol, 36*(4), 633-638. doi:10.1093/oxfordjournals.pcp.a078803
Großhans, J., Müller, H. A. J., & Wieschaus, E. (2003). Control of cleavage cycles in *Drosophila* embryos by frühstart. *Dev Cell, 5*(2), 285-294. doi:10.1016/s1534-5807(03)00208-9
Hallmann, A. (2006). Morphogenesis in the family Volvocaceae: different tactics for turning an embryo right-side out. *Protist, 157*(4), 445-461. doi:10.1016/j.protis.2006.05.010
Hanschen, E. R., Marriage, T. N., Ferris, P. J., Hamaji, T., Toyoda, A., Fujiyama, A., . . . Olson, B. J. (2016). The *Gonium pectorale* genome demonstrates co-option of cell cycle regulation during the evolution of multicellularity. *Nat Commun, 7*, 11370. doi:10.1038/ncomms11370
Heldt, F. S., Tyson, J. J., Cross, F. R., & Novak, B. (2020). A single light-responsive sizer can control multiple-fission cycles in *Chlamydomonas*. *Curr Biol, 30*(4), 634-644 e637. doi:10.1016/j.cub.2019.12.026
Herron, M. D., Hackett, J. D., Aylward, F. O., & Michod, R. E. (2009). Triassic origin and early radiation of multicellular volvocine algae. *Proc Natl Acad Sci U S A, 106*(9), 3254-3258. doi:10.1073/pnas.0811205106
Herron, M. D., & Michod, R. E. (2008). Evolution of complexity in the volvocine algae: transitions in individuality through Darwin's eye. *Evolution, 62*(2), 436-451. doi:10.1111/j.1558-5646.2007.00304.x
Johnson, C. H. (2010). Circadian clocks and cell division: what's the pacemaker? *Cell Cycle, 9*(19), 3864-3873. doi:10.4161/cc.9.19.13205
Jorgensen, P., Nishikawa, J. L., Breitkreutz, B. J., & Tyers, M. (2002). Systematic identification of pathways that couple cell growth and division in yeast. *Science, 297*(5580), 395-400. doi:10.1126/science.1070850
Kirk, D. L. (2003). Seeking the ultimate and proximate causes of *Volvox* multicellularity and cellular differentiation. *Integr Comp Biol, 43*(2), 247-253. doi:10.1093/icb/43.2.247
Kirk, D. L. (2005). A twelve-step program for evolving multicellularity and a division of labor. *Bioessays, 27*(3), 299-310. doi:10.1002/bies.20197
Kobayashi, Y., Imamura, S., Hanaoka, M., & Tanaka, K. (2011). A tetrapyrrole-regulated ubiquitin ligase controls algal nuclear DNA replication. *Nat Cell Biol, 13*(4), 483-487. doi:10.1038/ncb2203
Kofoid, C., & Swezy, O. (1915). Mitosis and multiple fission in trichomonad flagellates. *Proc Amer Acad Arts, 51*(6), 289-378. doi:10.2307/20025580
Koufopanou, V. (1994). The evolution of soma in the Volvocales. *Am Nat, 143*(5), 907-931. doi:10.1086/285639
Kuroiwa, T., Miyagishima, S. Y., Matsunaga, S., Sato, N., Nozaki, H., Tanaka, K., & Misumi, O. (2018). *Cyanidioschyzon merolae: a new model eukaryote for cell and organelle biology*: Springer.
Kuroiwa, T., Nagashima, H., & Fukuda, I. (1989). Chloroplast division without DNA synthesis during the life cycle of the unicellular alga *Cyanidium caldarium* M-8 as revealed by quantitative fluorescence microscopy. *Protoplasma, 149*(2-3), 120-129. doi:10.1007/bf01322984

Landry, B. D., Doyle, J. P., Toczyski, D. P., & Benanti, J. A. (2012). F-box protein specificity for G1 cyclins is dictated by subcellular localization. *PLoS Genet, 8*(7), e1002851. doi:10.1371/journal.pgen.1002851

Lerche, K., & Hallmann, A. (2009). Stable nuclear transformation of *Gonium pectorale*. *BMC Biotechnol, 9*(1), 64. doi:10.1186/1472-6750-9-64

Li, Y., Liu, D., Lopez-Paz, C., Olson, B. J., & Umen, J. G. (2016). A new class of cyclin dependent kinase in *Chlamydomonas* is required for coupling cell size to cell division. *Elife, 5*, e10767. doi:10.7554/eLife.10767

Lim, S., & Kaldis, P. (2013). Cdks, cyclins and CKIs: roles beyond cell cycle regulation. *Development, 140*(15), 3079-3093. doi:10.1242/dev.091744

Litsios, A., Huberts, D., Terpstra, H. M., Guerra, P., Schmidt, A., Buczak, K., . . . Heinemann, M. (2019). Differential scaling between G1 protein production and cell size dynamics promotes commitment to the cell division cycle in budding yeast. *Nat Cell Biol, 21*(11), 1382-1392. doi:10.1038/s41556-019-0413-3

Malumbres, M., & Barbacid, M. (2005). Mammalian cyclin-dependent kinases. *Trends Biochem Sci, 30*(11), 630-641. doi:10.1016/j.tibs.2005.09.005

Martin, S. G., & Berthelot-Grosjean, M. (2009). Polar gradients of the DYRK-family kinase Pom1 couple cell length with the cell cycle. *Nature, 459*(7248), 852-856. doi:10.1038/nature08054

Matt, G., & Umen, J. (2016). *Volvox*: A simple algal model for embryogenesis, morphogenesis and cellular differentiation. *Dev Biol, 419*(1), 99-113. doi:10.1016/j.ydbio.2016.07.014

McAteer, M., Donnan, L., & Peter, C. L. J. (1985). The timing of division in *Chlamydomonas*. *New Phytol, 99*(1), 41-56.

Merola, A., Castaldo, R., Luca, P. D., Gambardella, R., Musacchio, A., & Taddei, R. (2009). Revision of *Cyanidium caldarium.* Three species of acidophilic algae. *Giorn Bot Ital, 115*(4-5), 189-195. doi:10.1080/11263508109428026

Minoda, A., Sakagami, R., Yagisawa, F., Kuroiwa, T., & Tanaka, K. (2004). Improvement of culture conditions and evidence for nuclear transformation by homologous recombination in a red alga, *Cyanidioschyzon merolae* 10D. *Plant Cell Physiol, 45*(6), 667-671. doi:10.1093/pcp/pch087

Miyagishima, S. Y., Fujiwara, T., Sumiya, N., Hirooka, S., Nakano, A., Kabeya, Y., & Nakamura, M. (2014). Translation-independent circadian control of the cell cycle in a unicellular photosynthetic eukaryote. *Nat Commun, 5*, 3807. doi:10.1038/ncomms4807

Miyagishima, S. Y., Jong, L. W., Nozaki, H., & Hirooka, S. (2018). Cyanidiales: evolution and habitats. In T. Kuroiwa, S. Miyagishima, S. Matsunaga, N. Sato, H. Nozaki, K. Tanaka, & O. Misumi (Eds.), *Cyanidioschyzon merolae: a new model eukaryote for cell and organelle biology* (pp. 3-16): Springer Singapore.

Miyagishima, S. Y., Suzuki, K., Okazaki, K., & Kabeya, Y. (2012). Expression of the nucleus-encoded chloroplast division genes and proteins regulated by the algal cell cycle. *Mol Biol Evol, 29*(10), 2957-2970. doi:10.1093/molbev/mss102

Murphy, C. M., & Michael, W. M. (2013). Control of DNA replication by the nucleus/cytoplasm ratio in *Xenopus*. *J Biol Chem, 288*(41), 29382-29393. doi:10.1074/jbc.M113.499012

Nash, R., Tokiwa, G., Anand, S., Erickson, K., & Futcher, A. B. (1988). The WHI1+ gene of *Saccharomyces cerevisiae* tethers cell division to cell size and is a cyclin homolog. *EMBO J, 7*(13), 4335-4346.

Neganova, I., & Lako, M. (2008). G1 to S phase cell cycle transition in somatic and embryonic stem cells. *J Anat, 213*(1), 30-44. doi:10.1111/j.1469-7580.2008.00931.x

Newport, J., & Kirschner, M. (1982). A major developmental transition in early *Xenopus* embryos: I. characterization and timing of cellular changes at the midblastula stage. *Cell, 30*(3), 675-686. doi:10.1016/0092-8674(82)90272-0

Nozaki, H., Itoh, M., Sano, R., Uchida, H., Watanabe, M. M., & Kuroiwa, T. (1995). Phylogenetic relationships within the colonial Volvocales (Chlorophyta) inferred from rbcL gene seqquence data. *J Phycol, 31*(6), 970-979. doi:10.1111/j.0022-3646.1995.00970.x

O'Farrell, P. H. (2015). Growing an embryo from a single cell: a hurdle in animal life. *Cold Spring Harb Perspect Biol, 7*(11). doi:10.1101/cshperspect.a019042

O'Farrell, P. H., Stumpff, J., & Su, T. T. (2004). Embryonic cleavage cycles: how is a mouse like a fly? *Curr Biol, 14*(1), R35-45. doi:10.1016/j.cub.2003.12.022

Oesterhelt, C., Schnarrenberger, C., & Gross, W. (1999). Characterization of a sugar/polyol uptake system in the red alga *Galdieria sulphuraria*. *Eur J Phycol, 34*(3), 271-277. doi:10.1080/09670269910001736322

Oesterhelt, C., Vogelbein, S., Shrestha, R. P., Stanke, M., & Weber, A. P. (2008). The genome of the thermoacidophilic red microalga *Galdieria sulphuraria* encodes a small family of secreted class III peroxidases that might be involved in cell wall modification. *Planta, 227*(2), 353-362. doi:10.1007/s00425-007-0622-z

Oldenhof, H., Zachleder, V., & Van den Ende, H. (2007). The cell cycle of *Chlamydomonas reinhardtii*: the role of the commitment point. *Folia Microbiol (Praha), 52*(1), 53-60. doi:10.1007/BF02932138

Olson, B. J., Oberholzer, M., Li, Y., Zones, J. M., Kohli, H. S., Bisova, K., . . . Umen, J. G. (2010). Regulation of the *Chlamydomonas* cell cycle by a stable, chromatin-associated retinoblastoma tumor suppressor complex. *Plant Cell, 22*(10), 3331-3347. doi:10.1105/tpc.110.076067

Pan, K. Z., Saunders, T. E., Flor-Parra, I., Howard, M., & Chang, F. (2014). Cortical regulation of cell size by a sizer cdr2p. *Elife, 3*, e02040. doi:10.7554/eLife.02040

Parfrey, L. W., Lahr, D. J., Knoll, A. H., & Katz, L. A. (2011). Estimating the timing of early eukaryotic diversification with multigene molecular clocks. *Proc Natl Acad Sci U S A, 108*(33), 13624-13629. doi:10.1073/pnas.1110633108

Rigano, C., Aliotta, G., Rigano, V. D., Fuggi, A., & Vona, V. (1977). Heterotrophic growth patterns in the unicellular alga *Cyanidium caldarium.* A possible role for threonine dehydrase. *Arch Microbiol, 113*(3), 191-196. doi:10.1007/BF00492024

Rigano, C., Fuggi, A., Rigano, V. D. M., & Aliotta, G. (1976). Studies on utilization of 2-ketoglutarate, glutamate and other amino acids by the unicellular alga *Cyanidium caldarium*. *Arch Microbiol, 107*(2), 133-138. doi:10.1007/BF00446832

Setlikova, E., Setlik, I., Kupper, H., Kasalicky, V., & Prasil, O. (2005). The photosynthesis of individual algal cells during the cell cycle of *Scenedesmus quadricauda* studied by chlorophyll fluorescence kinetic microscopy. *Photosynth Res, 84*(1-3), 113-120. doi:10.1007/s11120-005-0479-6

Sleigh, M. A., & Sleigh, M. A. (1989). *Protozoa and other protists*. London: Edward Arnold.

Spudich, J. L., & Sager, R. (1980). Regulation of the *Chlamydomonas* cell cycle by light and dark. *J Cell Biol, 85*(1), 136-145. doi:10.1083/jcb.85.1.136

Sumiya, N., Fujiwara, T., Era, A., & Miyagishima, S. Y. (2016). Chloroplast division checkpoint in eukaryotic algae. *Proc Natl Acad Sci U S A, 113*(47), E7629-E7638. doi:10.1073/pnas.1612872113

Sumiya, N., Fujiwara, T., Kobayashi, Y., Misumi, O., & Miyagishima, S. Y. (2014). Development of a heat-shock inducible gene expression system in the red alga *Cyanidioschyzon merolae*. *PLoS One, 9*(10), e111261. doi:10.1371/journal.pone.0111261

Syed, S., Wilky, H., Raimundo, J., Lim, B., & Amodeo, A. A. (2020). The nuclear to cytoplasmic ratio directly regulates zygotic transcription in *Drosophila* through multiple modalities. *bioRxiv*, 766881. doi:10.1101/766881

Takahara, M., Takahashi, H., Matsunaga, S., Sakai, A., Kawano, S., & Kuroiwa, T. (2000). Isolation, characterization, and chromosomal mapping of an *ftsZ* gene from the unicellular primitive red alga *Cyanidium caldarium* RK-1. *Curr Genet, 37*(2), 143-151. doi:10.1007/s002940050021

Toplin, J. A., Norris, T. B., Lehr, C. R., McDermott, T. R., & Castenholz, R. W. (2008). Biogeographic and phylogenetic diversity of thermoacidophilic Cyanidiales in Yellowstone National Park, Japan, and New Zealand. *Appl Environ Microbiol, 74*(9), 2822-2833. doi:10.1128/AEM.02741-07

Tyers, M., Tokiwa, G., Nash, R., & Futcher, B. (1992). The Cln3-Cdc28 kinase complex of *S. cerevisiae* is regulated by proteolysis and phosphorylation. *EMBO J, 11*(5), 1773-1784.

Umen, J. G. (2005). The elusive sizer. *Curr Opin Cell Biol, 17*(4), 435-441. doi:10.1016/j.ceb.2005.06.001

Umen, J. G. (2018). Sizing up the cell cycle: systems and quantitative approaches in *Chlamydomonas*. *Curr Opin Plant Biol, 46*, 96-103. doi:10.1016/j.pbi.2018.08.003

Umen, J. G., & Goodenough, U. W. (2001). Control of cell division by a retinoblastoma protein homolog in *Chlamydomonas*. *Genes Dev, 15*(13), 1652-1661. doi:10.1101/gad.892101

Umen, J. G., & Olson, B. J. (2012). Genomics of volvocine algae. *Adv Bot Res, 64*, 185-243. doi:10.1016/B978-0-12-391499-6.00006-2

Vandepoele, K., Raes, J., De Veylder, L., Rouze, P., Rombauts, S., & Inze, D. (2002). Genome-wide analysis of core cell cycle genes in *Arabidopsis*. *Plant Cell, 14*(4), 903-916. doi:10.1105/tpc.010445

Verges, E., Colomina, N., Gari, E., Gallego, C., & Aldea, M. (2007). Cyclin Cln3 is retained at the ER and released by the J chaperone Ydj1 in late G1 to trigger cell cycle entry. *Mol Cell, 26*(5), 649-662. doi:10.1016/j.molcel.2007.04.023

Vitova, M., Bisova, K., Umysova, D., Hlavova, M., Kawano, S., Zachleder, V., & Cizkova, M. (2011). *Chlamydomonas reinhardtii*: duration of its cell cycle and phases at growth rates affected by light intensity. *Planta, 233*(1), 75-86. doi:10.1007/s00425-010-1282-y

Wang, H., Carey, L. B., Cai, Y., Wijnen, H., & Futcher, B. (2009). Recruitment of Cln3 cyclin to promoters controls cell cycle entry via histone deacetylase and other targets. *PLoS Biol, 7*(9), e1000189. doi:10.1371/journal.pbio.1000189

Wijnen, H., Landman, A., & Futcher, B. (2002). The G(1) cyclin Cln3 promotes cell cycle entry via the transcription factor Swi6. *Mol Cell Biol, 22*(12), 4402-4418. doi:10.1128/mcb.22.12.4402-4418.2002

Willis, L., & Huang, K. C. (2017). Sizing up the bacterial cell cycle. *Nat Rev Microbiol, 15*(10), 606-620. doi:10.1038/nrmicro.2017.79

Wilson, E. B. (1928). *The cell in development and heredity*. Retrieved from

Yoon, H. S., Ciniglia, C., Wu, M., Comeron, J. M., Pinto, G., Pollio, A., & Bhattacharya, D. (2006). Establishment of endolithic populations of extremophilic Cyanidiales (Rhodophyta). *BMC Evol Biol, 6*, 78. doi:10.1186/1471-2148-6-78

Yoon, H. S., Hackett, J. D., Ciniglia, C., Pinto, G., & Bhattacharya, D. (2004). A molecular timeline for the origin of photosynthetic eukaryotes. *Mol Biol Evol, 21*(5), 809-818. doi:10.1093/molbev/msh075

Zachleder, V., Bisova, K., Vitova, M., Kubin, S., & Hendrychova, J. (2002). Variety of cell cycle patterns in the alga *Scenedesmus quadricauda* (Chlorophyta) as revealed by application of illumination regimes and inhibitors. *Eur J Phycol, 37*(3), 361-371. doi:10.1017/s0967026202003815

Zachleder, V., Ivanov, I., Vitova, M., & Bisova, K. (2019). Cell cycle arrest by supraoptimal temperature in the alga *Chlamydomonas reinhardtii*. *Cells*, *8*(10), 1237. doi:10.3390/cells8101237

Acknowledgements

This doctoral study was carried out in Laboratory of Symbiosis and Cell Evolution in National Institute of Genetics (NIG), Mishima City, Japan from the year 2016 to 2021. I sincerely appreciate all kind of supports that I have received which made this study possible. I am deeply gratitude to my supervisor, Professor Shin-ya Miyagishima, for his patient, guidance and support throughout this study. He has reassessed my progress from time to time and provided his knowledge and valuable suggestions to improve my study plan. I also thanks for his strenuous effort to revise this doctoral thesis and other manuscripts, as well as the feedbacks provided for my various progress reports and presentations in my five years of study.

I would also like to express my great gratitude to Assistant Professor Takayuki Fujiwara for his experimental guidance provided with detailed explanations. He has given insightful discussions together with my supervisor, and also provided immerse feedbacks and suggestions for my experimental designs, progress presentations and manuscript preparation. He has also provided many algal strains for this study and has been my primary source for getting scientific questions answered. Big thanks also to Assistant Professor Shunsuke Hirooka for experimental guidance related to the study on *Cyanidium* spp. and *Galdieria* spp. He has also provided few algal strains for this study and has provided me various feedbacks throughout my study.

Sincere thanks also go out to all progress committee members Professor Jun Kitano, Professor Hitoshi Sawa, Professor Akatsuki Kimura and Professor Kazuhiro Maeshima for dedicating their time and effort to evaluate my study and provided useful suggestions to improve my study. I am grateful to Professor Jun Kitano for being my committee member chair for five years, continually following up and encouraging my study. In addition, I also would like to thank other teaching staffs in NIG for their valuable advices and suggestions on my study.

I have received many helps from the current and previous members of Laboratory of Symbiosis and Cell Evolution. Many thanks to Dr. Ryo Onuma for isolation of algal cells, suggestions on data analyses and numerous arrangements on laboratory related events. I am

grateful to Dr. Akihiro Uzuka for his information regarding PhD study, and for being my tutor during my first year of study and helped me in various procedures when I first arrived in NIG and settling in Mishima City. I would like to express my great gratitude to Ms. Uiko Sugimoto, Ms. Reiko Tomita, Ms. Reiko Ujigawa, Dr. Ryudo Ohbayashi, Dr. Yusuke Kobayashi, Ms. Kiyomi Hashimoto and Ms. Yoshiko Tanaka for various advices, supports in performing my experiments and also the help in administrative related works, which streamlined and reduced the effort required for this study. I also appreciate Ms. Sharlyn Chua for the help in the commitment assay of *Cyanidium* spp. and also the chance of being an instructor during NIG summer internship program.

I would also like to acknowledge Dr. Yoko Arakaki (The University of Tokyo) for providing various volvocine green algal strains and the information regarding synchronization of *T. socialis* culture. I also valued the help of Associate Professor Hisayoshi Nozaki (The University of Tokyo) in introducing me to my supervisor and accommodating me as a research student before I entered NIG. I am also thankful to Associate Professor Yamato Yoshida for being an examination committee member for this doctoral thesis.

I really appreciate the good support system provided by NIG and SOKENDAI for student and international members. Being an international student, I required and received many assistances. The staff members of Academic Services Division of SOKEDAI in NIG have always been supportive and helpful not only for my study but also on various arrangements for my stay in Mishima City. I also would like to thank to many SOKENDAI students which were always friendly and helped me to be integrated into life at NIG. Heartfelt thank also to my family and friends in Malaysia for the care, supports and encouragements throughout my study.

I have received various funding supports in undertaking this PhD study which I truly appreciate. This work was supported by Japanese Government (Monbukagakusho: MEXT) Scholarship from academic year of 2016 to 2017, SOKENDAI scholarship for academic year of 2018 and Japan Society for the Promotion of Science Research (JSPS) Fellowships for Young Scientists (no. 19J13366) from the academic year 2019 to 2020.